

# Cepheid Calibrations of Modern Type Ia Supernovae: Implications for the Hubble Constant<sup>1</sup>

Adam G. Riess<sup>2,3</sup>, Lucas Macri<sup>4</sup>, Weidong Li<sup>5</sup>, Hubert Lampeitl<sup>3,8</sup>, Stefano Casertano<sup>3</sup>, Henry C. Ferguson<sup>3</sup>, Alexei V. Filippenko<sup>5</sup>, Saurabh W. Jha<sup>6</sup>, , Ryan Chornock<sup>5</sup>, Lincoln Greenhill<sup>7</sup>, Max Mutchler<sup>3</sup>, Mohan Ganeshalingham<sup>5</sup>

## ABSTRACT

This is the first of two papers reporting measurements from a program to determine the Hubble constant to  $\sim 5\%$  precision from a refurbished distance ladder. We present new observations of 110 Cepheid variables in the host galaxies of two recent Type Ia supernovae (SNe Ia), NGC 1309 and NGC 3021, using the Advanced Camera for Surveys on the *Hubble Space Telescope* (*HST*). We also present new observations of the hosts previously observed with *HST* whose SNe Ia provide the most precise luminosity calibrations: SN 1994ae in NGC 3370, SN 1998aq in NGC 3982, SN 1990N in NGC 4639, and SN 1981B in NGC 4536, as well as the maser host, NGC 4258. Increasing the interval between observations enabled the discovery of new, longer-period Cepheids, including 57 with  $P > 60$  days, which extend these period-luminosity ( $P-L$ ) relations. We present 93 measurements of the metallicity parameter,  $12 + \log[\text{O}/\text{H}]$ , measured from H II regions in the vicinity of the Cepheids and show these are consistent with solar metallicity. We find the slope of the seven dereddened  $P-L$  relations to be consistent with that of the Large Magellanic Cloud Cepheids and with parallax measurements of Galactic Cepheids, and we address the implications for the Hubble constant. We also present multi-band light curves of SN 2002fk (in NGC 1309) and SN 1995al (in NGC 3021) which may be used to calibrate their luminosities. In the second paper we present observations of the Cepheids in the  $H$  band obtained with the Near Infrared Camera and Multi-Object Spectrometer on *HST*, further mitigating systematic errors

---

<sup>1</sup>Based on observations with the NASA/ESA *Hubble Space Telescope*, obtained at the Space Telescope Science Institute, which is operated by AURA, Inc., under NASA contract NAS 5-26555.

<sup>2</sup>Department of Physics and Astronomy, Johns Hopkins University, Baltimore, MD 21218.

<sup>3</sup>Space Telescope Science Institute, 3700 San Martin Drive, Baltimore, MD 21218; ariess@stsci.edu .

<sup>4</sup>George P. and Cynthia W. Mitchell Institute for Fundamental Physics and Astronomy, Department of Physics, Texas A&M University, 4242 TAMU, College Station, TX 77843-4242.

<sup>5</sup>Department of Astronomy, University of California, Berkeley, CA 94720-3411.

<sup>6</sup>Department of Physics and Astronomy, Rutgers University, 136 Frelinghuysen Road, Piscataway, NJ 08854.

<sup>7</sup>Smithsonian Astrophysical Observatory, Cambridge, MA

<sup>8</sup> Institute of Cosmology and Gravitation, University of Portsmouth, Portsmouth, PO1 3FX, UK

along the distance ladder resulting from dust and chemical variations. The quality and homogeneity of these SN and Cepheid data provide the basis for a more precise determination of the Hubble constant.

*Subject headings:* galaxies: distances and redshifts — cosmology: observations — cosmology: distance scale — supernovae: general

## 1. Introduction

The most accurate method to measure the Hubble constant,  $H_0$ , in the low-redshift Universe has been to meld the Type Ia supernova (SN Ia) and Cepheid distance scales through *Hubble Space Telescope* (*HST*) observations of Cepheid variables in SN Ia host galaxies within  $\sim 20$  Mpc. Having extremely high and moderately uniform luminosities, SNe Ia are the most precise distance indicators known for sampling the present expansion rate of the Universe. Methods which use the relationship between SN Ia light-curve shape and luminosity (Phillips 1993; Hamuy et al. 1995, 1996; Riess et al. 1995, 1996a, 1998; Perlmutter et al. 1997; Saha et al. 2001) and supernova color to constrain absorption by dust (Riess et al. 1996b; Phillips et al. 1999; Guy et al. 2005; Wang et al. 2009) yield distances with *relative* precision approaching 5% *if applied to modern photometry*. The  $\sim 100$  high-quality, modern SN Ia light curves currently published in the redshift range  $0.01 < z < 0.1$  establish the *relative* expansion rate to an unprecedented uncertainty of  $< 1\%$  (i.e., internal statistical error; Jha, Riess, Kirshner 2005). Yet because SNe Ia are a secondary distance indicator, the measurement of the *true* expansion rate is seriously limited by the few opportunities to calibrate their peak luminosity.

The SN Ia *HST* Calibration Program (Saha et al. 2001; Sandage et al. 2006) and the *HST* Key Project (Freedman et al. 2001) calibrated  $H_0$  via Cepheids and SNe Ia using Wide Field and Planetary Camera 2 (WFPC2). These measurements resolved decades of extreme uncertainty about the scale and age of the Universe. However, despite a great amount of careful work, the final estimates of  $H_0$  by the two teams differ by 20% and the overall uncertainty in each estimate has proved difficult to reduce to 10% or less. The bulk of this can be traced to systematic uncertainties among the many steps on the path to determining the luminosity of SNe Ia and to the known inaccuracy of the SN Ia calibration sample.

The use of the LMC as the anchor in the Key Project distance ladder presents specific challenges which result in several sources of systematic uncertainty if used for calibrating SNe Ia with Cepheids. The LMC distance is known to only 5% to 10% and its Cepheids, all observed from the ground, are of shorter mean period ( $\langle P \rangle \approx 5$  d) and lower metallicity than those found in the spiral galaxies that host SNe Ia beyond the Local Group. These mismatches propagate unwanted uncertainties to the measurement of the Hubble constant from the use of imperfectly known relations between Cepheid luminosity, metallicity, and period. The use of distance estimates to Galactic Cepheids as anchors by the *HST* Calibration Program also presents stiff challenges as discussed in §5.

Additional systematic uncertainties in both teams’ measurements of  $H_0$  result from the photometric idiosyncracies of the WFPC2 camera and the unreliability of those nearby SNe Ia which were *photographically* observed, highly reddened, atypical, or discovered after maximum brightness. Only three SNe Ia (SNe 1990N, 1981B, and 1998aq) were free from these aforementioned shortcomings, making ideal SNe a minority of the set used for calibrating  $H_0$  with WFPC2 (see Table 1). The use of many unreliable calibrators was necessitated by the limited reach of WFPC2, defining a volume within which Nature provides a suitable SN Ia only once every decade.

The installation of the Advanced Camera for Surveys (ACS; Ford et al. 2003) on board *HST* provided an important improvement in the optical imaging capabilities of the observatory. In regards to the distance ladder, the improved resolution and sensitivity of ACS extended the reach of *HST* Cepheid observations to about 35 Mpc, tripling the enclosed volume and the available number of potential calibrators of SNe Ia since the WFPC2 era. In Cycle 11 we (Riess et al. 2005) used ACS to measure Cepheid variables in the host of an ideal calibrator, SN 1994ae, situated in this extended volume. Two more opportunities to augment the very small, modern sample of calibrated SNe Ia are presented by SN 1995al in NGC 3021 and SN 2002fk in NGC 1309. These SNe Ia were discovered well before their maxima and were observed with the same *UBVRI* passbands and equipment we employed to measure the SNe Ia that help define the Hubble flow. These SNe Ia present two of the most complete photometric records ever of any SNe Ia (see §4). Calibration of  $H_0$  from SN 1995al and SN 2002fk would add only the fifth and sixth reliable SN Ia to Table 1 and, more importantly, only the second and third to use the more reliable and advantageous photometric system of ACS.

By replacing previous anchors of the distance scale with the “maser galaxy” NGC 4258 we can also wring additional precision for the Hubble constant. First, the distance to the masers has been measured geometrically to unprecedented precision for an extragalactic source (Herrnstein et al. 1999, Humphreys et al. 2005, 2008,2009). NGC 4258 also has the largest extragalactic set of long-period Cepheids observed with HST (Macri et al. 2006) Furthermore, we could bypass uncertainties in the determination of the photometric system zeropoints from the ground and space, and in the functional form of the period-luminosity ( $P-L$ ) relation, because we would only need to determine the relative magnitude offset between each galaxy’s set of Cepheids. To maximize this advantage we may also reobserve the hosts of nearby SNe Ia already observed with WFPC2 to place their Cepheids on the same photometric system and to find additional Cepheids whose periods would have been greater than the length of the WFPC2 campaigns. Lastly, the metallicity of the spiral hosts of Cepheid-calibratable SNe Ia is much more similar to that of NGC 4258 than to that of the LMC, reducing the overall dependence of  $H_0$  on metallicity corrections. Ultimately, the improved precision in  $H_0$  gained from a reduction in rungs on the distance ladder using NGC 4258 will be limited by the number of SN Ia hosts calibrated by ACS (due to the intrinsic scatter of SN Ia magnitudes).

In §2 we present the observations of (a) Cepheids in the new SN hosts, (b) new, longer period Cepheids in the previously observed hosts, and (c) measurements of the metallicities in the vicinity

of the Cepheids. The light curves of the SNe Ia are presented in §3. In §4 we describe the value of these data for the distance scale, a task undertaken in a companion paper (Riess et al. 2009).

Table 1: SN Ia Light Curves with *HST* Cepheid Calibration

SN Ia	Modern photometry? <sup>e</sup>	Low reddening? <sup>a</sup>	Observed before max?	Normal	Ideal?
1895B <sup>b</sup>	No	Unknown	No	Unknown	
1937C <sup>b</sup>	No	Yes	Yes	Yes	
1960F <sup>b</sup>	No	No	Yes	?	
1972E <sup>b</sup>	Yes	Yes	No	Yes	
1974G	No	No	Yes	?	
1981B <sup>b</sup>	Yes	Yes	Yes	Yes	✓
1989B <sup>b</sup>	Yes	No	Yes	Yes	
1990N <sup>b</sup>	Yes	Yes	Yes	Yes	✓
1991T <sup>b</sup>	Yes	Yes?	Yes	No	
1994ae <sup>c</sup>	Yes	Yes	Yes	Yes	✓
1995al <sup>d</sup>	Yes	Yes	Yes	Yes	✓
1998aq <sup>c</sup>	Yes	Yes	Yes	Yes	✓
1998bu	Yes	No	Yes	Yes	
1999by	Yes	Yes	Yes	No	
2002fk <sup>d</sup>	Yes	Yes	Yes	Yes	✓

<sup>a</sup> $A_V < 0.5$  mag.

<sup>b</sup>Calibrated by the Sandage/Tammann/Saha collaboration.

<sup>c</sup>Calibration presented by Riess et al. (2005).

<sup>d</sup>Calibration first presented in this paper.

<sup>e</sup>CCD or photoelectric, not photographic.

## 2. Cepheid Observations

The average of a small sample may be significantly impacted by a moderate systematic error among one of its members. Therefore, *it is essential that each SN Ia in the calibration sample have a reliable photometric record which is accurate and comparable to those of the SNe Ia used to measure the Hubble flow.* To define a reliable calibration sample we use the criteria for inclusion of a SN Ia given by Riess et al. (2005): (a) modern data (i.e., photoelectric or CCD), (b) observed before maximum brightness, (c) low reddening, and (d) spectroscopically typical. In addition, their hosts must be suitable targets for observations by *HST* of their Cepheids, which requires a relatively face-on, late-type host within  $\sim 35$  Mpc.

The recent SN 1995al in NGC 3021 and SN 2002fk in NGC 1309 provide two valuable additions to the small calibration set (shown in Table 2). The SN data are described in §4, but both are ideal candidates by the previous criteria and their magnitudes indicate distances of 30–35 Mpc. The host galaxies are moderately sized ( $1.5' \times 1.5'$  and  $2.0' \times 2.2'$ , respectively), face-on Sbc galaxies,

Table 2: Optical Observations of SN Ia Calibration Sample

Host	SN Ia	Initial campaign	Reobservation
NGC 4536	SN 1981B	WFPC2	WFPC2
NGC 4639	SN 1990N	WFPC2	ACS
NGC 3982	SN 1998aq	WFPC2	ACS
NGC 3370	SN 1994ae	ACS	ACS
NGC 3021	SN 1995al	ACS	ACS
NGC 1309	SN 2002fk	ACS	ACS

each fitting well within the ACS WFC field of view as shown in Figures 1 and 2.

In Cycle 14 (2005–2006, GO-10497) we observed NGC 1309 and NGC 3021 for 12 epochs of 4800 s each with ACS WFC *F555W* using a power-law spacing of intervals designed to reduce period aliasing up to the full monitoring duration of 52 d. We also observed each host at 5 epochs with *F814W* for 4800 s each. The telescope position and orientation were fixed for each host and a four-position dither (noninteger shift of 4.5 pixels in each detector coordinate) was performed to better sample the point-spread function (PSF) in the median image.

In Cycle 15 (2006–2007, GO-10802) we reobserved NGC 1309 and NGC 3021, as well as the other four hosts in the calibration sample of Table 2 at two epochs using ACS and *F555W* (each *F555W* observation was separated by  $\sim 10$  d) to constrain the phase of the Cepheid light curves for subsequent infrared (IR) observations with the Near Infrared Camera and Multi-Object Spectrometer (NICMOS; Riess et al. 2009) and to aid in the identification of Cepheids with  $P > 60$  d which were beyond the interval of the initial, contiguous campaigns.<sup>1</sup> Logs of the exposures for NGC 3021 and NGC 1309 are given in Tables 3 and 4, respectively.

## 2.1. ACS Photometry

For the four hosts with extensive ACS measurements NGC 1309, NGC 3021, NGC 3370 and NGC 4258, the data from programs GO-9810 (P.I. Greenhill), GO-9351 (P.I. Riess), GO-10497 (P.I. Riess), and GO-10802 (P.I. Riess) were retrieved from the *HST* archive. While ACS data for NGC 3370 (Riess et al. 2005) and NGC 4258 (Macri et al. 2006) were previously analyzed to identify Cepheids, the acquisition of the two new epochs of ACS imaging in program GO-10802, better calibration data, and the need for a homogeneous reduction process for the comparison of Cepheid magnitudes necessitated new data reductions undertaken here.

The data retrieval from the Space Telescope Science Institute (STScI) MAST archive made

---

<sup>1</sup>The Cycle 15 observations of NGC 4536 were obtained with WFPC2 due to the failure of ACS in February, 2007.

Table 3. Log of Observations for NGC 3021

Epoch #	MJD at mid exposure*	
	V	I
01	3686.0407	3686.1735
02	3686.1066	3686.2398
03	3696.4242	...
04	3696.5566	...
05	3704.6240	3704.7597
06	3704.6929	3704.8261
07	3708.7942	...
08	3708.8564	...
09	3712.7275	...
10	3712.7894	...
11	3715.7923	...
12	3715.8559	...
13	3716.7919	3716.9227
14	3716.8555	3717.0197
15	3718.8569	...
16	3718.9211	...
17	3721.9208	...
18	3722.0161	...
19	3725.7835	3725.9159
20	3725.8488	3726.0127
21	3730.5123	...
22	3730.5778	...
23	3737.5724	3737.7050
24	3737.6380	3737.7712
25	4058.9217	...
26	4066.7134	...

\*: JD-2450000.0

Table 4. Log of Observations for NGC 1309

Epoch #	MJD at mid exposure*	
	V	I
01	3588.6856	3588.8192
02	3588.7523	3588.8856
03	3599.9153	...
04	3599.9797	...
05	3606.7768	3606.9082
06	3606.8411	3606.9744
07	3609.9078	...
08	3609.9723	...
09	3615.5304	...
10	3615.6030	...
11	3616.9033	...
12	3617.0008	...
13	3618.5021	3618.6347
14	3618.5676	3618.7009
15	3620.9007	...
16	3620.9992	...
17	3623.9338	...
18	3624.0679	...
19	3629.7599	3629.9226
20	3629.8252	3630.0626
21	3633.3574	...
22	3633.4228	...
23	3640.4216	3640.5530
24	3640.4859	3640.6192
25	4015.3368	...
26	4032.5923	...

\*: JD-2450000.0

use of the most up-to-date calibration as applied by the software suite *calacs* in “pyraf.” Epoch-by-epoch photometry for all stellar sources identified in a master, composite image was measured for the images obtained in *F555W* and *F814W* using the DAOPHOT<sup>2</sup> set of routines following the procedures given by Stetson (1994), Stetson et al. (1998), Riess et al. (2005), and Macri et al. (2006). Magnitudes from PSF fitting were initially measured to include the charge within 0.5” radius apertures. These natural-system magnitudes for each candidate Cepheid at each observed epoch are given in Tables 5 and 6, evaluated as  $2.5 \log(e/s) - \text{CTE} + 25.0$ , where  $e/s$  is the measured flux (electrons per second) and CTE (charge transfer efficiency) is the magnitude loss given by Chiaberge et al. (2009) for a star as a function of observation date, pixel position, brightness, and background. The median uncertainty for an individual Cepheid magnitude in an epoch was 0.09 mag.

We selected Cepheids following the methodology outlined by Macri et al. (2006). Initially, Cepheid candidates were identified from the time-sampled data by selecting all stellar sources with a modified Welch/Stetson variability index  $J_S$  (Stetson 1996) in excess of 0.75 and that were detected in at least 12 of the 14 epochs of *F555W* data. These candidates were then subjected to a “minimum string-length analysis,” which identified as likely periods those that minimized the sum of magnitude variations for observations at similar trial phases (Stetson et al. 1998). Robust least-squares fits were then performed in the two bands, comparing the single-epoch magnitudes to template Cepheid light curves from Stetson et al. (1998), where six parameters representing (1) period, (2) *V*-band amplitude, (3) *I*-band amplitude, (4) epoch of zero phase, (5) mean magnitude in *V*, and (6) mean magnitude in *I* were free, but the shape of the light curve was a unique function of the assumed period. Finally, one of us (L.M.M.) applied experienced judgement in a visual comparison of the data to the best-fit Cepheid model, rejecting unconvincing candidates (approximately 10%). The criteria used to settle on the final set were (a) how well the light-curve sampling was distributed in phase, (b) the appearance of the characteristic rapid rise and slow fall of the light curve, and (c) the proximity of the amplitudes and colors to the expected range. This same partially subjective process was compared to a purely numerical selection by Riess et al. (2005) for the Cepheids in NGC 3370, resulting in small differences in Cepheid-list membership, and less than 0.04 mag difference in the intercept of the *P-L* relation. When the optimum fit had been achieved, the fitted light curves were converted to flux units and numerically integrated over a cycle to achieve flux-weighted mean apparent brightnesses in each bandpass; these were then converted back to magnitude units.

The photometric zeropoints (the magnitudes resulting in 1 electron  $\text{s}^{-1}$  in an infinite aperture) for our ACS magnitudes were obtained using the Vegamag system (i.e., Vega  $\equiv$  0 mag in all passbands). The official STScI ACS zeropoints were revised from those given by Sirianni et al.

---

<sup>2</sup>Past comparisons of photometry with the popular PSF fitting tools DoPHOT, DAOPHOT (Stetson 1987), and HSTphot by Gibson et al. (2000), Leonard et al. (2003), and Saha et al. (2001) show that the mean difference in *HST* photometry obtained with these packages is not significant.



(2005), and as of the beginning of 2009 have values of  $F555W = 25.744$  and  $F814W = 25.536$  for data obtained before 2006 July 4 when ACS operated at  $-77$  C, and  $F555W = 25.727$  and  $F814W = 25.520$  after that date when ACS operated at  $-81$  C. These are based on an empirical measurement of the system throughput at all wavelengths using the known spectral energy distribution of five white dwarfs. This approach is similar to that of Holtzman et al. (1995) for WFPC2.<sup>3</sup> The PSF magnitudes in Tables 5 and 6 were extended from the  $0.5''$  radius aperture to infinity using the aperture corrections given by Sirianni et al. (2005) of 0.092 and 0.087 mag in  $F555W$  and  $F814W$ , respectively. The natural-system magnitudes were converted to the Johnson system (for ease of comparison to non-*HST* Cepheid data) using the formulae in Sirianni et al. (2005). Thus, the natural-system magnitudes in Tables 5 and 6 with zeropoint 25.0 are converted to the Johnson system using the transformations

$$V = F555W + 0.744 - 0.092 - 0.054(V - I), \quad (1)$$

$$I = F814W + 0.536 - 0.087 - 0.002(V - I). \quad (2)$$

This transformation is performed during the simultaneous fitting of the  $V$  and  $I$  light-curve templates to interpolate the  $V - I$  color at epochs when only  $F555W$  was measured.

---

<sup>3</sup>The Key Project zeropoint is based on matching *HST* photometry of globular clusters (including 47 Tuc) to ground-based data obtained by Stetson (2000) on 22 nights from 12 distinct observing runs. Riess et al. (2005) found that the ACS photometric zeropoints of Sirianni et al. (2005),  $F555W = 25.704$  mag and  $F814W = 25.492$  mag, and those based on the Stetson (2000) system are quite consistent, with a mean difference of 0.015 mag in  $V$  and 0.026 mag in  $I$  for 250 calibrating stars in 47 Tuc.

Table 5. Cepheid photometry in NGC 3021<sup>a</sup>

#	F555W	F814W	F555W	F814W	F555W	F814W	F555W	F814W
	<b>31556P = 11.18 d</b>		<b>30672P = 13.93 d</b>		<b>08621P = 15.38 d</b>		<b>08102P = 18.71 d</b>	
1	26.841(189)	26.382(185)*	27.381(323)	26.677(182)	26.195(166)	25.881(145)	26.313(174)	25.904(148)
2	26.822(218)	26.807(199)	27.218(199)	26.799(206)	26.390(115)	25.942(135)	26.398(108)	26.110(122)
3	27.399(285)	...	26.600(165)	...	27.078(237)	...	...	...
4	26.981(188)	...	26.750(152)	...	26.742(190)	...	26.845(168)	...
5	26.576(137)	26.543(274)	27.297(236)	26.820(181)	26.614(183)	25.719(136)	26.625(171)	26.056(203)
6	26.708(207)	27.024(332)*	27.298(282)	26.854(185)	26.592(178)	26.011(124)	26.144(149)	26.189(117)
7	27.227(371)	...	26.593(132)	...	27.004(190)	...	26.213(248)	...
8	27.754(361)	...	26.632(074)	...	26.870(228)	...	26.543(184)	...
9	26.831(220)	...	27.134(337)	...	26.881(266)	...	27.108(361)	...
10	26.401(119)	...	27.175(176)	...	26.714(157)	...	27.116(242)	...
11	26.619(172)	...	27.871(309)	...	26.337(133)	...	27.021(294)	...
12	26.514(113)	...	27.663(252)	...	26.203(108)	...	27.012(191)	...
13	26.851(261)	26.678(282)	27.238(220)	27.041(300)	26.481(199)	25.949(179)	27.131(287)	26.539(215)
14	26.783(271)	26.592(270)	27.649(389)	26.889(161)	26.034(133)	25.944(134)	27.180(312)	26.485(290)
15	26.966(276)	...	26.737(144)	...	26.380(145)	...	27.416(372)	...
16	...	...	26.678(104)	...	26.640(163)	...	27.321(252)	...
17	26.872(220)	...	26.223(133)	...	26.731(223)	...	26.673(161)	...
18	27.396(250)	...	26.355(105)	...	26.448(172)	...	25.993(095)	...
19	26.103(110)	26.292(133)	26.843(148)	26.567(115)	27.327(363)	26.289(214)	26.601(175)	26.076(136)
20	26.139(150)	26.315(193)	26.730(212)	26.409(129)	26.561(189)	26.598(220)*	26.767(147)	26.062(144)
21	26.662(278)	...	26.788(193)	...	26.205(184)	...	26.570(205)	...
22	...	...	27.353(237)	...	26.366(166)	...	26.996(179)	...
23	26.470(138)	26.324(186)	26.411(151)	26.429(133)	27.314(338)	26.223(205)	27.215(172)	26.770(261)
24	26.582(121)	26.386(160)	27.000(180)	26.286(140)	27.209(365)	26.153(165)	27.468(228)	26.447(236)
25	26.798(252)	...	26.930(269)	...	26.720(342)	...	26.181(249)	...
26	27.510(391)	...	27.090(345)	...	26.601(256)	...	26.950(325)	...
	<b>20774P = 20.39 d</b>		<b>10786P = 21.16 d</b>		<b>47390P = 21.84 d</b>		<b>33607P = 23.14 d</b>	
1	26.427(141)	25.821(183)	26.590(179)	25.882(125)	26.292(189)	25.915(151)	26.733(116)	26.360(152)
2	26.349(157)	25.704(100)	26.658(188)	25.678(117)	26.178(118)	25.662(134)	27.329(359)	26.750(181)*
3	26.099(123)	...	26.737(145)	...	26.676(128)	...	26.743(208)	...
4	26.322(132)	...	27.291(294)	...	26.577(164)	...	26.391(143)	...
5	26.850(214)	26.140(181)	26.392(106)	26.056(185)	26.711(171)	25.925(166)	27.066(173)	26.446(181)
6	26.533(167)	26.034(194)	26.569(152)	25.866(172)	27.073(250)	26.096(165)	27.059(250)	26.477(156)
7	25.777(114)	...	26.686(176)	...	26.273(131)	...	27.111(193)	...
8	25.770(116)	...	26.819(186)	...	26.139(097)	...	27.160(225)	...
9	25.958(130)	...	27.281(294)	...	26.267(112)	...	26.431(181)	...
10	25.989(150)	...	26.880(175)	...	26.378(177)	...	26.517(160)	...
11	26.131(127)	...	27.315(326)	...	26.749(189)	...	26.520(094)	...
12	26.113(190)	...	27.177(317)	...	26.573(189)	...	26.246(114)	...
13	25.931(091)	25.698(123)	27.244(332)	26.259(175)	26.639(219)	26.128(224)	26.308(145)	25.972(098)
14	26.214(125)	25.588(100)	27.034(204)	26.031(166)	26.563(150)	26.037(167)	26.422(200)	25.953(107)
15	26.212(139)	...	26.738(167)	...	26.480(210)	...	26.870(206)	...
16	26.223(170)	...	26.653(134)	...	27.133(243)	...	26.643(112)	...
17	26.207(232)	...	26.241(107)	...	27.147(338)	...	26.762(161)	...
18	26.871(276)	...	26.069(144)	...	26.606(223)	...	26.720(148)	...

Table 5—Continued

#	F555W	F814W	F555W	F814W	F555W	F814W	F555W	F814W
19	26.463(168)	25.909(175)	26.574(183)	25.818(095)	27.102(338)	26.246(173)	26.966(202)	26.371(094)
20	26.531(170)	26.327(162)	26.254(105)	25.541(144)	26.792(194)	26.245(299)	26.708(105)	26.221(103)
21	25.676(088)	...	27.097(219)	...	26.112(130)	...	27.313(182)	...
22	25.692(127)	...	26.621(144)	...	26.321(178)	...	27.070(207)	...
23	25.955(121)	25.559(109)	27.115(256)	26.016(166)	26.478(133)	25.823(157)	26.267(095)	25.910(089)
24	26.157(166)	25.921(116)	26.833(330)	26.269(227)	26.426(142)	25.660(232)	26.090(108)	25.920(096)
25	25.806(128)	...	26.275(182)	...	25.896(128)	...	26.572(314)	...
26	26.451(229)	...	26.785(379)	...	26.498(185)	...	...	...
<b>32375P = 24.02 d</b>		<b>08636P = 24.36 d</b>		<b>32380P = 25.18 d</b>		<b>32088P = 25.78 d</b>		
1	26.158(059)	25.689(121)	26.586(139)	25.825(164)	26.736(212)	25.861(091)	27.179(229)	26.010(119)
2	26.311(168)	25.773(144)	26.710(201)	25.804(162)	26.686(113)	25.809(120)	27.158(276)	26.065(138)
3	27.245(174)	...	25.977(111)	...	25.841(061)	...	26.308(097)	...
4	26.929(174)	...	26.144(114)	...	25.846(064)	...	25.956(148)	...
5	26.938(299)	25.984(108)	26.343(140)	25.830(137)	26.476(179)	25.885(084)	26.656(136)	25.591(111)
6	26.507(171)	26.207(106)	26.398(156)	25.857(116)	26.634(226)	26.384(145)*	26.651(172)	25.673(127)
7	26.061(102)	...	26.709(234)	...	26.341(145)	...	27.113(190)	...
8	26.065(123)	...	26.581(171)	...	26.555(242)	...	26.761(173)	...
9	26.324(122)	...	26.574(172)	...	26.623(197)	...	27.390(317)	...
10	26.708(116)	...	26.786(228)	...	26.686(128)	...	26.499(229)	...
11	26.587(112)	...	25.942(139)	...	26.052(098)	...	27.373(255)	...
12	26.760(231)	...	26.154(119)	...	26.021(111)	...	...	...
13	26.485(133)	26.069(099)	25.850(093)	25.425(131)	25.635(105)	25.296(118)	27.096(277)	26.285(163)*
14	26.246(135)	26.084(125)	25.973(154)	25.469(074)	25.586(085)	25.220(079)	26.831(230)	25.895(073)
15	26.955(138)	...	25.715(094)	...	25.571(129)	...	25.873(142)	...
16	26.846(194)	...	25.752(138)	...	25.556(066)	...	26.026(139)	...
17	27.359(348)	...	25.994(138)	...	25.852(134)	...	26.389(106)	...
18	27.578(345)	...	26.043(124)	...	25.932(076)	...	26.137(105)	...
19	27.362(196)	26.397(166)	26.222(219)	25.653(138)	26.029(103)	25.473(112)	26.445(158)	25.795(106)
20	26.973(217)	26.608(205)	26.130(144)	25.484(133)	26.131(100)	25.621(095)	26.627(173)	25.549(106)
21	26.477(114)	...	26.472(160)	...	26.344(111)	...	26.714(145)	...
22	26.460(166)	...	26.543(231)	...	26.414(095)	...	26.638(217)	...
23	26.720(141)	25.934(086)	26.610(152)	26.039(184)	26.600(155)	26.099(183)	27.154(259)	26.008(099)
24	26.704(245)	25.695(081)	26.474(236)	26.254(275)*	26.602(126)	25.881(091)	26.978(230)	26.052(167)
25	...	...	25.636(159)	...	26.438(197)	...	26.282(252)	...
26	26.412(296)	...	26.186(208)	...	26.443(306)	...	26.751(342)	...
<b>26946P = 26.84 d</b>		<b>09028P = 31.90 d</b>		<b>23149P = 32.53 d</b>		<b>30428P = 32.61 d</b>		
1	26.398(158)	25.499(065)	25.256(079)	24.965(066)	25.527(084)	25.135(094)	26.108(083)	25.482(082)
2	26.790(230)	25.743(117)	25.248(069)	24.888(079)	25.723(092)	24.873(068)	26.015(076)	25.315(072)
3	26.221(105)	...	25.877(108)	...	26.344(102)	...	26.537(103)	...
4	26.366(157)	...	25.804(066)	...	26.111(128)	...	26.664(142)	...
5	25.885(090)	25.253(078)	25.989(130)	25.498(082)	26.753(106)	25.747(116)	25.395(064)	25.179(073)
6	26.078(136)	25.649(109)	25.927(086)	25.476(109)	26.604(166)	25.414(113)	25.478(051)	25.212(055)
7	26.128(123)	...	26.280(147)	...	26.317(174)	...	25.755(086)	...
8	26.153(170)	...	26.158(098)	...	26.236(195)	...	25.733(087)	...
9	26.442(180)	...	...	...	25.537(046)	...	25.860(073)	...
10	26.476(162)	...	26.083(092)	...	25.439(091)	...	25.541(133)	...

Table 5—Continued

#	F555W	F814W	F555W	F814W	F555W	F814W	F555W	F814W
11	26.654(141)	...	25.209(060)	...	25.577(069)	...	25.981(100)	...
12	26.691(155)	...	25.189(062)	...	25.559(090)	...	25.998(132)	...
13	26.780(152)	25.564(080)	25.165(081)	24.910(065)	25.777(068)	25.083(066)	26.022(093)	25.386(070)
14	26.551(125)	25.827(132)	25.192(051)	25.022(091)	25.749(093)	25.053(068)	26.165(095)	25.529(070)
15	26.461(162)	...	25.118(077)	...	25.721(090)	...	26.118(084)	...
16	26.567(187)	...	25.329(071)	...	25.750(128)	...	26.174(135)	...
17	26.740(112)	...	25.440(080)	...	25.822(083)	...	26.409(096)	...
18	26.923(256)	...	25.569(058)	...	25.788(076)	...	26.255(131)	...
19	25.674(058)	25.394(065)	25.677(081)	25.025(081)	26.138(098)	25.182(072)	26.229(090)	25.477(086)
20	25.750(082)	25.394(066)	25.657(068)	25.044(081)	25.915(127)	25.177(112)	26.559(141)	25.637(099)
21	25.685(078)	...	25.910(086)	...	26.306(128)	...	26.802(149)	...
22	25.984(116)	...	25.879(116)	...	26.106(190)	...	26.788(260)	...
23	26.461(096)	25.617(106)	26.022(182)	25.469(094)	27.130(245)*	26.004(168)	25.443(064)	25.194(100)
24	26.382(132)	25.787(099)	26.075(138)	25.278(092)	26.518(177)	25.742(143)	25.447(088)	25.162(052)
25	26.243(112)	...	26.254(197)	...	26.225(221)	...	26.428(194)	...
26	27.061(252)	...	25.183(106)	...	26.262(266)	...	25.610(139)	...
	<b>26126P = 34.88 d</b>		<b>12135P = 36.50 d</b>		<b>31803P = 37.28 d</b>		<b>45787P = 37.31 d</b>	
1	25.761(154)	25.336(104)	26.200(122)	25.161(130)	26.296(122)	25.437(061)	25.081(106)	24.810(154)
2	25.691(115)	25.309(092)	26.341(134)	25.482(149)	26.297(110)	25.434(069)	25.285(128)	24.707(134)
3	25.989(201)	...	25.886(112)	...	26.590(122)	...	25.353(167)	...
4	26.065(207)	...	25.793(088)	...	26.673(190)	...	25.273(126)	...
5	25.445(108)	25.081(084)	26.098(139)	25.228(094)	26.932(185)	...	25.629(208)	24.931(132)
6	25.569(085)	25.214(087)	26.498(143)	25.179(083)	26.780(110)	26.026(102)	25.566(161)	24.991(186)
7	25.422(075)	...	26.326(136)	...	26.861(179)	...	25.495(234)	...
8	25.509(129)	...	26.628(225)	...	26.738(138)	...	25.470(141)	...
9	25.595(110)	...	26.278(141)	...	26.511(212)	...	25.455(150)	...
10	25.629(120)	...	26.263(121)	...	26.213(130)	...	25.736(214)	...
11	25.620(129)	...	26.470(228)	...	25.868(100)	...	25.659(229)	...
12	25.830(123)	...	26.601(197)	...	25.904(079)	...	25.663(149)	...
13	25.861(139)	24.988(124)	26.387(124)	25.591(100)	25.931(125)	25.476(096)	25.235(171)	24.963(157)
14	25.607(090)	24.983(153)	26.570(152)	25.843(134)	25.923(096)	25.393(061)	25.703(227)	24.945(167)
15	25.757(163)	...	26.915(346)	...	26.049(121)	...	25.310(152)	...
16	25.874(189)	...	26.702(228)	...	26.400(180)	...	25.539(154)	...
17	25.907(181)	...	26.396(192)	...	26.144(080)	...	24.961(154)	...
18	26.040(138)	...	26.387(197)	...	26.222(118)	...	25.115(105)	...
19	25.967(190)	25.567(116)	25.917(124)	25.030(115)	26.257(096)	25.467(105)	25.314(151)	24.927(177)
20	25.896(197)	25.510(095)	25.743(104)	25.173(087)	26.409(121)	25.520(067)	25.198(135)	24.767(125)
21	26.023(204)	...	25.935(102)	...	26.768(126)	...	25.281(138)	...
22	26.216(201)	...	25.915(135)	...	26.410(095)	...	25.296(158)	...
23	25.314(116)	25.081(111)	25.924(116)	25.053(086)	26.909(181)	26.158(097)	25.449(163)	24.811(152)
24	25.346(090)	25.269(107)	26.118(111)	25.149(072)	26.646(106)	25.536(143)	25.605(216)	24.887(122)
25	25.508(124)	...	25.817(145)	...	26.206(202)	...	25.008(167)	...
26	25.908(244)	...	26.130(227)	...	26.502(215)	...	25.433(249)	...
	<b>26545P = 39.57 d</b>		<b>09402P = 39.78 d</b>		<b>25375P = 39.96 d</b>		<b>09611P = 40.49 d</b>	
1	26.064(106)	25.247(087)	26.664(143)	25.594(131)	25.225(085)	24.974(081)	25.934(110)	25.450(104)
2	26.176(115)	25.553(105)	26.603(198)	25.502(184)	25.219(072)	24.918(074)	25.941(160)	25.516(138)

Table 5—Continued

#	F555W	F814W	F555W	F814W	F555W	F814W	F555W	F814W
3	25.305(085)	...	26.449(154)	...	25.696(084)	...	25.614(110)	...
4	25.436(086)	...	26.343(252)	...	25.699(151)	...	25.866(120)	...
5	25.569(088)	24.824(057)	25.775(087)	25.006(070)	25.718(080)	25.552(113)	25.258(076)	24.963(061)
6	25.820(090)	25.026(091)	25.875(125)	25.063(105)	25.915(098)	25.438(175)	25.631(100)	24.901(109)
7	25.949(137)	...	25.979(134)	...	26.176(153)	...	25.485(101)	...
8	25.908(086)	...	26.105(210)	...	26.167(146)	...	25.451(106)	...
9	25.803(124)	...	26.234(112)	...	26.202(137)	...	25.627(089)	...
10	26.113(105)	...	26.259(190)	...	26.364(207)	...	25.532(141)	...
11	26.097(078)	...	26.352(115)	...	26.101(139)	...	25.563(129)	...
12	26.033(135)	...	26.272(178)	...	26.238(153)	...	25.685(133)	...
13	25.925(090)	25.102(054)	26.509(189)	25.244(090)	26.684(139)	26.098(179)	25.685(105)	25.352(119)
14	26.227(169)	25.408(105)	26.389(215)	25.261(086)	26.342(109)	26.034(207)	25.792(104)	25.096(079)
15	25.971(103)	...	26.824(287)	...	25.766(147)	...	25.819(115)	...
16	26.292(130)	...	26.527(269)	...	25.774(103)	...	26.166(180)	...
17	25.896(133)	...	26.517(147)	...	25.150(050)	...	25.950(127)	...
18	26.402(109)	...	26.614(206)	...	25.294(091)	...	25.945(133)	...
19	26.247(089)	25.216(074)	26.872(226)	25.350(104)	25.283(050)	25.037(088)	25.818(091)	25.481(080)
20	26.266(158)	25.476(102)	26.482(278)	25.397(147)	25.281(074)	25.093(087)	25.999(151)	25.645(107)
21	25.317(054)	...	26.678(184)	...	25.514(068)	...	25.958(133)	...
22	25.283(061)	...	27.014(343)	...	25.388(078)	...	25.984(164)	...
23	25.292(061)	24.746(049)	26.722(285)	25.589(138)	25.726(079)	25.283(107)	25.668(128)	25.144(094)
24	25.382(072)	24.846(058)	26.371(296)	25.325(105)	25.651(078)	25.179(074)	25.691(111)	25.190(151)
25	25.650(120)	...	25.611(146)	...	25.918(124)	...	25.801(227)	...
26	25.858(129)	...	25.772(156)	...	26.000(136)	...	25.145(167)	...
	<b>20415P = 51.51 d</b>		<b>12778P = 63.19 d</b>		<b>19817P = 68.61 d</b>		<b>07098P = 82.66 d</b>	
1	25.740(101)	25.076(112)	24.888(109)	24.425(057)	25.719(075)	24.711(061)	25.202(082)	24.700(084)
2	25.633(146)	24.819(078)	24.928(110)	24.532(058)	25.605(059)	24.715(056)	25.498(055)	24.723(062)
3	25.970(146)	...	24.954(090)	...	25.802(081)	...	25.668(137)	...
4	26.064(102)	...	25.018(090)	...	25.863(056)	...	25.746(080)	...
5	25.942(099)	25.094(095)	25.133(105)	24.845(079)	25.876(085)	24.982(086)	25.429(085)	25.004(074)
6	26.398(127)	25.098(078)	25.132(137)	24.732(060)	25.937(087)	24.861(046)	25.493(108)	25.107(091)
7	26.146(116)	...	25.150(114)	...	25.885(135)	...	25.176(377)	...
8	26.242(120)	...	25.201(094)	...	25.929(070)	...	25.119(062)	...
9	26.149(198)	...	25.297(147)	...	26.135(074)	...	25.113(047)	...
10	26.101(179)	...	25.198(114)	...	25.996(078)	...	24.992(056)	...
11	26.712(183)	...	25.118(158)	...	26.319(087)	...	25.010(077)	...
12	26.563(211)	...	25.185(129)	...	26.109(140)	...	25.013(051)	...
13	26.556(144)	25.228(077)	25.131(116)	24.883(071)	26.305(131)	25.230(074)	25.087(096)	24.623(071)
14	26.429(142)	25.293(079)	25.317(124)	24.863(086)	26.070(109)	25.084(042)	25.230(088)	24.515(087)
15	26.254(188)	...	25.165(105)	...	26.089(098)	...	25.000(144)	...
16	26.181(084)	...	25.253(118)	...	25.973(082)	...	25.037(093)	...
17	25.962(129)	...	25.215(075)	...	25.946(088)	...	25.031(063)	...
18	25.757(130)	...	25.252(105)	...	25.869(082)	...	25.155(074)	...
19	25.593(102)	25.216(071)*	24.920(103)	24.506(097)	25.777(113)	24.898(063)	25.175(062)	24.616(086)
20	25.535(068)	24.757(081)	25.080(088)	24.698(068)	25.611(077)	24.864(049)	24.800(062)	24.497(066)
21	25.865(094)	...	24.786(093)	...	25.551(054)	...	25.408(179)	...

Table 5—Continued

#	F555W	F814W	F555W	F814W	F555W	F814W	F555W	F814W
22	25.402(109)	...	24.717(092)	...	25.407(082)	...	25.076(067)	...
23	25.887(085)	25.119(081)	24.719(064)	24.552(069)	25.421(080)	24.652(041)	25.329(067)	24.754(075)
24	25.812(086)	24.791(050)	24.834(097)	24.479(061)	25.403(062)	24.599(044)	25.339(077)	24.633(040)
25	26.002(132)	...	24.923(138)	...	25.903(138)	...	25.139(102)	...
26	26.139(283)	...	24.888(141)	...	25.867(117)	...	25.002(120)	...
	<b>09558P = 88.19 d</b>		<b>12013P = 90.73 d</b>		<b>10203P = 95.91 d</b>			
1	26.736(277)	25.005(092)	25.268(161)	24.460(073)	25.184(099)	24.440(076)		
2	26.487(194)	25.118(089)	25.246(152)	24.444(096)	25.192(069)	24.435(072)		
3	26.526(264)	...	25.350(127)	...	25.077(071)	...		
4	27.003(317)	...	25.336(156)	...	25.007(058)	...		
5	...	25.258(123)	25.176(080)	24.477(074)	25.089(089)	24.475(083)		
6	26.893(281)	25.319(085)	25.358(130)	24.624(111)	25.231(080)	24.543(118)		
7	26.688(281)	...	25.139(116)	...	25.063(072)	...		
8	26.439(196)	...	25.022(106)	...	25.163(088)	...		
9	26.263(161)	...	24.851(109)	...	25.113(091)	...		
10	26.276(152)	...	24.980(120)	...	25.243(094)	...		
11	26.072(116)	...	24.848(078)	...	25.268(105)	...		
12	26.095(181)	...	24.982(120)	...	25.200(061)	...		
13	26.107(147)	24.836(091)	24.874(123)	24.209(056)	25.344(099)	24.501(078)		
14	26.050(170)	24.846(090)	24.997(089)	24.327(081)	25.266(100)	24.437(086)		
15	25.918(127)	...	25.024(107)	...	25.377(093)	...		
16	25.999(120)	...	24.960(145)	...	25.302(065)	...		
17	26.253(208)	...	24.835(070)	...	25.610(117)*	...		
18	25.991(143)	...	25.004(094)	...	25.357(043)	...		
19	26.135(149)	24.915(063)	24.980(119)	24.351(096)	25.348(058)	24.509(100)		
20	25.876(105)	24.756(065)	25.044(110)	24.247(082)	25.318(082)	24.485(055)		
21	25.983(188)	...	25.069(118)	...	25.293(065)	...		
22	25.922(149)	...	24.994(115)	...	25.367(078)	...		
23	25.989(180)	24.821(058)	25.060(123)	24.405(097)	25.162(083)	24.571(097)		
24	26.032(167)	24.878(080)	25.089(094)	24.390(098)	25.253(081)	24.418(065)		
25	26.416(219)	...	25.384(182)	...	25.407(158)*	...		
26	26.369(199)	...	25.199(195)	...	25.152(096)	...		

\* Data point rejected in light curve fit

<sup>a</sup>  $1\sigma$  uncertainties (units of 0.001 mag) are given in parentheses.

Table 6. Cepheid photometry in NGC 1309 <sup>a</sup>

#	F555W	F814W	F555W	F814W	F555W	F814W	F555W	F814W
	<b>21599P = 20.93 d</b>		<b>09778P = 21.98 d</b>		<b>08610P = 23.23 d</b>		<b>06631P = 24.82 d</b>	
1	27.127(234)	26.249(129)	27.137(249)	27.083(303)*	27.039(291)	26.456(166)	25.882(101)	25.646(127)
2	26.627(221)	26.238(114)	27.535(393)	26.796(228)	26.965(368)	26.012(148)*	25.574(167)	25.750(085)
3	26.833(225)	...	26.316(252)	...	26.751(269)	...	26.543(262)	...
4	27.354(217)	...	26.378(245)	...	25.896(130)	...	26.628(223)	...
5	27.289(283)	26.931(180)*	...	26.242(181)	26.792(209)	26.160(105)	26.636(135)	26.135(154)
6	...	26.529(128)	26.999(280)	26.442(153)	26.709(249)	25.796(142)*	...	26.241(139)
7	27.012(101)	...	26.937(181)	...	26.954(277)	...	26.483(107)	...
8	27.005(209)	...	27.278(334)	...	26.677(214)	...	26.730(248)	...
9	26.414(086)	...	26.900(233)	...	27.256(255)	...	25.924(130)	...
10	26.304(127)	...	27.180(266)	...	27.265(332)	...	26.061(151)	...
11	26.426(098)	...	26.348(174)	...	27.385(364)	...	26.103(095)	...
12	26.359(089)	...	26.308(097)	...	27.153(228)	...	26.501(174)	...
13	26.743(109)	26.483(131)	26.306(132)	26.080(155)	27.174(294)	26.681(220)*	26.186(149)	25.706(134)
14	26.778(129)	26.126(074)	26.535(124)	26.041(099)	27.111(266)	26.333(152)	26.188(132)	25.754(089)
15	26.759(200)	...	26.301(122)	...	26.446(099)	...	26.242(135)	...
16	26.910(122)	...	26.573(108)	...	26.742(212)	...	26.320(149)	...
17	27.266(252)	...	26.806(207)	...	26.351(146)	...	26.469(126)	...
18	27.273(150)	...	...	...	26.194(099)	...	26.640(218)	...
19	27.630(254)	26.684(180)	27.228(297)	26.922(331)	26.584(151)	25.946(101)	26.945(216)	26.357(153)
20	27.341(292)	26.751(183)	27.361(275)	26.912(205)	26.441(137)	26.113(147)	26.888(188)	26.171(197)
21	26.394(088)	...	27.622(356)	...	26.915(151)	...	26.318(149)	...
22	26.489(109)	...	27.123(273)	...	...	...	26.713(174)	...
23	26.674(172)	26.192(187)	26.603(201)	26.079(149)	27.276(280)	26.306(162)	26.030(107)	25.791(114)
24	26.521(100)	26.256(135)	26.210(148)	26.306(104)	27.118(374)	26.364(181)	26.182(153)	25.755(083)
25	26.723(213)	...	26.557(280)	...	...	...	26.353(215)	...
26	26.163(132)	...	26.956(209)	...	27.080(346)	...	26.341(161)	...
	<b>06737P = 25.46 d</b>		<b>34523P = 25.52 d</b>		<b>44606P = 25.84 d</b>		<b>48719P = 26.71 d</b>	
1	27.050(175)	26.533(152)	26.914(221)	26.315(135)	26.729(170)	26.484(175)	26.634(166)	25.954(126)
2	26.777(152)	26.638(175)	...	26.662(367)*	26.344(177)	26.601(177)	26.261(177)	25.903(110)
3	26.711(184)	...	26.367(200)	...	26.447(178)	...	26.186(191)	...
4	26.129(117)	...	26.188(159)	...	26.613(169)	...	26.553(235)	...
5	26.306(094)	25.957(078)	26.076(095)	25.989(084)	27.009(178)	26.784(248)	26.890(180)	25.998(109)
6	26.758(247)	26.093(080)	26.306(159)	25.782(138)	26.653(130)	26.418(130)	27.562(394)*	26.167(137)
7	27.053(155)	...	26.678(170)	...	27.134(162)	...	27.216(247)	...
8	26.661(092)	...	26.657(219)	...	26.464(146)	...	26.767(342)	...
9	27.102(199)	...	27.084(212)	...	27.065(219)	...	26.166(144)	...
10	27.320(196)	...	26.833(327)	...	27.159(191)	...	26.299(138)	...
11	27.498(212)	...	26.707(165)	...	26.486(154)	...	25.961(219)	...
12	27.512(246)	...	27.487(297)	...	26.619(112)	...	25.798(161)	...
13	27.047(209)	26.379(090)	27.209(310)	26.152(145)	25.837(059)	25.961(162)	26.128(116)	25.815(101)
14	26.951(154)	26.372(117)	26.963(316)	26.182(154)	25.846(070)	25.989(126)	26.267(148)	25.760(092)
15	27.351(221)	...	26.668(180)	...	26.083(071)	...	26.352(162)	...
16	27.072(176)	...	26.632(302)	...	25.816(090)	...	26.074(144)	...
17	26.830(129)	...	26.674(174)	...	26.319(086)	...	26.350(132)	...
18	27.190(196)	...	26.635(230)	...	26.197(096)	...	26.371(155)	...

Table 6—Continued

#	F555W	F814W	F555W	F814W	F555W	F814W	F555W	F814W
19	26.451(086)	25.861(081)	26.403(181)	25.941(140)	26.569(106)	26.500(160)	26.575(273)	25.853(137)
20	26.535(106)	26.038(078)	26.369(261)	25.779(091)	26.338(140)	26.347(164)	26.571(172)	25.909(113)
21	26.404(076)	...	26.390(124)	...	26.752(104)	...	26.839(183)	...
22	26.560(137)	...	26.270(194)	...	26.748(184)	...	26.705(173)	...
23	26.944(163)	26.216(155)	27.144(215)	26.127(158)	26.849(172)	26.055(150)	26.853(262)	26.246(233)
24	27.307(228)	26.360(086)	26.747(325)	25.992(219)	26.966(233)	27.248(267)*	27.049(288)	25.951(115)
25	26.516(161)	...	...	...	26.610(242)	...	26.503(211)	...
26	26.496(179)	...	26.609(213)	...	25.731(087)	...	26.743(225)	...
<b>55736P = 27.18 d</b>		<b>54039P = 27.65 d</b>		<b>41542P = 27.72 d</b>		<b>12340P = 27.84 d</b>		
1	26.689(145)	26.246(132)	26.191(116)	25.624(105)	26.548(237)	25.788(147)	26.047(147)	25.748(173)
2	27.067(180)	26.409(154)*	26.049(132)	25.529(076)	26.091(135)	25.803(119)	25.888(131)	25.770(130)
3	27.122(175)	...	26.922(295)	...	26.939(351)	...	26.033(241)	...
4	27.235(185)	...	26.517(117)	...	...	...	26.458(331)	...
5	26.473(084)	25.924(084)	27.491(373)	26.316(130)	25.941(136)	25.528(110)	26.378(216)	26.374(282)
6	26.366(202)	26.011(111)	27.547(248)	26.316(108)	25.939(090)	25.785(104)	26.838(308)	26.203(263)
7	26.533(079)	...	26.747(164)	...	26.179(160)	...	27.044(306)	...
8	26.545(095)	...	26.550(103)	...	26.121(179)	...	26.638(256)	...
9	26.900(159)	...	26.116(078)	...	26.538(201)	...	25.923(155)	...
10	26.979(136)	...	26.091(086)	...	26.423(143)	...	25.993(125)	...
11	26.874(114)	...	26.347(290)	...	26.634(165)	...	25.940(138)	...
12	26.612(106)	...	26.294(085)	...	26.487(250)	...	25.821(085)	...
13	26.964(185)	26.314(066)	26.423(119)	25.870(076)	26.419(142)	25.880(172)	25.928(124)	25.762(138)
14	27.174(195)	26.039(123)	26.064(098)	25.713(086)	26.715(173)	25.877(173)	26.068(152)	25.815(124)
15	27.059(220)	...	26.547(137)	...	26.733(272)	...	26.168(156)	...
16	26.957(121)	...	26.153(094)	...	26.645(155)	...	25.989(145)	...
17	27.111(185)	...	26.365(100)	...	27.139(331)	...	26.411(234)	...
18	27.159(172)	...	26.336(106)	...	26.585(220)	...	26.335(201)	...
19	27.179(172)	26.792(090)*	27.407(238)	26.149(110)	26.789(227)	25.941(130)	26.318(183)	26.792(090)*
20	27.205(147)	26.418(097)	26.690(119)	26.134(118)	26.695(252)	26.188(168)	26.502(214)	26.430(247)
21	26.453(081)	...	26.696(181)	...	26.208(115)	...	26.971(328)	...
22	26.375(126)	...	26.966(171)	...	26.108(149)	...	26.804(283)	...
23	26.548(097)	26.079(095)	26.273(106)	25.782(088)	26.319(158)	25.533(200)	...	26.539(326)
24	26.799(263)	25.985(089)	26.271(117)	25.926(067)	26.322(144)	25.704(102)	26.725(202)	26.564(304)
25	26.310(105)	...	26.988(311)	...	27.123(356)	...	26.213(258)	...
26	26.974(213)	...	26.342(157)	...	26.423(209)	...	26.174(250)	...
<b>52644P = 29.17 d</b>		<b>02343P = 29.62 d</b>		<b>23076P = 30.67 d</b>		<b>85974P = 30.86 d</b>		
1	27.333(193)*	26.185(092)	27.333(193)*	26.785(171)	27.518(360)	26.180(090)	26.158(120)	25.702(162)
2	26.851(157)	26.098(125)	27.113(292)	26.628(179)	26.752(274)	26.269(310)	25.871(125)	25.687(108)
3	26.047(134)	...	26.565(220)	...	26.253(134)	...	26.407(165)	...
4	25.825(058)	...	25.997(178)	...	26.238(137)	...	26.730(301)	...
5	26.255(078)	25.902(065)	26.932(194)	26.091(084)	26.653(145)	25.879(067)	26.624(138)	27.053(273)*
6	26.481(112)	25.698(132)	26.753(146)	25.794(127)	26.609(344)	26.006(190)	26.820(236)	26.240(120)
7	26.419(089)	...	26.794(147)	...	26.623(190)	...	26.674(174)	...
8	26.502(104)	...	26.640(167)	...	26.575(270)	...	26.656(235)	...
9	26.628(143)	...	26.750(145)	...	...	...	25.754(090)	...
10	26.644(112)	...	26.927(167)	...	27.382(317)	...	25.706(165)	...



Table 6—Continued

#	F555W	F814W	F555W	F814W	F555W	F814W	F555W	F814W
11	26.613(200)	...	27.129(220)	...	27.059(264)	...	25.451(111)	...
12	26.505(122)	...	27.214(230)	...	27.152(307)	...	25.748(139)	...
13	26.905(135)	26.089(093)	27.233(207)	27.036(193)*	27.034(215)	26.180(124)	26.127(148)	25.871(142)
14	26.718(104)	26.235(079)	26.855(219)	26.652(156)	26.644(172)	26.213(151)	26.027(167)	25.348(137)*
15	26.890(108)	...	26.632(132)	...	27.513(391)	...	26.157(086)	...
16	26.718(105)	...	26.396(090)	...	26.574(152)	...	25.870(140)	...
17	26.066(066)	...	25.804(101)	...	27.069(214)	...	26.250(200)	...
18	25.900(060)	...	25.758(066)	...	26.768(282)	...	26.482(133)	...
19	25.836(078)	25.502(060)	26.295(126)	25.899(089)	26.269(116)	26.568(172)*	26.690(167)	26.098(144)
20	25.844(073)	25.561(043)	26.367(150)	25.849(090)	26.303(120)	25.717(124)	26.622(195)	26.066(107)
21	26.150(071)	...	26.408(110)	...	26.554(156)	...	26.754(164)	...
22	26.309(126)	...	26.359(100)	...	26.155(125)	...	26.314(175)	...
23	26.477(103)	25.824(075)	26.512(149)	26.119(104)	26.712(395)	26.462(228)*	26.523(196)	26.038(208)
24	26.416(135)	25.787(086)	26.876(234)	25.958(137)	26.494(223)	26.072(165)	26.555(202)	26.346(176)
25	26.385(126)	...	26.220(134)	...	27.448(335)	...	25.804(208)	...
26	26.033(154)	...	26.945(236)	...	26.271(121)	...	...	...
	<b>07224P = 30.91 d</b>		<b>07255P = 31.16 d</b>		<b>50024P = 31.69 d</b>		<b>59151P = 32.62 d</b>	
1	26.148(115)	25.785(092)	26.495(215)	26.092(139)	27.409(329)	26.107(099)	26.200(190)	25.599(076)
2	26.274(111)	25.972(086)	26.488(176)	25.918(175)	26.909(175)	25.988(144)	26.298(149)	25.681(104)
3	26.828(205)	...	26.765(241)	...	26.759(212)	...	26.156(187)	...
4	27.385(302)	...	27.086(324)	...	26.637(190)	...	26.382(188)	...
5	26.965(242)	26.370(113)	26.257(152)	25.978(094)	26.299(061)	25.681(110)	25.839(088)	25.582(088)
6	27.813(288)	26.274(112)	26.475(108)	25.968(096)	26.236(094)	25.737(143)	25.620(188)	25.311(083)*
7	26.913(183)	...	26.192(118)	...	26.542(120)	...	25.738(095)	...
8	27.146(173)	...	26.081(108)	...	26.610(198)	...	25.672(128)	...
9	26.331(089)	...	26.355(114)	...	26.714(163)	...	25.686(144)	...
10	26.318(107)	...	26.485(114)	...	26.797(163)	...	25.664(130)	...
11	26.156(090)	...	26.519(163)	...	27.039(191)	...	26.192(107)	...
12	26.117(112)	...	26.539(164)	...	26.876(176)	...	25.999(113)	...
13	26.174(109)	25.857(079)	27.035(250)	25.989(108)	26.881(182)	25.909(115)	26.329(119)	25.690(096)
14	26.111(061)	25.834(081)	26.572(164)	26.004(100)	26.623(151)	25.813(134)	25.942(130)	25.513(072)
15	26.379(140)	...	26.776(232)	...	26.612(113)	...	26.128(122)	...
16	26.352(105)	...	26.894(223)	...	27.380(257)	...	25.984(113)	...
17	26.295(149)	...	26.896(267)	...	27.172(190)	...	26.456(091)	...
18	26.556(109)	...	26.872(308)	...	27.802(386)*	...	26.225(100)	...
19	26.771(121)	26.049(081)	27.067(250)	26.444(145)	27.206(178)	25.980(107)	26.628(170)	25.933(084)
20	27.610(236)	26.329(105)	27.325(287)	26.260(117)	27.521(280)	26.259(140)	26.659(131)	26.057(108)
21	27.378(238)	...	27.004(254)	...	26.657(142)	...	26.471(132)	...
22	27.412(195)	...	26.682(302)	...	26.704(151)	...	26.845(239)	...
23	27.500(266)	26.324(131)	26.157(126)	25.823(139)	26.112(138)	25.513(114)	25.853(076)	25.697(069)
24	27.820(314)	26.469(133)	26.294(110)	25.791(137)	26.418(119)	25.497(111)	25.824(100)	25.598(138)
25	26.842(274)	...	26.170(142)	...	26.266(130)	...	26.233(141)	...
26	26.820(276)	...	...	...	26.846(223)	...	25.643(083)	...
	<b>60583P = 32.95 d</b>		<b>04322P = 33.26 d</b>		<b>30349P = 33.51 d</b>		<b>03108P = 33.71 d</b>	
1	26.639(189)	25.974(111)	26.847(211)	26.037(101)	26.621(250)	26.222(213)	26.758(134)	26.192(103)
2	26.968(248)	...	26.521(105)	25.904(116)	26.775(273)	26.057(185)	26.859(168)	26.205(114)

Table 6—Continued

#	F555W	F814W	F555W	F814W	F555W	F814W	F555W	F814W
3	26.627(345)	...	25.701(079)	...	25.930(159)	...	26.172(118)	...
4	26.083(123)	...	25.812(072)	...	26.238(186)	...	25.922(086)	...
5	27.005(349)	25.806(113)	26.185(109)	25.619(084)	26.423(197)	25.861(159)	26.863(166)	25.804(096)
6	27.470(385)	25.616(109)	26.002(094)	25.582(098)	26.436(176)	25.982(178)	26.455(094)	25.617(061)
7	26.979(212)	...	26.199(119)	...	26.651(214)	...	26.398(134)	...
8	...	...	25.836(104)	...	26.587(210)	...	26.538(166)	...
9	27.276(231)	...	26.246(090)	...	26.714(216)	...	27.005(204)	...
10	26.781(192)	...	26.211(122)	...	26.301(144)	...	26.649(130)	...
11	26.853(201)	...	26.443(104)	...	26.824(228)	...	26.498(150)	...
12	27.482(352)	...	26.544(120)	...	26.909(210)	...	26.857(157)	...
13	26.599(166)	26.250(174)	26.541(186)	26.021(097)	26.751(226)	26.133(179)	26.981(140)	26.006(130)
14	27.271(351)	26.082(182)	26.520(131)	25.847(084)	...	26.352(172)	26.667(145)	25.748(125)
15	27.160(235)	...	26.703(151)	...	26.640(278)	...	26.737(153)	...
16	26.786(283)	...	26.339(147)	...	...	...	26.701(177)	...
17	25.903(101)	...	26.980(206)	...	26.700(183)	...	26.574(161)	...
18	25.807(092)	...	26.786(103)	...	27.232(389)	...	26.521(091)	...
19	26.021(110)	25.405(116)	26.443(113)	25.961(104)	25.780(142)	25.574(128)	26.092(103)	25.557(082)
20	26.219(143)	25.578(144)	26.600(200)	25.973(115)	26.203(142)	25.976(157)*	25.986(138)	25.711(091)
21	26.321(133)	...	25.672(086)	...	25.965(184)	...	25.983(074)	...
22	26.075(126)	...	25.607(047)	...	26.316(149)	...	26.247(089)	...
23	26.744(213)	25.710(078)	25.776(083)	25.321(079)*	26.765(218)	26.044(124)	26.758(195)	25.889(143)
24	26.256(148)	25.747(125)	25.852(090)	25.503(084)	26.143(169)	26.350(260)*	26.513(132)	25.744(090)
25	27.017(381)	...	26.398(134)	...	26.643(231)	...	26.457(153)	...
26	26.596(205)	...	25.660(103)	...	25.818(127)	...	25.848(091)	...
	<b>09099P = 33.74 d</b>		<b>30771P = 33.75 d</b>		<b>14063P = 34.08 d</b>		<b>59846P = 35.12 d</b>	
1	26.140(148)	25.794(139)	27.290(194)	26.421(175)	25.971(119)	25.323(165)	26.360(152)	25.806(144)
2	26.406(250)	25.960(175)	27.206(221)	26.252(132)	25.928(168)	25.762(155)	26.508(183)	25.643(125)
3	26.725(395)	...	26.370(245)	...	25.800(188)	...	...	...
4	...	...	26.284(115)	...	25.941(111)	...	26.695(306)	...
5	26.786(243)	26.506(266)*	26.717(188)	26.112(170)	26.288(164)	25.856(173)	25.869(178)	25.598(108)
6	26.422(231)	26.064(172)	26.517(141)	25.844(143)	26.321(369)	25.753(112)	26.046(154)	25.516(102)
7	26.854(200)	...	27.031(199)	...	27.037(261)	...	25.862(116)	...
8	26.618(186)	...	26.925(176)	...	26.270(166)	...	25.711(083)	...
9	26.405(237)	...	26.942(223)	...	26.486(212)	...	26.076(108)	...
10	26.236(163)	...	26.407(169)	...	26.781(293)	...	26.080(147)	...
11	26.070(139)	...	27.308(236)	...	26.488(214)	...	26.170(142)	...
12	25.955(133)	...	26.980(197)	...	26.734(240)	...	26.278(200)	...
13	25.957(105)	25.761(138)	...	26.524(162)	26.525(271)	25.891(114)	26.403(164)	25.661(124)
14	26.352(199)	25.741(140)	27.347(166)	26.216(159)	26.943(302)	26.126(210)	25.873(116)	25.740(133)
15	26.189(126)	...	26.970(307)	...	26.012(145)	...	26.241(115)	...
16	25.921(161)	...	26.681(225)	...	26.198(167)	...	26.025(099)	...
17	26.408(159)	...	...	...	25.610(128)	...	26.597(223)	...
18	26.214(206)	...	27.438(218)	...	25.676(090)	...	26.414(182)	...
19	26.198(184)	25.901(173)	26.161(067)	26.011(134)	25.911(132)	25.377(076)	26.871(261)	25.855(155)
20	26.169(151)	26.164(195)	26.301(106)	25.785(115)	25.761(092)	25.404(093)	26.500(185)	25.910(160)
21	26.793(280)	...	26.174(079)	...	25.930(159)	...	26.784(232)	...

Table 6—Continued

#	F555W	F814W	F555W	F814W	F555W	F814W	F555W	F814W
22	26.594(238)	...	26.465(121)	...	26.005(143)	...	26.740(225)	...
23	26.694(247)	25.973(161)	26.408(088)	26.009(119)	25.990(150)	25.593(150)	25.982(112)	25.374(110)
24	27.180(376)	26.504(196)*	26.819(210)	25.847(091)	26.119(176)	25.472(088)	25.913(167)	25.305(093)
25	...	...	26.950(231)	...	26.300(188)	...	26.241(231)	...
26	26.347(225)	...	26.603(231)	...	25.749(139)	...	25.762(194)	...
	<b>31655P = 35.83 d</b>		<b>07868P = 36.17 d</b>		<b>69637P = 37.23 d</b>		<b>41024P = 38.63 d</b>	
1	25.836(092)	25.331(080)	27.187(303)	26.410(114)	25.915(184)	25.298(120)	26.011(126)	25.619(095)
2	25.658(075)	25.056(093)*	26.607(154)	26.188(146)	25.321(079)	25.378(091)	26.147(123)	25.703(122)
3	26.120(134)	...	26.249(138)	...	25.488(146)	...	26.524(210)	...
4	26.074(099)	...	26.181(105)	...	25.932(232)	...	26.986(399)	...
5	26.237(078)	25.677(092)	26.375(116)	25.894(148)	26.158(186)	25.294(100)	26.605(168)	26.271(199)
6	26.404(147)	25.681(073)	26.438(133)	25.918(106)	26.430(172)	25.360(158)	27.239(276)	26.285(204)
7	26.187(088)	...	26.978(175)	...	26.273(177)	...	...	...
8	26.039(109)	...	26.508(147)	...	26.057(200)	...	26.282(172)	...
9	25.781(071)	...	26.724(126)	...	26.469(370)	...	25.998(157)	...
10	25.988(095)	...	26.707(162)	...	26.538(274)	...	26.115(154)	...
11	25.766(094)	...	27.319(160)	...	26.138(154)	...	25.795(121)	...
12	25.844(067)	...	26.880(138)	...	26.058(169)	...	25.909(115)	...
13	25.873(086)	25.438(052)	27.027(178)	26.179(122)	26.450(250)	25.646(128)	25.923(108)	25.788(185)
14	25.941(135)	25.482(091)	26.856(118)	26.033(121)	26.110(152)	25.726(164)	25.894(129)	25.708(139)
15	25.698(086)	...	26.984(134)	...	26.785(338)	...	26.001(156)	...
16	25.696(060)	...	26.913(176)	...	26.144(113)	...	25.997(120)	...
17	25.867(083)	...	27.042(167)	...	26.390(181)	...	25.860(086)	...
18	25.780(106)	...	27.062(205)	...	26.098(196)	...	26.229(165)	...
19	25.898(116)	25.323(084)	26.861(194)	26.208(102)	25.765(097)	25.281(126)	26.015(156)	25.867(149)
20	25.945(051)	25.565(064)	26.683(159)	26.083(096)	25.748(128)	25.230(096)	26.246(149)	26.186(181)
21	25.944(112)	...	26.254(106)	...	25.842(098)	...	26.748(272)	...
22	26.044(086)	...	26.189(114)	...	25.645(164)	...	26.770(257)	...
23	26.088(148)	25.540(071)	26.788(130)	25.852(073)	25.990(187)	25.241(135)	26.789(257)	26.456(215)
24	26.224(117)	25.632(101)	26.257(111)	25.758(101)	25.958(184)	25.375(115)	26.860(281)	26.736(286)*
25	25.695(092)	...	26.995(316)	...	...	...	26.226(176)	...
26	26.475(235)	...	26.022(152)	...	25.885(174)	...	...	...
	<b>34163P = 39.34 d</b>		<b>07989P = 39.42 d</b>		<b>44069P = 39.90 d</b>		<b>27980P = 39.92 d</b>	
1	26.427(188)	25.711(108)	26.517(139)	25.983(166)	26.566(196)	26.075(132)	26.737(129)	25.678(087)
2	26.267(168)	25.606(091)	26.413(197)	25.795(108)	26.243(125)	25.854(245)	26.322(221)	25.614(175)
3	26.671(215)	...	27.221(364)	...	26.015(138)	...	26.666(152)	...
4	26.471(206)	...	27.133(267)	...	26.066(139)	...	27.836(375)	...
5	25.812(113)	25.343(080)	...	26.162(113)	26.507(143)	25.823(106)	26.172(134)	25.584(086)
6	25.508(096)	25.278(089)	...	26.337(091)	26.156(290)	25.752(117)	26.707(234)	25.644(136)
7	25.847(082)	...	27.187(203)	...	26.657(150)	...	25.966(103)	...
8	25.686(110)	...	27.314(271)	...	26.105(133)	...	25.595(079)	...
9	25.920(141)	...	27.009(283)	...	26.540(215)	...	26.027(090)	...
10	25.951(117)	...	26.981(149)	...	26.654(225)	...	26.053(094)	...
11	25.958(128)	...	26.542(169)	...	26.743(265)	...	26.157(071)	...
12	26.268(189)	...	26.579(139)	...	27.028(315)	...	26.143(140)	...
13	26.260(159)	25.546(145)	26.540(135)	25.657(086)	26.910(295)	26.668(172)*	26.180(104)	25.530(076)

Table 6—Continued

#	F555W	F814W	F555W	F814W	F555W	F814W	F555W	F814W
14	25.998(166)	25.300(085)	26.642(136)	25.816(090)	26.535(219)	26.081(123)	26.342(179)	25.395(112)
15	25.971(098)	...	26.399(097)	...	26.767(185)	...	26.425(127)	...
16	25.897(117)	...	26.856(204)	...	26.318(151)	...	26.448(109)	...
17	26.620(234)	...	26.366(152)	...	26.939(278)	...	26.782(131)	...
18	26.068(182)	...	26.482(130)	...	26.376(200)	...	26.320(141)	...
19	26.277(116)	25.749(104)	26.481(125)	25.992(103)	26.262(125)	25.743(079)	26.518(177)	25.638(071)
20	26.201(187)	25.739(098)	26.814(237)	25.933(086)	26.018(106)	25.417(182)*	26.752(153)	25.648(105)
21	26.655(191)	...	26.635(167)	...	25.870(076)	...	27.060(216)	...
22	26.194(123)	...	26.815(130)	...	25.689(068)	...	26.706(154)	...
23	25.904(188)	25.535(131)	27.008(200)	26.150(160)	25.912(115)	25.774(112)	27.373(305)	25.919(106)
24	26.195(113)	25.672(119)	26.896(194)	26.321(095)	25.822(121)	25.478(067)	27.434(380)	25.924(140)
25	26.055(328)	...	26.283(113)	...	26.431(191)	...	26.145(131)	...
26	26.383(207)	...	27.072(286)	...	25.789(115)	...	26.670(232)	...
	<b>52975P = 40.52 d</b>		<b>07994P = 40.69 d</b>		<b>01166P = 41.11 d</b>		<b>76534P = 41.86 d</b>	
1	26.361(109)	25.699(148)	26.870(249)	25.585(117)	26.677(130)	25.601(101)	26.319(262)	25.836(166)
2	26.341(128)	25.875(100)	26.592(152)	25.653(113)	26.602(095)	25.543(084)	26.052(272)	25.215(143)*
3	26.759(175)	...	...	...	27.001(237)	...	26.463(286)	...
4	26.900(200)	...	27.268(394)	...	26.626(096)	...	...	...
5	27.122(141)	26.400(149)	26.028(084)	25.651(073)	26.994(186)	25.969(090)	26.159(249)	25.821(169)
6	26.980(218)	26.393(105)	26.303(099)	25.670(095)	27.684(295)	26.019(099)	26.477(387)	26.154(216)*
7	27.459(301)	...	25.764(093)	...	27.149(189)	...	25.816(257)	...
8	27.305(243)	...	25.927(069)	...	27.316(175)	...	26.066(210)	...
9	26.879(165)	...	25.870(113)	...	27.332(266)	...	25.773(136)	...
10	...	...	25.927(109)	...	27.035(150)	...	25.641(185)	...
11	26.990(155)	...	25.895(116)	...	27.197(139)	...	25.917(228)	...
12	26.630(146)	...	25.954(089)	...	27.069(142)	...	25.890(244)	...
13	26.433(121)	25.832(112)	26.032(076)	25.376(076)	26.936(126)	25.959(090)	25.876(149)	25.457(123)
14	26.245(126)	25.654(091)	26.130(107)	25.445(092)	26.834(133)	25.945(115)	25.561(161)	25.266(116)
15	26.268(097)	...	26.295(118)	...	26.542(100)	...	25.748(183)	...
16	26.163(080)	...	25.941(066)	...	26.617(129)	...	25.506(118)	...
17	26.387(142)	...	26.380(154)	...	26.269(088)	...	25.901(143)	...
18	26.213(072)	...	25.990(125)	...	26.309(067)	...	26.003(211)	...
19	26.516(133)	25.856(111)	26.392(160)	25.671(083)	26.470(112)	25.758(066)	26.126(204)	25.470(115)
20	26.879(129)	26.107(088)	26.344(092)	25.466(106)	26.574(085)	25.701(084)	26.145(199)	25.587(142)
21	26.522(147)	...	26.545(133)	...	26.560(095)	...	26.143(196)	...
22	26.599(132)	...	26.523(118)	...	26.535(119)	...	26.213(182)	...
23	26.572(171)	26.530(197)	26.703(217)	25.994(125)	26.815(178)	25.777(108)	26.363(341)	25.337(131)*
24	26.817(143)	26.403(125)	26.861(155)	26.107(095)	26.629(112)	25.852(081)	26.854(365)	25.692(221)
25	27.328(310)	...	25.928(092)	...	26.649(189)	...	26.232(378)	...
26	...	...	...	...	26.437(220)	...	25.550(222)	...
	<b>22918P = 42.03 d</b>		<b>02032P = 42.54 d</b>		<b>48747P = 42.68 d</b>		<b>67393P = 42.74 d</b>	
1	26.146(115)	25.443(072)	25.570(099)	25.066(088)	27.048(334)	25.967(140)	26.453(277)	25.409(168)
2	26.155(137)	25.448(082)	25.495(091)	25.043(071)	26.934(187)	25.792(128)	26.365(266)	25.330(158)
3	26.523(181)	...	26.016(205)	...	27.115(223)	...	25.575(119)	...
4	27.023(367)	...	25.968(106)	...	...	...	25.409(145)	...
5	25.503(062)	25.185(092)	26.236(127)	25.303(074)	26.153(090)	25.862(107)	25.614(105)	25.076(143)

Table 6—Continued

#	F555W	F814W	F555W	F814W	F555W	F814W	F555W	F814W
6	25.883(172)	25.343(071)	26.096(139)	25.408(061)	26.397(091)	25.761(095)	25.573(130)	25.151(128)
7	25.629(070)	...	25.850(105)	...	26.420(120)	...	25.939(126)	...
8	25.631(103)	...	26.104(077)	...	25.898(113)	...	26.076(228)	...
9	26.290(198)	...	26.304(139)	...	26.714(137)	...	26.373(247)	...
10	25.770(088)	...	26.356(124)	...	26.118(210)	...	25.943(176)	...
11	25.792(126)	...	26.455(110)	...	26.532(173)	...	26.079(133)	...
12	26.015(118)	...	26.707(123)	...	26.269(111)	...	26.222(216)	...
13	25.769(101)	25.140(089)	26.752(137)	25.561(071)	26.431(108)	25.730(123)	25.458(174)*	25.394(150)
14	25.890(081)	25.381(078)	26.609(109)	25.632(062)	26.265(081)	25.708(059)	25.959(144)	25.242(140)
15	25.836(109)	...	26.269(122)	...	26.464(122)	...	26.173(199)	...
16	25.885(121)	...	26.436(097)	...	26.218(114)	...	26.114(199)	...
17	25.963(092)	...	25.714(101)	...	26.720(258)	...	25.952(157)	...
18	26.295(125)	...	25.535(103)	...	26.712(105)	...	26.206(182)	...
19	26.411(179)	25.545(091)	25.889(197)	25.194(049)	26.967(328)	25.932(089)	26.333(349)	25.436(199)
20	26.303(149)	25.601(089)	25.351(080)	25.084(072)	26.927(179)	26.056(086)	26.342(187)	25.459(145)
21	26.512(162)	...	25.592(100)	...	27.328(296)	...	26.208(213)	...
22	26.484(142)	...	25.552(037)	...	...	...	26.246(210)	...
23	27.061(336)	25.905(130)	25.705(118)	25.199(076)	27.107(319)	26.573(206)	25.565(144)	25.047(129)
24	26.656(257)	25.721(090)	25.677(068)	25.191(074)	27.345(297)	26.397(153)	25.458(130)	25.171(127)
25	26.600(288)	...	25.529(067)	...	26.790(197)	...	26.322(256)	...
26	25.744(075)	...	26.274(124)	...	26.474(195)	...	25.796(187)	...
	<b>58298P = 43.53 d</b>		<b>07331P = 44.59 d</b>		<b>02979P = 44.91 d</b>		<b>01732P = 45.00 d</b>	
1	26.495(216)	25.602(107)	25.252(102)	25.228(127)	25.705(085)	25.003(066)	25.371(112)	25.001(075)
2	26.333(099)	25.690(157)	25.528(090)	25.331(113)	25.733(108)	25.112(063)	25.228(079)	24.767(099)
3	25.928(149)	...	25.886(196)	...	26.120(204)	...	25.843(109)	...
4	26.039(062)	...	25.648(130)	...	25.834(131)	...	25.648(080)	...
5	25.703(165)	25.288(146)	25.603(181)	25.236(106)	26.245(129)	25.527(095)	25.828(087)	25.168(068)
6	25.758(083)	25.244(102)	25.993(147)	25.225(162)	26.460(311)	25.441(055)	25.775(138)	25.125(091)
7	25.775(105)	...	25.681(119)	...	26.230(091)	...	25.764(072)	...
8	25.859(079)	...	25.965(150)	...	26.169(095)	...	25.711(118)	...
9	25.923(096)	...	26.622(320)*	...	26.259(106)	...	25.885(084)	...
10	25.844(099)	...	26.008(147)	...	26.319(126)	...	25.744(082)	...
11	26.091(124)	...	25.782(127)	...	26.430(122)	...	25.863(073)	...
12	25.943(070)	...	26.526(218)*	...	26.388(182)	...	25.947(078)	...
13	25.990(100)	25.311(056)	25.945(092)	25.532(126)	26.356(112)	25.593(087)	25.918(076)	25.281(047)
14	25.931(072)	25.341(085)	26.207(136)	25.961(126)*	26.283(080)	25.559(055)	25.748(124)	25.131(083)
15	26.078(094)	...	26.205(135)	...	25.976(089)	...	25.844(048)	...
16	26.374(110)	...	26.099(146)	...	26.095(081)	...	25.708(070)	...
17	26.107(153)	...	26.116(100)	...	25.581(097)	...	25.780(075)	...
18	26.184(085)	...	26.210(120)	...	25.519(081)	...	25.824(106)	...
19	26.492(110)	25.653(056)	25.406(188)	25.554(116)	25.444(064)	25.015(033)	25.546(064)	25.092(046)
20	26.535(121)	25.622(090)	25.766(093)	25.494(082)	25.538(093)	25.084(058)	25.345(091)	24.890(104)
21	26.445(124)	...	25.255(097)	...	25.618(056)	...	25.371(053)	...
22	26.664(111)	...	25.513(083)	...	25.506(043)	...	25.356(095)	...
23	26.607(233)	25.871(130)	26.630(202)*	25.297(139)	25.678(058)	25.090(048)	25.527(064)	24.931(057)
24	26.561(158)	25.965(117)	25.562(071)	25.330(132)	25.684(079)	25.206(073)	25.383(073)	24.844(071)

Table 6—Continued

#	F555W	F814W	F555W	F814W	F555W	F814W	F555W	F814W
25	26.278(229)	...	26.021(162)	...	26.378(130)	...	25.720(103)	...
26	26.465(221)	...	25.577(091)	...	25.318(087)	...	25.576(088)	...
	<b>19368P = 45.25 d</b>		<b>49584P = 45.67 d</b>		<b>16143P = 46.74 d</b>		<b>15346P = 46.85 d</b>	
1	26.320(180)	25.378(127)	26.172(218)	25.415(119)	25.992(141)	25.301(115)	26.400(184)	25.581(123)
2	26.381(130)	25.631(094)	26.067(132)	25.571(094)	25.915(077)	25.171(066)*	26.489(178)	25.412(092)
3	26.163(168)	...	26.400(205)	...	26.132(136)	...	25.694(163)	...
4	26.807(207)*	...	26.484(170)	...	26.346(119)	...	25.865(127)	...
5	25.693(131)	25.269(110)	26.577(211)	25.822(154)	26.322(116)	25.434(086)	25.731(132)	25.148(102)*
6	26.067(120)	25.364(086)	26.667(187)	25.882(141)	26.314(149)	25.549(083)	26.281(206)*	25.382(090)
7	25.731(088)	...	26.447(153)	...	26.530(202)	...	25.743(086)	...
8	25.818(091)	...	26.336(159)	...	26.519(124)	...	25.680(073)	...
9	25.674(083)	...	26.717(262)	...	26.700(211)	...	25.891(163)	...
10	25.720(078)	...	26.444(131)	...	26.607(120)	...	26.002(102)	...
11	25.598(110)	...	26.546(167)	...	26.597(195)	...	25.887(111)	...
12	25.841(120)	...	26.833(170)	...	26.334(170)	...	26.094(135)	...
13	25.568(081)	25.135(107)	26.201(127)	25.801(112)	26.746(199)	25.310(071)*	25.860(149)	25.237(088)*
14	25.665(060)	25.216(102)	26.349(172)	25.803(105)	26.767(179)	25.731(089)	26.012(106)	25.508(072)
15	25.432(095)	...	25.956(092)	...	26.681(166)	...	25.793(157)	...
16	25.788(085)	...	26.183(105)	...	26.870(179)	...	26.149(126)	...
17	25.679(112)	...	25.833(114)	...	26.584(164)	...	26.084(133)	...
18	25.942(086)	...	25.895(083)	...	26.927(134)	...	26.166(156)	...
19	25.885(147)	25.202(109)	25.790(098)	25.298(091)	26.831(171)	25.640(119)	26.335(133)	25.654(100)
20	26.093(114)	25.181(102)	25.968(080)	25.474(080)	26.717(195)	25.904(095)	26.400(171)	25.672(094)
21	26.054(101)	...	26.086(113)	...	26.314(116)	...	26.476(134)	...
22	26.132(096)	...	26.045(083)	...	26.788(247)	...	26.806(212)	...
23	26.338(147)	25.461(126)	26.186(104)	25.362(067)	26.137(100)	25.110(122)*	25.973(111)	25.501(100)
24	26.469(146)	25.556(130)	26.455(166)	25.331(120)	26.084(086)	25.368(054)	25.985(072)	25.500(106)
25	25.936(141)	...	...	...	25.991(174)	...	26.026(108)	...
26	25.829(139)	...	25.998(093)	...	26.985(215)	...	25.835(143)	...
	<b>54502P = 47.14 d</b>		<b>59642P = 47.39 d</b>		<b>52566P = 47.42 d</b>		<b>52170P = 47.99 d</b>	
1	26.998(240)	26.000(097)	25.399(081)	25.305(105)	26.028(126)	25.623(070)	26.131(092)	25.338(070)
2	26.922(207)	25.971(114)	25.705(091)	25.256(113)	26.036(110)	25.547(094)	26.197(073)	25.301(062)
3	26.101(130)	...	25.988(174)	...	26.350(182)	...	26.371(172)	...
4	26.207(125)	...	26.080(175)	...	26.619(233)	...	26.512(148)	...
5	25.912(076)	25.334(061)	25.805(101)	25.434(148)	26.161(108)	25.996(105)	26.737(269)	25.642(073)
6	25.775(125)	25.392(097)	26.188(201)	25.606(116)	26.291(129)	25.822(086)	26.533(112)	25.571(086)
7	26.200(101)	...	25.999(103)	...	25.892(090)	...	26.710(145)	...
8	25.772(160)	...	25.888(106)	...	25.936(090)	...	26.765(137)	...
9	26.152(096)	...	26.283(147)	...	25.569(080)	...	27.124(250)	...
10	26.629(161)	...	25.818(105)	...	25.547(068)	...	26.935(156)	...
11	26.263(097)	...	26.128(154)	...	25.839(099)	...	26.908(200)	...
12	26.271(112)	...	26.250(214)	...	25.741(111)	...	26.859(115)	...
13	26.157(073)	25.595(078)	26.145(108)	25.865(137)	25.835(084)	25.425(054)	26.653(118)	25.680(110)
14	26.509(248)	25.492(085)	26.260(174)	26.076(142)*	25.604(104)	25.438(071)	26.558(112)	25.682(062)
15	26.456(120)	...	26.398(197)	...	25.829(093)	...	26.478(098)	...
16	26.446(146)	...	26.206(140)	...	25.859(114)	...	26.199(072)	...

Table 6—Continued

#	F555W	F814W	F555W	F814W	F555W	F814W	F555W	F814W
17	26.483(100)	...	26.188(152)	...	25.897(117)	...	26.094(121)	...
18	26.319(145)	...	25.931(113)	...	25.765(113)	...	26.017(108)	...
19	26.698(199)	25.701(068)	25.445(111)	25.205(081)	26.132(126)	25.534(065)	26.058(098)	25.344(071)
20	27.248(340)	25.894(095)	25.500(103)	25.367(076)	25.806(084)	25.500(070)	26.037(075)	25.057(111)*
21	27.133(156)	...	25.502(094)	...	26.116(098)	...	25.843(076)	...
22	27.249(316)	...	25.380(079)	...	26.104(132)	...	26.054(055)	...
23	26.910(236)	25.937(115)	25.815(136)	25.309(147)	26.345(140)	25.864(091)	25.967(172)	25.378(119)
24	27.028(200)	26.146(164)	25.426(140)	25.346(099)	26.190(116)	25.903(113)	26.112(090)	25.340(082)
25	26.944(209)	...	25.553(083)	...	26.307(150)	...	26.030(126)	...
26	25.956(087)	...	25.812(142)	...	26.431(171)	...	26.373(141)	...
	<b>04882P = 48.92 d</b>		<b>68817P = 49.93 d</b>		<b>15318P = 51.46 d</b>		<b>71911P = 51.99 d</b>	
1	26.580(212)	25.925(137)	25.861(155)	25.719(170)*	25.737(075)	25.333(078)	25.290(117)	24.699(107)*
2	27.448(367)*	26.166(111)*	25.851(155)	25.428(111)	25.662(069)	25.081(062)	25.049(099)*	24.873(113)
3	25.940(140)	...	25.592(160)	...	25.592(105)	...	25.493(107)	...
4	25.927(078)	...	25.794(189)	...	25.599(073)	...	25.385(097)	...
5	25.943(108)	25.452(077)	25.993(106)	25.779(135)	25.972(118)	25.331(085)	25.399(092)	24.834(105)
6	...	25.470(069)	26.078(197)	25.611(101)	25.911(069)	25.167(061)	25.742(139)	25.010(094)
7	25.960(112)	...	26.120(115)	...	25.955(077)	...	25.466(074)	...
8	26.544(250)	...	25.926(104)	...	25.824(142)	...	25.789(133)	...
9	26.204(118)	...	25.388(166)*	...	26.144(065)	...	25.707(141)	...
10	26.321(127)	...	25.711(125)*	...	26.177(101)	...	25.625(104)	...
11	26.473(118)	...	26.220(175)	...	26.206(101)	...	25.840(097)	...
12	26.611(127)	...	26.421(232)	...	26.026(078)	...	25.783(114)	...
13	26.198(164)	25.582(092)	26.505(202)	25.682(155)	26.150(082)	25.535(091)	25.771(109)	24.973(104)
14	26.423(114)	25.645(060)	26.540(204)	25.784(153)	26.158(086)	25.191(064)*	25.668(118)	25.074(098)
15	26.315(137)	...	26.461(141)	...	26.166(072)	...	25.766(074)	...
16	26.514(120)	...	26.080(144)	...	26.282(090)	...	25.845(125)	...
17	26.362(149)	...	26.412(194)	...	26.497(128)	...	25.642(102)	...
18	26.208(161)	...	26.332(146)	...	26.401(101)	...	25.720(111)	...
19	...	25.849(101)	26.039(136)	25.635(127)	26.710(125)	25.791(101)	25.912(164)	25.240(088)
20	26.844(121)	25.925(077)	26.056(089)	25.600(163)	26.545(147)	25.833(091)	25.841(088)	25.149(120)
21	26.697(126)	...	25.690(121)	...	26.387(089)	...	25.725(134)	...
22	26.836(135)	...	25.872(115)	...	26.459(167)	...	25.699(094)	...
23	25.813(079)	25.494(070)	25.586(178)	25.369(116)	25.544(064)	25.217(077)	25.402(108)	24.945(105)
24	25.905(076)	25.457(076)	25.544(069)	25.476(110)	25.627(063)	25.107(066)	25.421(070)	24.896(091)
25	26.599(138)	...	26.136(189)	...	25.626(087)	...	25.419(097)	...
26	25.838(091)	...	25.766(160)	...	26.045(153)	...	25.734(125)	...
	<b>28132P = 52.24 d</b>		<b>06581P = 58.98 d</b>		<b>25965P = 59.02 d</b>		<b>06542P = 59.13 d</b>	
1	26.453(175)	25.354(126)	27.137(286)	26.085(188)	25.895(182)	25.408(125)	26.177(110)	25.233(064)
2	26.540(213)	25.731(077)*	26.164(199)	25.765(118)	25.791(131)	25.450(095)	26.138(097)	25.211(048)
3	26.758(212)	...	26.246(205)	...	25.785(214)	...	26.141(174)	...
4	26.505(250)	...	25.630(115)	...	25.925(162)	...	26.171(115)	...
5	26.330(121)	25.325(068)	26.116(122)	25.582(155)	26.189(235)	25.680(128)	26.181(084)	25.589(113)*
6	26.480(162)	25.443(112)	25.822(292)	25.019(064)*	26.201(167)	25.851(148)	26.444(151)	25.492(122)
7	26.211(118)	...	25.800(075)	...	26.378(192)	...	26.233(080)	...
8	25.737(110)	...	25.875(056)	...	26.465(245)	...	26.257(113)	...

Table 6—Continued

#	F555W	F814W	F555W	F814W	F555W	F814W	F555W	F814W
9	25.935(123)	...	25.636(130)	...	26.295(207)	...	25.709(102)	...
10	25.858(096)	...	25.933(090)	...	26.360(259)	...	25.960(063)	...
11	25.988(089)	...	26.387(189)	...	26.437(226)	...	25.965(066)	...
12	25.891(105)	...	25.971(106)	...	26.486(288)	...	25.959(070)	...
13	25.964(078)	25.325(068)	26.467(141)	25.645(140)	26.179(204)	25.632(128)	25.852(074)	25.193(049)
14	25.985(082)	25.243(078)	26.128(135)	25.303(101)	25.737(182)	25.785(143)	25.743(090)	25.207(070)
15	26.037(115)	...	26.371(217)	...	25.906(132)	...	25.766(057)	...
16	25.969(109)	...	25.857(133)	...	26.057(156)	...	25.651(076)	...
17	26.005(109)	...	26.665(168)	...	25.772(117)	...	25.627(102)	...
18	25.973(098)	...	26.159(075)	...	25.598(081)	...	25.704(054)	...
19	26.047(163)	25.330(070)	26.185(138)	25.716(154)	25.800(134)	25.397(109)	25.709(062)	25.078(048)
20	26.181(120)	25.433(093)	26.515(130)	25.468(080)	25.728(172)	25.233(107)	25.724(084)	25.087(062)
21	26.453(108)	...	26.669(237)	...	25.717(120)	...	25.706(104)	...
22	26.046(103)	...	26.544(094)	...	25.752(140)	...	25.759(082)	...
23	26.194(106)	25.481(120)	26.892(208)	25.620(115)	25.710(099)	25.386(112)	25.939(049)	25.103(058)
24	26.294(175)	25.465(114)	26.857(179)	26.036(109)	25.936(193)	25.262(171)	25.993(081)	25.046(066)
25	26.817(279)	...	25.652(076)	...	26.052(185)	...	26.222(110)	...
26	25.874(165)	...	26.229(132)	...	26.017(212)	...	25.790(103)	...
	<b>53187P = 59.75 d</b>		<b>69494P = 60.18 d</b>		<b>02647P = 60.68 d</b>		<b>17049P = 61.25 d</b>	
1	25.912(111)	25.775(091)	25.823(113)	25.576(073)	25.553(061)	24.792(082)	25.438(085)	24.751(062)
2	25.989(117)	25.536(074)	25.975(098)	25.473(064)	25.834(084)	24.975(076)	25.272(089)	24.742(098)
3	26.133(162)	...	25.927(182)	...	25.814(169)	...	25.050(128)*	...
4	26.101(157)	...	26.413(192)	...	25.819(117)	...	25.582(128)	...
5	25.996(106)	25.696(096)	26.471(190)	25.465(111)	25.916(102)	25.170(099)	25.438(109)	24.956(074)
6	26.249(170)	25.688(095)	26.784(190)	25.677(100)	26.774(308)*	25.434(054)*	25.716(127)	24.879(098)
7	26.418(184)	...	26.550(132)	...	26.089(077)	...	25.618(100)	...
8	26.476(184)	...	26.415(123)	...	26.559(143)	...	25.639(123)	...
9	26.450(157)	...	26.434(156)	...	26.145(108)	...	25.635(112)	...
10	26.367(116)	...	26.502(190)	...	26.316(128)	...	25.554(102)	...
11	26.922(191)*	...	26.752(211)	...	26.208(149)	...	25.554(103)	...
12	26.589(213)	...	26.706(298)	...	26.056(126)	...	26.028(122)	...
13	26.512(160)	26.112(131)	26.666(204)	25.806(116)	25.980(106)	25.228(075)	25.599(079)	25.128(108)
14	25.780(287)*	26.026(173)	26.611(168)	25.836(102)	26.361(119)	25.386(083)	25.777(148)	25.048(097)
15	26.282(162)	...	26.809(206)	...	25.781(087)	...	25.900(109)	...
16	26.171(123)	...	26.845(128)	...	25.722(098)	...	25.900(101)	...
17	26.506(100)	...	26.632(160)	...	25.338(094)	...	26.122(133)	...
18	26.403(142)	...	26.931(280)	...	25.590(061)	...	25.698(124)	...
19	26.113(095)	25.645(105)	27.291(293)	25.911(095)	25.136(056)	24.737(066)	26.231(193)	25.173(122)
20	25.995(093)	25.621(103)	26.944(247)	26.047(135)	25.198(085)	25.012(087)	25.796(179)	25.318(125)
21	25.765(115)	...	26.909(242)	...	25.328(064)	...	25.910(093)	...
22	25.926(079)	...	27.478(292)	...	25.204(075)	...	25.886(119)	...
23	26.056(108)	25.633(090)	26.772(230)	25.728(111)	25.408(079)	24.736(081)	25.974(109)	24.966(112)
24	25.961(093)	25.879(120)*	26.451(138)	25.880(113)	25.390(084)	24.795(058)	26.099(201)	25.235(169)
25	26.143(117)	...	26.124(173)	...	25.704(075)	...	25.498(111)	...
26	26.303(147)	...	...	...	26.006(126)	...	25.493(137)	...
	<b>19918P = 64.95 d</b>		<b>64757P = 65.03 d</b>		<b>13102P = 66.34 d</b>		<b>45088P = 71.41 d</b>	



Table 6—Continued

#	F555W	F814W	F555W	F814W	F555W	F814W	F555W	F814W
1	25.588(088)	24.915(089)	25.949(090)	25.135(066)	25.510(091)	24.923(056)	...	26.346(209)*
2	25.454(079)	24.804(083)	25.928(082)	25.186(101)	25.434(072)	24.984(080)	26.697(279)	25.847(198)
3	25.702(087)	...	26.102(159)	...	25.462(068)	...	26.578(228)	...
4	25.718(089)	...	25.900(108)	...	25.451(083)	...	26.465(254)	...
5	26.008(107)	25.189(079)	26.077(123)	25.179(070)	25.688(080)	24.984(083)	26.729(229)	26.144(177)
6	26.184(184)	25.146(083)	26.051(190)	25.295(123)	25.574(154)	24.984(087)	26.500(153)	26.052(166)
7	25.956(099)	...	26.171(077)	...	25.819(103)	...	27.028(292)	...
8	25.978(092)	...	26.335(117)	...	25.528(128)	...	26.517(350)	...
9	25.969(111)	...	26.208(107)	...	25.886(122)	...	26.773(316)	...
10	25.987(102)	...	26.358(162)	...	25.891(113)	...	26.099(129)	...
11	25.845(124)	...	26.291(104)	...	25.951(075)	...	26.336(164)	...
12	25.858(109)	...	26.090(100)	...	25.943(124)	...	26.313(192)	...
13	25.781(083)	25.188(112)	26.019(148)	25.252(062)	26.062(115)	25.129(068)	26.228(233)	25.791(136)
14	25.771(113)	25.222(091)	26.233(133)	25.270(079)	25.979(093)	25.136(107)	26.112(160)	25.900(189)
15	25.558(062)	...	26.433(223)	...	25.976(079)	...	25.988(126)	...
16	25.532(068)	...	26.392(122)	...	25.842(057)	...	25.747(229)	...
17	25.424(078)	...	26.259(146)	...	26.220(122)	...	25.913(128)	...
18	25.274(078)	...	26.537(166)	...	26.023(089)	...	25.615(082)	...
19	25.394(073)	24.592(143)*	26.785(235)	25.386(078)	26.237(133)	25.418(073)	25.518(074)	25.189(108)
20	25.341(053)	24.927(086)	26.385(098)	25.383(090)	26.363(090)	25.433(097)	25.519(079)	25.078(079)
21	25.443(069)	...	26.661(151)	...	26.281(083)	...	25.571(083)	...
22	25.436(058)	...	26.633(131)	...	26.379(078)	...	25.652(103)	...
23	25.426(104)	24.836(092)	26.343(176)	25.408(054)	25.701(083)	25.093(100)	25.736(110)	25.081(077)
24	25.486(087)	24.853(084)	26.561(162)	25.441(085)	25.698(074)	24.987(072)	25.622(138)	24.964(068)
25	25.315(081)	...	26.582(242)	...	25.847(140)	...	26.580(257)	...
26	25.418(112)	...	26.351(182)	...	26.247(176)	...	26.794(238)	...
	<b>03836P = 73.28 d</b>		<b>07702P = 73.76 d</b>		<b>49485P = 74.19 d</b>		<b>23616P = 82.14 d</b>	
1	26.006(143)	25.194(122)	25.521(109)	24.995(062)	25.159(077)	24.761(072)*	26.527(101)	25.424(089)
2	25.780(084)	24.973(066)	25.539(066)	24.969(068)	25.115(101)	25.081(059)	26.198(083)	25.535(093)
3	26.203(158)	...	25.923(147)	...	25.381(107)	...	25.818(129)	...
4	26.003(076)	...	25.775(080)	...	25.347(161)	...	25.839(115)	...
5	26.504(108)	25.511(093)	25.838(100)	25.095(057)	25.369(080)	24.656(054)*	25.462(068)	25.050(070)
6	26.088(169)	25.212(066)	26.338(201)	24.954(077)	25.648(163)	25.131(082)	26.051(167)	25.065(056)
7	26.023(090)	...	25.893(081)	...	25.523(080)	...	25.921(062)	...
8	26.097(153)	...	25.936(086)	...	25.365(065)	...	25.622(057)	...
9	25.629(104)	...	25.975(088)	...	25.449(073)	...	25.412(064)	...
10	25.778(064)	...	26.107(085)	...	25.481(131)	...	25.289(088)	...
11	25.914(073)	...	26.213(137)	...	25.661(105)	...	25.387(063)	...
12	25.744(086)	...	26.024(090)	...	26.019(126)	...	25.696(046)	...
13	25.934(097)	25.171(091)	26.114(091)	25.150(071)	25.579(068)	24.957(072)*	25.360(073)	24.833(076)
14	25.675(066)	25.023(062)	25.974(070)	25.208(087)	25.777(124)	25.174(092)	25.584(068)	25.082(045)
15	25.715(087)	...	26.194(101)	...	25.624(075)	...	25.431(094)	...
16	25.472(092)	...	26.101(133)	...	25.639(145)	...	25.488(058)	...
17	25.605(087)	...	26.255(129)	...	25.471(054)	...	25.554(077)	...
18	25.402(075)	...	26.384(075)	...	25.869(096)	...	25.646(036)	...
19	25.511(098)	24.930(085)	26.523(183)	25.694(106)	25.871(076)	25.020(063)*	25.676(111)	24.833(075)

However we note that our determination of  $H_0$  in Riess et al. (2009) is insensitive to the value of the optical zeropoints and aperture corrections since we will make use of *the difference* in the photometry of Cepheids in NGC 4258 and the SN hosts.

The impact of blending and crowding on Cepheid magnitudes in optical *HST* data has been addressed through Monte Carlo “artificial star” experiments. Ferrarese et al. (2000) have shown that the impact of crowding on the measured magnitudes is largely eliminated by application of the previously described selection criteria, whose effect is to reject Cepheids that are significantly contaminated by a close companion. The presence of significant contamination will alter the shape parameters of the Cepheid light curves, reducing the amplitude of variation and flattening the “sawtooth” near minimum light (by contributing a greater fraction to the total flux when the Cepheid is faint). Alternatively, a partial blend will result in a poor PSF fit and a large reported uncertainty, rendering the apparent variability less significant, and also causing a Cepheid candidate to fail one or more of the previous criteria. Ferrarese et al. (2000) found that for multi-epoch data, the net crowding bias on the distance modulus is only  $\sim 1\%$ . Riess et al. (2005) similarly found that candidates in “crowded” environments (defined here as having an additional source within at least  $0.1''$  which contributes at least  $\sim 10\%$  of the peak flux of the variable candidate) usually failed one or more of the previously discussed selection criteria.

The *net* effect of even modest crowding and blending on the distance scale is further reduced by the use NGC 4258 (instead of the LMC or the Galaxy) as an anchor of the distance scale. As shown in Riess et al. (2009), the effect of crowding is reduced to the *difference* in crowding between the SN hosts and NGC 4258, which is negligible as determined from artificial-star tests.

## 2.2. Cepheids in NGC 3021, NGC 1309, and NGC 3370

Here we present the first identification of Cepheids in NGC 1309 and NGC 3021. Each host yielded a sufficient number of Cepheids to provide a mean distance precision which is greater than the SN it hosts.

For NGC 1309 we identified 79 Cepheids, all with  $P > 20$  d, providing one of the largest sets of extragalactic Cepheids observed by *HST*. NGC 3021, a third the size of NGC 1309, not surprisingly yielded fewer Cepheids, a total of 31 with 27 at  $P > 20$  d. Their light curves are shown in Figures 3 and 4, and the parameters of the Cepheids are given in Tables 7 and 8. The  $P$ - $L$  relations in  $V$  and  $I$  are shown in Figures 5 and 6.

Cepheid samples in a magnitude-limited survey may suffer selection bias at the short-period end due to the loss of Cepheids faint for their period (e.g., Ferrarese et al. 2006, Leonard et al. 2003). Such Cepheids may fall below the detection limit or their light curves may be dominated by blending, reducing the significance of their variability. Riess et al. (2005) found this bias to apply for those Cepheids with  $P < 20$  d for NGC 3370. This limit applies to NGC 3021 which has similar Cepheid magnitudes at a given period as NGC 3370. As seen in Figure 6, the few Cepheids found

Table 6—Continued

#	F555W	F814W	F555W	F814W	F555W	F814W	F555W	F814W
20	25.543(078)	24.876(065)	26.491(085)	25.574(085)	26.095(257)	25.557(125)	25.602(055)	24.981(046)
21	25.571(101)	...	26.470(122)	...	25.810(155)	...	25.646(138)	...
22	25.491(076)	...	26.485(100)	...	26.062(107)	...	25.827(056)	...
23	25.553(086)	24.847(100)	26.125(124)	25.331(107)	25.678(093)	25.075(068)*	26.100(104)	25.137(105)
24	25.706(119)	25.114(089)	26.098(080)	25.438(070)	25.662(098)	25.485(124)	25.910(052)	25.096(087)
25	25.856(102)	...	25.527(075)	...	25.527(134)	...	25.881(122)	...
26	25.720(078)	...	25.770(106)	...	25.206(087)	...	25.851(127)	...
	<b>19777P = 82.39 d</b>		<b>65015P = 89.04 d</b>		<b>04908P = 97.90 d</b>			
1	25.481(131)	24.927(089)	26.073(154)	25.109(127)	25.906(107)	25.072(087)		
2	25.819(132)	25.129(077)	26.073(168)	25.202(102)	25.829(089)	25.004(057)		
3	25.579(120)	...	25.928(163)	...	25.911(229)	...		
4	25.907(103)	...	25.985(180)	...	25.872(108)	...		
5	25.992(132)	25.115(110)	26.405(145)	25.417(123)	25.930(102)	24.917(090)		
6	26.193(190)	25.195(098)	26.263(160)	25.247(130)	26.011(146)	24.911(062)		
7	26.044(133)	...	26.390(158)	...	25.761(091)	...		
8	25.703(124)	...	26.113(120)	...	25.502(068)	...		
9	25.887(174)	...	26.478(218)	...	25.402(101)	...		
10	25.906(139)	...	26.609(198)	...	25.400(071)	...		
11	25.788(108)	...	26.684(290)	...	25.558(079)	...		
12	26.122(114)	...	...	...	25.493(077)	...		
13	25.939(175)	25.176(105)	26.194(242)	25.843(167)*	25.498(059)	24.723(079)		
14	25.663(119)	25.185(081)	26.465(170)	25.497(171)	25.423(081)	24.791(062)		
15	25.714(133)	...	...	...	25.393(062)	...		
16	25.574(075)	...	26.515(195)	...	25.390(076)	...		
17	25.503(127)	...	26.209(142)	...	25.465(080)	...		
18	25.726(113)	...	25.980(130)	...	25.435(052)	...		
19	25.525(111)	24.754(079)	25.897(099)	25.255(142)	25.254(072)	24.612(056)		
20	25.470(086)	24.950(071)	25.814(168)	25.018(087)	25.378(071)	24.729(067)		
21	25.324(076)	...	25.975(163)	...	25.338(076)	...		
22	25.443(071)	...	25.810(096)	...	25.364(054)	...		
23	25.401(119)	24.731(077)	25.741(137)	25.022(162)	25.446(077)	24.522(074)*		
24	25.300(084)	24.996(069)	25.753(109)	25.040(122)	25.374(072)	24.710(067)		
25	25.869(165)	...	25.799(190)	...	25.160(097)	...		
26	25.793(142)	...	26.162(177)	...	25.454(066)	...		

\* Data point rejected in light curve fit

<sup>a</sup>  $1\sigma$  uncertainties (units of 0.001 mag) are given in parentheses.

with  $P < 20$  d tend to be brighter than expected, though no such bias appears for the Wesenheit reddening-free magnitudes (defined in §3; see Madore 1982 and Figure 8). For NGC 1309, whose Cepheids indicate a greater distance than NGC 3370 or NGC 3021, the periods with apparent bias rises to  $P < 38$  d (see Fig. 5). Again, the Wesenheit magnitudes do not show this bias at shorter periods (see Figure 8). In both cases this would imply that the Cepheids with periods shorter than the bias limit suffer a modest amount of blending from bluer sources which is largely removed by the color correction. While the Wesenheit magnitudes appear useful at lower periods, it is safer to restrict the use of Cepheids to those with periods greater than the range where their selection appears biased in the individual passbands.

Our additional imaging of NGC 3370 in Cycle 15 allowed us to identify new Cepheids with periods in excess of the original 60 day campaign as well as a few more at shorter periods. For NGC 3370, we have detected 127 Cepheids of which 110 have  $P > 20$  d, nearly double the sample found by Riess et al. (2005) and reducing the mean wesenheim magnitudes by 0.035 mag. These are shown in Figure 7 and their parameters are given in Table 9 (where  $L_V$  is the  $V$ -band variability index).

Table 7. Cepheid Candidates in NGC 3021

id	$\alpha$ (J2000)	$\delta$ (J2000)	period (days)	$\langle V \rangle$ (mag)	$\langle I \rangle$ (mag)	Amp <sub>V</sub> (mag)	Amp <sub>I</sub> (mag)	$L_V$	$t_0$ (2400000+)
31556	147.72782	33.55528	11.17	27.418(0.243)	27.052(0.072)	0.600	0.322	0.804	54071.48
30672	147.72778	33.54702	13.92	27.489(0.224)	26.996(0.137)	0.618	0.429	1.187	54082.60
8621.	147.74838	33.55002	15.37	27.225(0.209)	26.479(0.111)	0.470	0.206	0.908	54083.98
8102.	147.74935	33.55170	18.71	27.391(0.251)	26.760(0.121)	0.536	0.270	0.991	54077.91
20774	147.73750	33.55041	20.38	26.770(0.144)	26.179(0.174)	0.447	0.268	1.313	54077.16
10786	147.74693	33.55663	21.16	27.242(0.176)	26.349(0.152)	0.465	0.243	1.256	54081.52
47390	147.73410	33.55873	21.84	27.186(0.165)	26.373(0.151)	0.455	0.212	1.300	54080.90
33607	147.72083	33.55514	23.13	27.328(0.160)	26.626(0.050)	0.450	0.268	1.532	54084.59
32375	147.72586	33.55581	24.01	27.280(0.210)	26.461(0.148)	0.552	0.301	1.530	54092.85
8636.	147.74871	33.55237	24.36	26.848(0.085)	26.116(0.102)	0.451	0.288	1.588	54083.61
32380	147.72645	33.56000	25.18	26.769(0.095)	26.040(0.134)	0.560	0.346	2.752	54096.04
32088	147.72678	33.55614	25.77	27.199(0.228)	26.220(0.103)	0.552	0.245	1.733	54080.94
26946	147.73211	33.54878	26.84	26.816(0.152)	25.974(0.149)	0.587	0.170	2.380	54102.95
9028.	147.74791	33.55032	31.89	26.356(0.095)	25.642(0.071)	0.516	0.277	3.677	54099.86
23149	147.73688	33.55930	32.53	26.633(0.108)	25.713(0.157)	0.555	0.367	2.523	54104.49
30428	147.72812	33.54750	32.60	26.636(0.123)	25.849(0.088)	0.576	0.244	3.384	54097.22
26126	147.73336	33.55230	34.87	26.319(0.111)	25.721(0.150)	0.328	0.176	1.092	54086.75
12135	147.74553	33.55600	36.50	26.743(0.146)	25.721(0.127)	0.426	0.303	1.492	54092.92
31803	147.72789	33.55893	37.27	27.039(0.114)	26.152(0.156)	0.486	0.353	1.601	54088.95
45787	147.73632	33.55657	37.31	26.023(0.122)	25.330(0.059)	0.282	0.125	0.709	54095.88
26545	147.73249	33.54885	39.57	26.327(0.139)	25.461(0.140)	0.590	0.323	3.045	54089.38
9402.	147.74757	33.55109	39.78	26.885(0.162)	25.729(0.104)	0.623	0.317	1.558	54100.07
25375	147.73388	33.55151	39.95	26.359(0.150)	25.850(0.118)	0.614	0.560	3.372	54083.58
9611.	147.74740	33.55142	40.49	26.295(0.117)	25.663(0.101)	0.400	0.396	0.963	54106.75
20415	147.73892	33.55806	51.51	26.551(0.163)	25.467(0.124)	0.476	0.220	1.712	54088.40
12778	147.74489	33.55619	63.19	25.613(0.070)	25.097(0.095)	0.278	0.198	1.265	54113.26
19817	147.73982	33.56093	68.61	26.322(0.089)	25.253(0.057)	0.370	0.259	2.211	54146.16
7098.	147.75116	33.55414	82.66	25.913(0.129)	25.182(0.138)	0.344	0.186	1.127	54131.46
9558.	147.74734	33.55075	88.18	26.884(0.152)	25.435(0.085)	0.435	0.262	0.932	54164.64
12013	147.74545	33.55484	90.73	25.735(0.065)	24.819(0.094)	0.237	0.119	0.757	54172.44
10203	147.74683	33.55170	95.91	25.756(0.063)	24.909(0.049)	0.170	0.020	0.908	54135.11

Table 8. Cepheid Candidates in NGC 1309

id	$\alpha$ (J2000)	$\delta$ (J2000)	period (days)	$\langle V \rangle$ (mag)	$\langle I \rangle$ (mag)	Amp <sub>V</sub> (mag)	Amp <sub>I</sub> (mag)	$L_V$	$t_0$ (2400000+)
21599	50.52930	-15.41687	20.93	27.434(0.201)	26.744(0.187)	0.555	0.162	1.631	54053.33
9778.	50.53294	-15.38609	21.98	27.453(0.199)	26.869(0.194)	0.513	0.279	1.159	54057.75
8610.	50.53423	-15.39811	23.22	27.310(0.182)	26.615(0.091)	0.541	0.219	1.031	54064.55
6631.	50.53610	-15.41348	24.81	26.988(0.150)	26.405(0.070)	0.498	0.267	1.304	54060.05
6737.	50.53598	-15.41296	25.45	27.336(0.217)	26.628(0.152)	0.541	0.279	1.291	54060.20
34523	50.52358	-15.40722	25.52	27.211(0.198)	26.476(0.110)	0.521	0.210	1.266	54061.51
44606	50.51955	-15.40855	25.84	27.082(0.228)	26.699(0.228)	0.563	0.242	2.614	54059.06
48719	50.51726	-15.40686	26.70	27.142(0.167)	26.370(0.098)	0.516	0.142	1.036	54045.30
55736	50.50417	-15.38446	27.18	27.440(0.125)	26.670(0.101)	0.419	0.300	1.534	54069.83
54039	50.50975	-15.38449	27.64	27.223(0.235)	26.415(0.069)	0.545	0.353	1.301	54057.11
41542	50.52035	-15.39916	27.71	27.075(0.141)	26.293(0.103)	0.463	0.222	1.187	54051.06
12340	50.53212	-15.39489	27.84	26.987(0.165)	26.575(0.137)	0.445	0.378	1.169	54063.03
52644	50.51172	-15.37853	29.17	26.875(0.136)	26.244(0.098)	0.574	0.338	2.819	54064.19
2343.	50.54025	-15.40458	29.61	27.084(0.182)	26.489(0.221)	0.602	0.402	1.923	54068.76
23076	50.52816	-15.40843	30.66	27.288(0.261)	26.467(0.104)	0.496	0.239	1.192	54061.02
85974	50.51896	-15.40298	30.86	26.900(0.155)	26.396(0.104)	0.521	0.301	1.776	54047.85
7224.	50.53585	-15.41538	30.90	27.390(0.257)	26.555(0.092)	0.683	0.268	2.330	54050.49
7255.	50.53427	-15.38705	31.15	27.265(0.159)	26.531(0.064)	0.452	0.265	1.162	54045.49
50024	50.51566	-15.39516	31.69	27.299(0.214)	26.290(0.124)	0.512	0.302	1.724	54048.75
59151	50.53574	-15.41413	32.61	26.772(0.174)	26.180(0.082)	0.445	0.241	1.602	54065.95
60583	50.53360	-15.39877	32.95	27.064(0.296)	26.136(0.094)	0.684	0.423	1.746	54054.39
4322.	50.53615	-15.38579	33.25	26.793(0.132)	26.208(0.068)	0.612	0.327	2.840	54067.55
30349	50.52525	-15.40856	33.51	27.043(0.212)	26.430(0.136)	0.528	0.236	0.899	54066.02
3108.	50.53807	-15.38939	33.71	26.989(0.180)	26.245(0.149)	0.472	0.238	1.974	54067.12
9099.	50.53391	-15.39736	33.74	27.050(0.186)	26.379(0.116)	0.458	0.135	0.698	54057.49
30771	50.52352	-15.38006	33.74	27.297(0.228)	26.524(0.124)	0.530	0.266	1.816	54069.89
14063	50.53191	-15.40485	34.07	26.754(0.188)	26.033(0.151)	0.519	0.334	1.382	54068.80
59846	50.53441	-15.40029	35.12	26.831(0.157)	26.052(0.173)	0.475	0.144	1.036	54065.28
31655	50.52487	-15.41096	35.82	26.606(0.123)	25.976(0.077)	0.297	0.132	1.204	54049.49
7868.	50.53405	-15.38828	36.17	27.244(0.184)	26.456(0.080)	0.472	0.270	1.354	54069.11
69637	50.52730	-15.39672	37.23	26.591(0.260)	25.841(0.085)	0.532	0.175	1.073	54074.11
41024	50.52078	-15.40182	38.62	26.958(0.216)	26.440(0.171)	0.525	0.352	1.006	54043.19
34163	50.52292	-15.39251	39.34	26.687(0.183)	25.985(0.090)	0.423	0.282	1.016	54079.33
7989.	50.53524	-15.41099	39.42	27.391(0.166)	26.482(0.149)	0.410	0.304	0.784	54055.14
44069	50.51958	-15.40478	39.90	26.868(0.213)	26.258(0.117)	0.487	0.367	1.629	54072.88
27980	50.52622	-15.41000	39.92	27.127(0.253)	26.059(0.043)	0.815	0.238	1.739	54050.36
52975	50.51305	-15.41224	40.52	27.301(0.155)	26.533(0.217)	0.510	0.355	1.691	54067.73
7994.	50.53392	-15.38694	40.69	26.936(0.169)	26.038(0.078)	0.602	0.371	1.340	54059.04
1166.	50.54164	-15.39645	41.11	27.386(0.175)	26.279(0.062)	0.514	0.270	1.478	54076.96
76534	50.52410	-15.40276	41.86	26.645(0.162)	26.005(0.132)	0.490	0.315	0.853	54073.82
22918	50.52824	-15.40865	42.03	26.707(0.193)	25.889(0.096)	0.595	0.262	1.397	54071.01
2032.	50.54017	-15.39411	42.53	26.497(0.183)	25.768(0.056)	0.624	0.246	2.908	54053.85
48747	50.51610	-15.38609	42.68	27.234(0.182)	26.373(0.111)	0.566	0.356	1.002	54079.41
67393	50.52880	-15.39772	42.74	26.533(0.131)	25.685(0.061)	0.443	0.162	1.433	54068.90
58298	50.53507	-15.38553	43.52	26.694(0.111)	25.922(0.095)	0.521	0.341	1.704	54083.59

Table 8—Continued

id	$\alpha$ (J2000)	$\delta$ (J2000)	period (days)	$\langle V \rangle$ (mag)	$\langle I \rangle$ (mag)	Amp <sub>V</sub> (mag)	Amp <sub>I</sub> (mag)	$L_V$	$t_0$ (2400000+)
7331.	50.53498	-15.40072	44.58	26.382(0.145)	25.850(0.092)	0.377	0.195	1.042	54080.80
2979.	50.53940	-15.40977	44.90	26.467(0.123)	25.737(0.073)	0.503	0.320	3.097	54076.82
1732.	50.54059	-15.39462	45.00	26.252(0.094)	25.525(0.096)	0.261	0.170	1.854	54082.39
19368	50.52978	-15.40833	45.25	26.566(0.158)	25.759(0.117)	0.442	0.238	1.308	54065.50
49584	50.51619	-15.39832	45.67	26.838(0.143)	26.046(0.107)	0.409	0.322	1.434	54082.05
16143	50.53022	-15.39054	46.74	27.014(0.173)	26.015(0.090)	0.476	0.296	1.459	54058.63
15346	50.53148	-15.40689	46.85	26.746(0.147)	25.925(0.081)	0.409	0.091	0.722	54068.16
54502	50.50920	-15.39192	47.13	26.996(0.205)	26.100(0.080)	0.666	0.332	1.593	54075.84
59642	50.53436	-15.39644	47.39	26.428(0.155)	25.925(0.071)	0.379	0.311	1.889	54059.19
52566	50.51322	-15.40390	47.41	26.641(0.105)	26.095(0.092)	0.425	0.331	1.436	54088.98
52170	50.51350	-15.39881	47.99	26.915(0.134)	25.940(0.024)	0.520	0.235	2.161	54058.99
4882.	50.53701	-15.41209	48.91	26.808(0.158)	26.046(0.087)	0.576	0.246	1.970	54084.46
68817	50.52830	-15.40526	49.93	26.578(0.160)	26.036(0.081)	0.406	0.190	1.546	54086.75
15318	50.53038	-15.38675	51.46	26.562(0.088)	25.781(0.124)	0.615	0.354	2.909	54055.96
71911	50.52661	-15.40578	51.99	26.207(0.098)	25.447(0.057)	0.287	0.169	1.137	54059.51
28132	50.52604	-15.40768	52.24	26.820(0.129)	25.815(0.068)	0.405	0.073	0.883	54084.04
6581.	50.53598	-15.41154	58.98	26.810(0.262)	26.005(0.177)	0.637	0.254	1.363	54073.09
25965	50.52610	-15.39321	59.02	26.562(0.148)	25.964(0.071)	0.371	0.265	0.757	54100.04
6542.	50.53606	-15.41233	59.12	26.575(0.093)	25.663(0.020)	0.311	0.220	1.889	54096.28
53187	50.51202	-15.39909	59.75	26.757(0.119)	26.179(0.098)	0.300	0.191	1.006	54113.61
69494	50.52808	-15.40923	60.17	27.077(0.173)	26.150(0.087)	0.619	0.250	1.337	54069.54
2647.	50.53992	-15.40867	60.67	26.278(0.127)	25.452(0.097)	0.553	0.305	3.064	54115.54
17049	50.53025	-15.39867	61.24	26.272(0.154)	25.415(0.137)	0.363	0.189	0.959	54082.07
19918	50.52958	-15.40892	64.94	26.241(0.086)	25.425(0.093)	0.351	0.189	2.152	54082.93
64757	50.53107	-15.40794	65.03	26.796(0.138)	25.710(0.041)	0.345	0.156	0.934	54107.87
13102	50.53150	-15.38948	66.34	26.331(0.115)	25.506(0.076)	0.539	0.243	2.231	54113.61
45088	50.51857	-15.39463	71.40	26.699(0.197)	25.912(0.156)	0.662	0.607	2.057	54128.10
3836.	50.53789	-15.40643	73.27	26.390(0.128)	25.504(0.120)	0.401	0.195	1.401	54066.32
7702.	50.53554	-15.41410	73.76	26.473(0.110)	25.596(0.089)	0.615	0.342	1.718	54094.45
49485	50.51648	-15.40236	74.19	26.071(0.155)	25.670(0.045)	0.451	0.267	1.158	54099.77
23616	50.52841	-15.41752	82.13	26.481(0.178)	25.579(0.091)	0.450	0.242	1.307	54107.33
19777	50.52881	-15.39393	82.38	26.246(0.135)	25.437(0.105)	0.325	0.193	1.002	54128.08
65015	50.53048	-15.40066	89.03	26.625(0.137)	25.576(0.087)	0.343	0.238	1.220	54084.36
4908.	50.53644	-15.40175	97.89	26.201(0.098)	25.247(0.069)	0.309	0.210	1.559	54115.33

Table 9. Cepheid Candidates in NGC 3370

id	$\alpha$ (J2000)	$\delta$ (J2000)	period (days)	$\langle V \rangle$ (mag)	$\langle I \rangle$ (mag)	Amp <sub>V</sub> (mag)	Amp <sub>I</sub> (mag)	$L_V$	$t_0$ (2400000+)
88045	161.77365	17.27522	14.45	27.620(0.262)	26.950(0.179)	0.526	0.228	1.523	54087.72
35527	161.76834	17.26353	15.09	27.634(0.188)	26.544(0.134)	0.450	0.493	1.255	54074.51
8849.	161.75805	17.27787	15.39	27.414(0.215)	26.445(0.074)	0.615	0.318	1.662	54085.07
52153	161.78670	17.27016	15.77	27.495(0.188)	26.804(0.142)	0.557	0.293	1.502	54088.84
2204.	161.75537	17.28996	16.22	27.626(0.135)	26.723(0.118)	0.479	0.273	1.749	54071.32
24497	161.76928	17.28204	16.78	27.609(0.256)	26.737(0.175)	0.556	0.438	1.757	54084.18
4668.	161.75797	17.28751	17.26	27.494(0.251)	26.660(0.110)	0.563	0.277	1.310	54081.86
78990	161.76383	17.26409	17.37	27.381(0.182)	26.474(0.217)	0.498	0.297	1.892	54077.47
2638.	161.75400	17.28417	17.46	27.290(0.179)	26.530(0.042)	0.586	0.459	2.549	54081.90
37156	161.76811	17.26012	17.84	27.603(0.138)	26.792(0.165)	0.551	0.313	2.003	54086.86
9842.	161.75587	17.26928	18.39	27.747(0.321)	27.056(0.180)	0.593	0.224	1.623	54075.80
11908	161.76236	17.28264	18.76	27.238(0.173)	26.209(0.150)	0.400	0.126	1.463	54088.84
8367.	161.75989	17.28410	18.88	27.693(0.250)	26.772(0.249)	0.607	0.282	1.741	54078.46
44450	161.77260	17.25851	19.10	27.693(0.248)	26.843(0.130)	0.556	0.350	1.411	54078.88
5394.	161.75420	17.27504	19.21	27.432(0.181)	26.475(0.168)	0.544	0.272	2.211	54080.20
21444	161.76766	17.28206	19.64	27.452(0.222)	26.525(0.114)	0.477	0.271	1.670	54090.17
52086	161.78246	17.25879	19.91	27.201(0.122)	26.347(0.053)	0.500	0.418	2.413	54089.91
45559	161.78086	17.27835	20.21	27.272(0.172)	26.524(0.119)	0.567	0.414	2.188	54076.41
45280	161.77907	17.27414	20.27	27.603(0.215)	26.766(0.225)	0.570	0.259	0.854	54077.95
51454	161.78510	17.26936	20.51	27.328(0.166)	26.400(0.062)	0.434	0.176	1.151	54083.93
50670	161.77931	17.25660	20.52	27.237(0.131)	26.399(0.140)	0.479	0.241	2.157	54079.69
26546	161.76597	17.26987	21.57	27.028(0.206)	26.160(0.054)	0.472	0.068	1.625	54080.85
11992	161.75778	17.26972	21.78	27.509(0.192)	26.547(0.082)	0.587	0.319	1.590	54093.66
10540	161.76365	17.28919	21.79	27.442(0.243)	26.607(0.153)	0.578	0.245	1.771	54092.36
51357	161.78000	17.25566	23.43	27.198(0.144)	26.349(0.088)	0.517	0.349	2.023	54092.68
871.0	161.75495	17.29607	23.66	27.329(0.165)	26.322(0.130)	0.543	0.281	2.276	54091.36
8807.	161.75882	17.28007	23.72	27.484(0.158)	26.425(0.129)	0.524	0.175	1.537	54085.34
47494	161.77627	17.25957	24.43	27.215(0.195)	25.988(0.101)	0.532	0.217	2.100	54073.89
23575	161.76105	17.26054	24.46	27.310(0.123)	26.353(0.108)	0.448	0.273	1.512	54099.40
47059	161.77441	17.25595	24.49	27.332(0.190)	26.402(0.090)	0.589	0.436	1.913	54098.58
53228	161.78689	17.25998	24.73	27.490(0.198)	26.634(0.141)	0.487	0.289	1.719	54085.77
61720	161.75875	17.28389	25.43	26.630(0.137)	25.724(0.114)	0.429	0.236	1.991	54082.44
21354	161.76299	17.26917	25.59	27.131(0.220)	26.459(0.105)	0.380	0.271	1.186	54097.74
23818	161.76845	17.28078	26.33	27.098(0.230)	26.043(0.109)	0.486	0.230	1.355	54095.29
22838	161.76132	17.26232	26.38	27.246(0.157)	26.248(0.193)	0.476	0.256	1.916	54085.26
81239	161.77044	17.27853	26.42	27.013(0.192)	26.342(0.134)	0.551	0.430	1.258	54082.13
39583	161.77518	17.27540	26.87	26.958(0.213)	26.006(0.185)	0.552	0.157	1.950	54086.41
18872	161.76209	17.27022	27.02	27.024(0.160)	26.347(0.118)	0.583	0.480	2.014	54076.36
22029	161.76515	17.27416	27.32	26.772(0.221)	25.836(0.149)	0.422	0.036	1.325	54084.89
48470	161.78219	17.27266	27.35	27.344(0.201)	26.261(0.193)	0.518	0.259	1.982	54079.93
5744.	161.75647	17.28052	27.74	27.299(0.131)	26.232(0.106)	0.755	0.352	2.625	54090.86
51334	161.78015	17.25611	28.79	27.496(0.266)	26.509(0.088)	0.669	0.476	2.088	54100.09
49159	161.77565	17.25210	29.07	26.890(0.183)	26.049(0.116)	0.512	0.366	2.097	54107.61
4531.	161.75831	17.28893	29.23	27.124(0.162)	26.124(0.128)	0.581	0.276	1.516	54092.40
62219	161.75791	17.28025	29.43	27.323(0.242)	26.218(0.172)	0.785	0.434	2.143	54088.70



Table 9—Continued

id	$\alpha$ (J2000)	$\delta$ (J2000)	period (days)	$\langle V \rangle$ (mag)	$\langle I \rangle$ (mag)	Amp <sub>V</sub> (mag)	Amp <sub>I</sub> (mag)	$L_V$	$t_0$ (2400000+)
46992	161.77485	17.25741	29.60	27.119(0.218)	26.168(0.075)	0.627	0.278	2.739	54101.12
4032.	161.76154	17.29942	29.78	26.756(0.114)	25.898(0.118)	0.547	0.249	3.155	54095.81
51430	161.78069	17.25719	30.43	27.408(0.207)	26.352(0.126)	0.518	0.244	1.715	54101.23
27556	161.77156	17.28401	30.69	27.202(0.140)	26.227(0.126)	0.421	0.230	1.872	54094.43
19943	161.76245	17.26963	30.80	26.582(0.088)	25.845(0.084)	0.343	0.206	1.649	54083.47
35299	161.77125	17.27173	31.20	26.483(0.162)	25.569(0.109)	0.371	0.218	0.759	54100.86
13380	161.76194	17.27869	31.74	26.477(0.126)	25.603(0.102)	0.261	0.162	0.810	54080.07
13249	161.76203	17.27921	31.78	27.010(0.195)	26.180(0.141)	0.440	0.274	1.494	54102.53
32684	161.77068	17.27447	32.04	26.620(0.138)	25.511(0.113)	0.460	0.272	1.661	54104.72
15081	161.76554	17.28584	32.56	27.510(0.166)	26.281(0.076)	0.423	0.343	1.419	54086.09
4710.	161.75647	17.28320	32.62	27.231(0.150)	26.150(0.108)	0.470	0.207	1.513	54108.24
18200	161.76118	17.26863	32.87	27.001(0.150)	25.894(0.104)	0.463	0.305	2.597	54090.74
26416	161.76487	17.26700	33.40	27.044(0.178)	25.851(0.084)	0.495	0.182	1.799	54097.26
52428	161.78414	17.26088	33.48	26.998(0.131)	25.962(0.128)	0.483	0.214	2.033	54098.93
31439	161.77252	17.28137	33.49	26.970(0.170)	25.953(0.104)	0.428	0.139	1.968	54092.83
17886	161.76336	17.27517	33.56	26.800(0.203)	25.557(0.043)	0.688	0.289	2.100	54101.75
49211	161.78007	17.26419	33.57	27.125(0.175)	26.169(0.110)	0.484	0.259	1.834	54104.43
52279	161.78547	17.26580	33.69	27.022(0.167)	25.987(0.131)	0.445	0.359	2.101	54094.93
33812	161.77245	17.27762	34.07	26.916(0.138)	26.034(0.111)	0.488	0.380	1.673	54105.37
4345.	161.75620	17.28353	34.07	27.348(0.144)	26.141(0.116)	0.739	0.360	2.373	54089.34
17595	161.76259	17.27355	34.22	27.176(0.229)	26.021(0.152)	0.741	0.375	2.019	54095.37
1320.	161.75212	17.28576	34.58	27.551(0.156)	26.487(0.097)	0.414	0.196	1.104	54084.23
17969	161.76144	17.26969	34.71	26.941(0.206)	25.778(0.161)	0.673	0.328	2.096	54108.94
10677	161.76072	17.28069	35.24	27.152(0.175)	26.027(0.077)	0.645	0.381	2.083	54090.46
40369	161.77544	17.27471	35.41	27.592(0.225)	26.062(0.069)	0.581	0.208	1.189	54098.72
19618	161.76333	17.27244	35.66	26.758(0.222)	25.544(0.184)	0.509	0.209	1.731	54109.86
22097	161.76764	17.28103	36.02	26.679(0.119)	25.681(0.133)	0.480	0.246	1.666	54093.05
50582	161.78077	17.26097	36.69	26.958(0.167)	25.899(0.062)	0.489	0.343	1.736	54105.54
59919	161.75710	17.28387	36.99	26.703(0.165)	25.819(0.162)	0.506	0.377	2.357	54108.29
45614	161.77520	17.26245	37.02	26.788(0.144)	25.958(0.103)	0.526	0.171	2.055	54090.95
21445	161.76923	17.28640	37.10	27.064(0.150)	25.975(0.077)	0.618	0.284	1.887	54090.02
16214	161.75886	17.26535	37.21	27.394(0.171)	26.191(0.127)	0.513	0.189	1.208	54110.28
30965	161.77252	17.28201	37.28	26.549(0.097)	25.594(0.105)	0.606	0.322	3.412	54094.59
20306	161.76295	17.27049	37.28	26.834(0.131)	26.072(0.106)	0.257	0.214	0.871	54082.04
21506	161.76844	17.28412	38.54	26.163(0.098)	25.409(0.067)	0.480	0.339	2.652	54103.44
31251	161.77276	17.28228	39.30	26.314(0.094)	25.373(0.071)	0.337	0.179	2.062	54118.69
47492	161.77587	17.25844	39.41	27.278(0.185)	26.133(0.059)	0.396	0.157	1.264	54084.59
7613.	161.75941	17.28456	39.50	27.209(0.196)	26.166(0.167)	0.442	0.239	1.149	54120.64
18990	161.76910	17.28952	40.01	26.664(0.136)	25.855(0.037)	0.522	0.325	3.251	54097.25
13355	161.76178	17.27834	41.09	26.420(0.123)	25.492(0.126)	0.412	0.168	1.564	54116.06
20732	161.76774	17.28324	41.55	26.881(0.124)	25.715(0.042)	0.389	0.169	1.612	54099.06
29982	161.76730	17.26882	42.75	26.440(0.149)	25.523(0.055)	0.386	0.250	1.278	54107.93
9431.	161.76075	17.28388	43.10	26.126(0.109)	25.287(0.044)	0.447	0.310	2.588	54087.71
6440.	161.75761	17.28213	43.94	26.483(0.135)	25.311(0.065)	0.632	0.248	3.243	54087.45
85483	161.77245	17.27666	44.57	26.444(0.136)	25.310(0.107)	0.362	0.116	1.106	54088.24

### 2.3. Long-Period Cepheids

The initial *HST* imaging campaigns of the SN hosts were too brief to reliably identify Cepheids with  $P > 60$  d as their duration was shorter than a full pulsation cycle. While long-period Cepheids are rarer than their older cousins, their greater brightness and contrast makes them easier to detect and they are very valuable for extending the range of Cepheids as distance indicators. At  $P > 100$  d, the  $P$ - $L$  relations flatten (e.g., Freedman et al. 1992) and such Cepheids require the use of different relations as discussed by Bird et al. (2009). While we have as yet no Cepheids with  $P > 100$  days in our sample, in the future such objects could be useful for extending the range to which SNe Ia may be calibrated.

For the three SN hosts exclusively observed with ACS (NGC 3370, 1309, and 3021), we have identified a total of 39 and 18 Cepheids with periods greater than 60 and 75 d, respectively. For NGC 4258 we identified additional Cepheids using the new epochs beyond those analyzed by Macri et al. (2006), 149 in all including 68 with  $P > 20$  d, 6 with  $P > 60$  d, and 3 with  $P > 75$  d. The optical Cepheid data for NGC 4258 are given by Macri et al. (2009). In Table 10 we indicate the number of Cepheids with long periods found in the previously discussed hosts.

The new epochs of imaging of the three hosts initially observed with WFPC2 (NGC 3982, NGC 4536, and NGC 4639) also enabled the discovery of new Cepheids at  $P > 60$  d not previously identified. However, the fractional coverage of these hosts is less, limited by the smaller field of WFPC2. To look for such objects we retrieved the WFPC2 data which originated from programs GO-5427, GO-5981, and GO-8100 (SN Ia *HST* Calibration Program, P.I. Sandage) to combine with the Cycle 15 data from our SHOES (Supernovae and  $H_0$  for the Equation of State) program. These data were processed in the same manner as the ACS data described in the previous section while making use of the latest WFPC2 CTE corrections. The search for Cepheids in these hosts netted a dozen Cepheids with  $P > 60$  d to augment those previously detected in the original analyses of Saha et al. (1996, 1997, 2001), Gibson et al. (2000) and Stetson & Gibson (2001).<sup>4</sup> Additional imaging might reveal so-called “ultra long-period Cepheids” ( $P > 100$  d; e.g., Bird et al. 2009) of future value.

### 2.4. Cepheid Homogeneity

The reliable use of Cepheids along the distance ladder relies on their homogeneity. To test this we constructed composite light curves in the well-sampled  $V$  band, as shown in Figure 9. We limited inclusion to long period Cepheids, i.e., those with  $P > 10$  d, resulting in averages of 20 to 40 d in the hosts. We find that these mean light curves in each galaxy to be quite homogeneous. Table 11 gives the mean half-amplitude for the SN hosts, each of which is measured to 1% to 2%

---

<sup>4</sup>We rediscovered  $\sim 90\%$  the Cepheids presented in the previous analyses. For these Cepheids we found a negligible difference (0.3 d) in their mean period, with a dispersion about the difference of 1.3 d.

Table 9—Continued

id	$\alpha$ (J2000)	$\delta$ (J2000)	period (days)	$\langle V \rangle$ (mag)	$\langle I \rangle$ (mag)	Amp <sub>V</sub> (mag)	Amp <sub>I</sub> (mag)	$L_V$	$t_0$ (2400000+)
25870	161.76779	17.27589	44.81	26.379(0.155)	25.410(0.139)	0.523	0.336	1.405	54099.75
37212	161.77170	17.26998	44.87	26.705(0.175)	25.701(0.141)	0.529	0.225	2.175	54121.50
28504	161.76514	17.26491	44.97	26.387(0.101)	25.564(0.073)	0.378	0.287	1.768	54109.23
9014.	161.75980	17.28234	45.10	27.106(0.190)	25.985(0.160)	0.563	0.234	2.191	54101.07
40168	161.77694	17.27923	45.40	26.626(0.095)	25.606(0.076)	0.552	0.288	2.503	54122.22
5439.	161.75713	17.28309	45.82	26.409(0.124)	25.424(0.052)	0.576	0.258	2.602	54089.11
46830	161.77864	17.26849	45.88	27.114(0.232)	26.032(0.132)	0.602	0.355	1.969	54104.19
34313	161.77155	17.27429	47.19	26.634(0.204)	25.659(0.049)	0.451	0.204	2.193	54099.56
20949	161.77120	17.29254	47.37	26.415(0.120)	25.453(0.074)	0.431	0.216	2.543	54098.79
2074.	161.75695	17.29511	49.85	26.699(0.143)	25.738(0.079)	0.480	0.244	2.455	54129.77
46035	161.78023	17.27523	50.13	26.580(0.110)	25.497(0.106)	0.636	0.286	3.021	54112.43
28129	161.76619	17.26830	50.57	26.245(0.122)	25.118(0.092)	0.465	0.233	2.670	54127.73
5361.	161.75695	17.28274	50.60	25.948(0.115)	25.052(0.086)	0.394	0.255	1.797	54115.05
28534	161.77050	17.27974	51.15	26.929(0.146)	25.944(0.062)	0.462	0.333	1.986	54095.76
48903	161.77827	17.26024	51.69	26.717(0.161)	25.620(0.139)	0.668	0.323	2.414	54136.82
15864	161.76420	17.28080	52.41	26.144(0.067)	25.109(0.042)	0.357	0.243	1.478	54109.82
4367.	161.75525	17.28084	52.72	26.941(0.148)	25.723(0.064)	0.312	0.181	1.130	54088.61
13303	161.76500	17.28732	52.74	26.716(0.122)	25.561(0.043)	0.539	0.245	2.246	52817.50
1528.	161.75194	17.28407	60.68	25.982(0.076)	25.156(0.043)	0.350	0.217	2.805	54113.52
5501.	161.75677	17.28193	62.71	26.093(0.053)	24.833(0.025)	0.176	0.050	0.853	54142.71
6706.	161.75874	17.28466	64.79	26.238(0.096)	25.267(0.072)	0.559	0.224	2.216	54148.62
7014.	161.75977	17.28685	66.71	25.781(0.104)	24.700(0.070)	0.320	0.198	2.104	54126.33
33669	161.76845	17.26671	67.23	26.670(0.154)	25.282(0.126)	0.408	0.184	1.565	54115.81
9063.	161.75862	17.27891	68.90	25.687(0.045)	24.875(0.038)	0.201	0.136	1.571	54135.47
22612	161.76869	17.28313	69.35	25.746(0.069)	24.703(0.073)	0.391	0.212	2.692	54095.88
29662	161.76544	17.26415	71.53	26.272(0.119)	25.366(0.110)	0.484	0.259	1.869	54152.55
22718	161.76805	17.28118	73.36	25.673(0.108)	24.763(0.042)	0.430	0.207	1.547	54112.11
1454.	161.75252	17.28609	79.26	26.521(0.092)	25.188(0.094)	0.674	0.374	2.578	54159.30
33346	161.76861	17.26770	80.85	26.002(0.121)	25.105(0.064)	0.407	0.216	0.979	54171.59
33195	161.77345	17.28137	81.04	25.895(0.072)	24.884(0.048)	0.281	0.164	1.654	54177.57
4471.	161.75697	17.28539	83.28	27.010(0.093)	25.584(0.095)	0.351	0.213	1.314	54158.04
22098	161.76770	17.28115	86.33	25.892(0.116)	24.822(0.129)	0.247	0.112	1.918	54146.68
3205.	161.75284	17.27851	88.25	26.112(0.120)	25.097(0.083)	0.356	0.186	1.005	54172.21
31067	161.76816	17.26970	88.54	25.667(0.100)	24.516(0.046)	0.330	0.131	1.147	54130.16
48741	161.77799	17.26004	96.49	25.522(0.051)	24.561(0.028)	0.248	0.146	2.139	54131.89
8038.	161.76096	17.28786	96.82	26.286(0.101)	25.194(0.080)	0.336	0.182	2.181	54135.30
17501	161.76206	17.27215	98.72	26.034(0.131)	24.952(0.051)	0.295	0.208	2.189	54158.29

Table 10: Long-Period Cepheids

Host	SN Ia	$P > 60$ d	$P > 75$ d
NGC 4536	SN 1981B	5	4
NGC 4639	SN 1990N	2	1
NGC 3982	SN 1998aq	5	3
NGC 3370	SN 1994ae	19	10
NGC 3021	SN 1995al	6	4
NGC 1309	SN 2002fk	14	4
NGC 4258	————	6	3

precision and is consistent with the sample average of 0.48, including that of the inner field of NGC 4258. The exception may be the outer field of NGC 4258 whose mean is 13% lower than the sample mean, though this difference is not significant due to the small number of long-period Cepheids in this field. *Individual* half-amplitudes for the Cepheids range from 0.15 to 0.80 mag.

There are pertinent reasons why the *mean* shape or amplitude of the light curve might vary from galaxy to galaxy. A difference in blending would alter the apparent amplitudes, reducing them in the presence of greater blending. Chemical composition may also affect Cepheid amplitudes. Paczyński & Pindor (2000) found that the mean amplitude of Cepheids in the Galaxy is 7% greater than in the LMC, and the mean amplitude of Cepheids in the Small Magellanic Cloud is 25% smaller than in the LMC; they suggested that a natural explanation for the difference is their relative metal content. This difference would be in the same direction as the low metallicity of the outer region of NGC 4258, though more data would be required to see if this is a significant difference. Pulsation models also indicate a dependence between amplitude and chemical composition (Bono et al. 1999; Marconi et al. 2005). Finally, Cepheid amplitudes also vary with temperature or color, resulting in the amplitude-color relations (e.g., Kanbur & Ngeow 2006).

The 2% limit on the difference in the mean of the half amplitude for NGC 4258 (inner field) and the SN hosts constrains the *differential blending* between NGC 4258 and the SN hosts to  $< 5\%$  of the mean Cepheid flux. The uniformity of the observed amplitudes is also consistent with the finding in §3 that the metallicities near the Cepheids are homogeneous.

In Figure 10 we show the composite light curves of all Cepheids with  $P > 60$  d. These have lower mean amplitudes, as expected, but the characteristic sawtooth shape clearly demonstrates their authenticity.

### 3. Cepheid Metallicities and Pulsation Relations

Past work (Kochanek 1997; Kennicutt et al. 1998; Sakai et al. 2004; Macri et al. 2006) has demonstrated a significant dependence between the apparent magnitudes of Cepheids at a fixed

Table 11: V-Band Half-Amplitudes

Host	Mean $V$ ( $\sigma$ )	$\sigma$ from sample mean	No. $P > 10$ d
NGC 3370	0.486(0.011)	0.56	130
NGC 1309	0.474(0.013)	−0.48	86
NGC 3021	0.464(0.020)	−0.78	33
NGC 4536	0.467(0.024)	−0.54	34
NGC 3982	0.490(0.019)	0.56	37
NGC 4639	0.483(0.017)	0.14	30
NGC 4258i	0.472(0.011)	−0.72	144
NGC 4258o	0.418(0.045)	−1.39	7

period and the metallicity in the environment of the Cepheid. This dependence and its uncertainty propagates as one of the largest sources of systematic error in the Hubble constant measured via the LMC,  $\sim 4\%$  (Freedman et al. 2001). The SHOES program was designed to mitigate the sensitivity of the Hubble constant measurement to metallicity by 1) utilizing Cepheids in a narrow range of the metallicity parameter  $[O/H]$ , and by 2) measuring Cepheids in the near-infrared where the metallicity dependence is diminished (Alibert et al. 1999; Persson et al. 2004; Marconi et al. 2005; Gieren et al. 2008).

Nevertheless, to account for even a modest metallicity dependence and its uncertainty, we measured the  $[O/H]$  abundance from 93 H II regions in the vicinity of the Cepheids in all of the galaxies in Table 2 using slit masks with the Low Resolution Imaging Spectrometer on the Keck I telescope (Oke et al. 1995). Our analysis methods are described in §2.5 of Riess et al. (2005) and follow the calibration from Zaritsky et al. (1994), for which  $[O/H]_{\text{solar}} = 7.9 \times 10^{-4}$  and the solar abundance is  $12 + \log[O/H] = 8.9$ . The result is the measurement of a gradient in  $12 + \log[O/H]$  for each galaxy across the deprojected radii occupied by the Cepheids (Table 12), as shown in Figure 11. The intercepts and gradients were used to estimate the metallicity at the deprojected radius of each individual Cepheid.

Table 12: Metallicity ( $12 + \log[O/H]$ ) of SHOES Hosts

Host	at $r = 30''$	change per $10''$	avg. at Cepheid positions	dispersion
NGC1309	9.013	−0.098	8.90	0.19
NGC3021	9.018	−0.224	8.94	0.25
NGC4536	9.104	−0.025	8.79	0.12
NGC4639	9.130	−0.086	8.96	0.14
NGC4258 <sup>a</sup>	9.015	−0.006	8.94	0.05
NGC3370	9.030	−0.090	8.82	0.19
NGC3982	8.998	−0.152	8.74	0.25

<sup>a</sup>For inner field of Macri et al. (2006); outer field average = 8.72, dispersion = 0.03.

The mean value of  $12 + \log[\text{O}/\text{H}]$  at the positions of the Cepheids in the SN hosts is quite similar to that in the *inner field* of NGC 4258, with a difference that is less than the dispersion of the means of the SN hosts. This statement is independent of the normalization of the metallicity scale as it depends on the difference in metallicity. Thus, a correction to the distance scale is unwarranted when comparing these Cepheids.<sup>5</sup> The exception is the outer field of NGC 4258 whose values are determined to be  $8.72 \pm 0.03$ .

Interestingly, the metallicities of the Cepheids in the SN hosts and the inner field of NGC 4258 are very similar to the solar neighborhood value of 8.9 and the value of 8.81 measured for 68 Galactic Cepheids (Andrievsky et al. 2002, 2004). Thus, in principle, Galactic Cepheids could provide a suitable calibration of the luminosities of our Cepheid sample in the SN hosts independent of NGC 4258. In practice, the calibration of Galactic Cepheid luminosities is compromised by the precision and accuracy of their distance estimates, their large extinction, and the inhomogeneity of their photometry.

Sandage & Tammann (2008) contend that the *slope* of the Cepheid  $P$ - $L$  relation is sensitive to chemical composition and that solar-metallicity Cepheids used in the distance scale should be calibrated with Galactic Cepheids. This conclusion could have important consequences for the determination of the distance scale via the LMC. Tammann et al. (2003) used a mixture of Baade-Becker-Wesselink and cluster-based distance estimates to Galactic Cepheids to calibrate the  $V$ -band and  $I$ -band  $P$ - $L$  relations which should then be applicable to the solar-metallicity Cepheids in SN Ia hosts. Corrections for the extinction of Cepheids in SN hosts are subsequently made by the use of two colors and a Galactic reddening law (Saha et al. 2006). This is equivalent to the use of a “Wesenheit reddening-free” mean magnitude,  $m_w$ , defined by Madore (1982) as

$$m_w = m_V - R(m_V - m_I) = a_w \log P + b_w, \quad (3)$$

where  $R \equiv A_V/(A_V - A_I)$ , and  $a_w$  and  $b_w$  are the slope and intercept of this  $P - w$  relation, respectively.

The Tammann et al. (2003) Cepheid analysis provides a slope for the  $P - w$  relation in equation (3) of  $-3.75 \pm 0.09$  mag, which is used by Saha et al. (2006) to determine distances to the SN Ia hosts. This slope is the steepest estimate of the Galactic relation to date (Tammann et al. 2003) and is much steeper than the LMC  $P - w$  slope of  $-3.2$  to  $-3.3$  mag (Udalski et al. 1999). Because the mean period for Cepheids seen in SN hosts,  $\langle P \rangle = 30 - 35$  days, is longer than that in the LMC,  $\langle P \rangle = 5$  days, this steeper slope results in the bulk of the 15% increase in the Sandage et al. (2006) determination of the distance scale from that of Freedman et al. (2001).

---

<sup>5</sup>However, even using the Sakai et al. (2004) zeropoint relation of  $\delta(m - M)\delta[\text{O}/\text{H}] = -0.24 \pm 0.05$  and these Cepheids to calibrate the distance scale would result in a modest 1% correction to the Hubble constant with a systematic error of 0.2%, a substantially reduced sensitivity from past use of LMC Cepheids and their values of  $12 + \log[\text{O}/\text{H}] = 8.5$ .

As seen in Table 12, the measurements here provide the largest sample of Cepheids to date with solar metallicity (mean  $12 + \log[\text{O}/\text{H}] = 8.9$ ), long periods (Kanbur & Ngeow 2004, beyond the break in the LMC relation at  $P = 10$  d), and uniform measurements. Here we use them to measure the slope of the  $P - w$  relation, whose value is vital to measurements of the Hubble constant.

For the Cepheids in each host we fit equation (3) to determine the slope and zeropoint. We used an iterative clipping of  $\pm 3\sigma$  from the mean to remove outliers and limited the fit to Cepheids with  $10 < P < 100$  d to avoid the possibility of a break at  $P = 10$  d and a change of slope at  $P > 100$  days (Bird, Stanek, and Prieto 2009). In the SN hosts we also limited the Cepheids to  $20 < P < 100$  d to mitigate selection as discussed in §2.2. We did not include the outer field of NGC 4258 because it has too few Cepheids (7 with  $P > 10$  d, 2 with  $P > 20$  d) to yield a reliable result. The values and uncertainties of the slopes based on the 445 Cepheids are given in Table 13, and the results are plotted versus the host metallicity in Figure 12. The mean slope for all Cepheids was  $-2.98 \pm 0.07$  mag. Changing the lower period cutoff to  $P > 10$  d for the Cepheids in the SN hosts gives a mean of  $-3.00 \pm 0.07$  mag. Setting the lower period cutoff for each galaxy individually based on the completeness boundaries like those shown in Figures 6 to 8 yields a mean slope of  $-2.98 \pm 0.08$  mag. Overall, we found the mean slope to be insensitive to the period range, with a moderately shallower slope at the longest periods as expected (Bird et al. 2009). This finding is consistent with the analysis by (Madore & Freedman 2009) who show that a color tilt in the monochromatic  $P - L$  slope due to metallicity is diminished in the  $P - w$  due to dereddening.

We find no evidence that the slope is steeper than the LMC slope, as ours is consistent with the LMC though  $1\sigma$  to  $2\sigma$  shallower. The mean slope is significantly lower and inconsistent with the results from Tammann et al. (2003). (Even the poorly determined mean slope of the 3 hosts observed with WFPC2 yield  $-3.26 \pm 0.22$  which is  $> 2\sigma$  shallower than the Tammann et al. slope). We discuss likely origins of this difference in §5.

Table 13: Cepheid  $P - w$  slopes

Host	slope (mag)	$\sigma$
NGC 3370	-2.94	0.14
NGC 1309	-2.82	0.21
NGC 3021	-2.60	0.24
NGC 3982	-3.15	0.42
NGC 4639	-3.07	0.55
NGC 4536	-3.38	0.30
NGC 4258i	-3.05	0.10

#### 4. Light Curves of SN 1995al and SN 2002fk

Use of the Cepheid data in the previous sections and the flux-calibrated light curves of the new SNe presented in this section provide the means to determine their luminosity.

Both SN 1995al (NGC 3021) and SN 2002fk (NGC 1309) were spectroscopically normal SNe Ia (Wei et al. 1995; Ayani & Yamaoka 2002).

SN 2002fk was extensively monitored by the 0.76 m Katzman Automatic Imaging Telescope (KAIT; Li et al. 2000; Filippenko et al. 2001) commencing 13 d before  $B$ -band maximum. The SN photometry was measured with the benefit of galaxy subtraction and PSF fitting relative to stars in the field of the SN. These field stars were later calibrated on five photometric nights with KAIT and the Nickel 1 m telescope at the Lick Observatory using Landolt (1992) standards.

The mean magnitudes of the field stars are given in Table 14 and their positions are shown in Figure 13. The light curves of the SN are shown in Figure 14 compared to their model fits using the MLCS2k2 (Jha et al. 2007) algorithm. The fits are consistent with those obtained for well-observed SNe Ia and are sufficient to constrain the relative distance modulus to a precision of 0.068 mag or 0.105 mag, with the intrinsic contribution of 0.08 mag (Jha et al. 2007) added in quadrature.

For SN 1995al, photometric monitoring was conducted starting 5 d before  $B$ -band maximum with the FLWO 1.2 m telescope equipped with a thick, front-illuminated Loral CCD (“Andycam”) and a set of Johnson  $UBV$  and Kron-Cousins  $RI$  filters. The observations were initially presented by Riess et al. (1999) as a member of a set of 22 SNe Ia and we direct the reader there for additional details. The photometry presented by Riess et al. lacked the benefit of galaxy template subtraction and multiple zeropoint calibrations. These steps can improve the precision of SN Ia photometry and a reanalysis is warranted for including this SN in the small calibration set. We have now undertaken the galaxy subtraction and obtained zeropoint calibrations on 5 independent nights using the Landolt (1992) standard stars for the fundamental calibration.

The mean magnitudes of the field stars are given in Table 15 and their positions are shown in Figure 13. The photometric differences with the version from Riess et al. (1999) are a few hundredths of a magnitude in all bands except  $I$ , which differed in the mean by 0.1 mag. The light curves of the SNe are shown in Figure 14 compared to their model fits using the MLCS2k2 (Jha et al. 2007) algorithm.

Photometry of the two SNe is given in Tables 16 and 17 and their photometric parameters in Table 18.

It is important to insure that the photometry of the other 4 SNe Ia in Table 2 is also reliable. For SN 1990N, Lira et al. (1999) undertook a comprehensive recalibration of SN 1990N. SN 1994ae was recalibrated using galaxy subtraction in Riess et al. (2005) which also contained the calibration of SN 1998aq using the same techniques.

We have also verified the photometric calibration of SN 1981B presented by Buta & Turner



Table 14. Comparison Stars for SN 2002fk

Star	<i>U</i>	N	<i>B</i>	N	<i>V</i>	N	<i>R</i>	N	<i>I</i>	N
1	—	0	16.255(0.007)	5	15.748(0.013)	5	15.441(0.006)	3	15.034(0.010)	3
2	—	0	16.415(0.006)	5	15.784(0.012)	3	15.405(0.015)	3	15.002(0.002)	2
3	—	0	16.331(0.009)	5	15.787(0.007)	5	15.444(0.012)	4	15.047(0.015)	4
4	—	0	17.513(0.010)	3	16.954(0.012)	5	16.611(0.014)	2	16.176(0.009)	2

Table 15. Comparison Stars for SN 1995al

Star	<i>U</i>	N	<i>B</i>	N	<i>V</i>	N	<i>R</i>	N	<i>I</i>	N
0	15.078(0.019)	3	14.619(0.004)	4	13.795(0.004)	4	13.307(0.004)	3	12.836(0.008)	3
1	19.027(0.079)	2	18.050(0.051)	2	16.865(0.007)	2	16.067(0.002)	2	15.350(0.011)	2
2	13.633(0.021)	2	13.686(0.009)	2	13.246(0.015)	2	12.977(0.013)	2	12.692(0.004)	2
3	14.586(0.025)	3	14.628(0.006)	3	14.132(0.008)	3	13.842(0.008)	3	13.551(0.009)	3
4	15.390(0.018)	3	14.870(0.002)	4	14.050(0.006)	4	13.620(0.005)	3	13.244(0.006)	3
5	16.536(0.012)	3	16.744(0.002)	4	16.322(0.007)	4	16.042(0.009)	4	15.737(0.012)	4
6	18.499(0.007)	2	17.451(0.013)	4	16.425(0.005)	4	15.822(0.012)	4	15.326(0.014)	4
7	16.894(0.027)	2	16.667(0.004)	4	15.990(0.004)	4	15.609(0.008)	4	15.250(0.010)	4
8	17.893(0.012)	3	17.538(0.006)	4	16.757(0.006)	4	16.295(0.009)	4	15.881(0.017)	4
9	17.558(0.019)	2	16.878(0.009)	4	15.967(0.011)	4	15.429(0.011)	4	14.928(0.015)	4
10	99.999(9.999)	0	17.371(0.015)	4	15.879(0.003)	4	14.820(0.005)	3	13.629(0.016)	3
11	15.432(0.021)	3	15.291(0.009)	4	14.654(0.006)	4	14.296(0.005)	4	13.951(0.009)	4
12	17.086(0.006)	3	16.860(0.012)	4	16.132(0.015)	4	15.693(0.013)	4	15.318(0.008)	4

Table 16. Photometry of SN 2002fk

JD-2.4e6	<i>B</i>	<i>V</i>	<i>R</i>	<i>I</i>
52535.99	15.061(0.010)	15.152(0.032)	15.090(0.049)	14.879(0.025)
52537.00	14.667(0.011)	14.760(0.010)	14.721(0.038)	14.518(0.020)
52537.97	14.347(0.010)	14.450(0.012)	14.396(0.033)	14.238(0.011)
52541.99	13.600(0.010)	13.714(0.011)	13.693(0.042)	13.603(0.015)
52544.00	13.472(0.010)	13.592(0.028)	13.529(0.016)	13.557(0.020)
52544.96	13.386(0.010)	13.508(0.020)	13.462(0.010)	13.510(0.011)
52548.99	13.327(0.010)	13.366(0.011)	13.382(0.011)	13.573(0.010)
52549.98	13.311(0.010)	13.363(0.010)	13.380(0.010)	13.589(0.011)
52550.95	13.349(0.011)	13.400(0.010)	13.380(0.010)	13.654(0.012)
52551.97	13.383(0.011)	13.424(0.010)	13.397(0.013)	13.691(0.010)
52553.95	13.519(0.011)	13.468(0.011)	13.481(0.013)	13.784(0.012)
52555.94	13.658(0.010)	13.549(0.010)	13.647(0.036)	13.953(0.010)
52559.95	13.973(0.013)	13.766(0.010)	13.941(0.035)	14.199(0.012)
52562.89	14.298(0.011)	13.957(0.010)	14.111(0.033)	14.292(0.010)
52565.90	14.669(0.010)	14.127(0.013)	14.187(0.049)	14.296(0.034)
52570.95	—	14.372(0.025)	14.191(0.030)	14.179(0.039)
52574.87	15.549(0.013)	14.569(0.022)	14.269(0.040)	14.023(0.011)
52576.89	15.757(0.042)	14.684(0.011)	14.378(0.038)	14.044(0.010)
52579.90	15.977(0.048)	14.859(0.016)	14.488(0.010)	14.121(0.011)
52582.87	16.109(0.031)	15.055(0.026)	14.690(0.010)	14.293(0.010)
52588.93	16.363(0.038)	15.367(0.025)	15.024(0.034)	—
52594.84	16.513(0.018)	15.538(0.021)	15.263(0.017)	15.003(0.028)
52604.83	16.650(0.017)	15.819(0.012)	15.635(0.011)	15.490(0.026)
52607.80	16.751(0.027)	15.884(0.014)	15.705(0.049)	15.600(0.018)
52610.85	16.812(0.034)	15.996(0.019)	15.826(0.024)	15.755(0.026)
52613.81	16.799(0.017)	16.037(0.020)	15.955(0.014)	15.917(0.032)
52616.79	16.873(0.038)	16.161(0.027)	16.011(0.033)	16.097(0.060)
52619.77	16.889(0.020)	16.223(0.037)	16.147(0.053)	16.090(0.035)
52631.79	17.153(0.028)	16.547(0.026)	16.584(0.063)	16.595(0.069)
52644.73	17.323(0.048)	16.830(0.018)	16.977(0.020)	17.103(0.074)
52657.72	17.301(0.084)	17.148(0.036)	17.309(0.050)	17.792(0.135)
52673.63	17.723(0.101)	17.551(0.035)	17.903(0.050)	18.125(0.139)

(1983). For the Buta & Turner stars A, B, and C, we found respective differences in the  $B$ -band of 0.02, -0.01, and 0.02 mag (an average of 0.01 mag), where a positive difference indicates our photometry is brighter. For the  $V$  band we found differences of 0.01, 0.00, and 0.00 mag, respectively.

## 5. Discussion

In a companion paper (Riess et al. 2009), we present IR measurements from NICMOS on *HST* of the Cepheids analyzed here. Although the new, optical photometry of SNe Ia and Cepheids presented here already addresses some of the largest sources of systematic error in the determination of the Hubble constant, the *remaining* errors are further reduced from observations of these Cepheids at longer wavelengths.

One of the biggest of these remaining uncertainties results from the corrections applied for Cepheid reddening. Systematic errors in the apparent color excess arise from differences in the photometric system used to measure Cepheid colors in the SN hosts and the anchor galaxy or from intrinsic differences in color resulting from those in metallicity. Errors in the optical color excess are further amplified by use of a  $V - I$  reddening ratio,  $R = \frac{A_V}{E_{V-I}} \approx 2.5$ . Another source of error arises from differences in the value of  $R$  from host to host or sight line to sight line for which Galactic variations in  $R$  are  $\sim 0.2$  (Valencic, Clayton and Gordon 2004). Reobserving the Cepheids with a single instrument (to negate photometric system differences) and at redder wavelengths (reducing the scale of  $R$  and its variations) would mitigate these uncertainties. We therefore defer our full analysis of the Hubble constant resulting from the data presented here to Riess et al. (2009), where we present the long-wavelength observations from NICMOS.

However, we note here that the two new SNe Ia, SN 1995al and SN 2002fk, and the Cepheids in their hosts yield estimates of the SN Ia luminosity (corrected to the fiducial of the luminosity-light curve shape relation) which are quite consistent with the other SNe in Table 2. Due to the relationship between luminosity and light curve shape, the value of the fiducial luminosity depends on which light curve shape within a family of light curves is chosen to be the fiducial. Based on the maser distance to NGC 4258 and its Cepheids, Riess et al. (2009) find for the MLCS2k2 light curve family (Jha, Riess, Kirshner 2005) the fiducial, dereddened absolute magnitude,  $M_V^0$  (defined at the time of  $B$  max) of SN 1995al and SN 2002fk is  $-18.99 \pm 0.14$  and  $-19.16 \pm 0.12$  mag, respectively, in good agreement with the average of  $-19.05 \pm 0.07$  mag for the mean of the previous four (also from Riess et al. 2009). Thus the average for all 6 is  $M_V^0 = -19.06 \pm 0.05$ .

From our analysis it appears that the slopes for  $P-L$  and  $P - w$  derived by Tammann et al. (2003) from Galactic Cepheids are inaccurate. Even limiting the analysis of the Tammann et al. Cepheids to the 27 with  $P > 10$  d, in order to remove more rapid ones not represented in our sample, we find a slope of  $-4.37 \pm 0.18$ . The Galactic Cepheids have the *same metallicity* as those presented here yet the Tammann et al. slope is  $7\sigma$  greater than the mean of  $-2.98 \pm 0.07$  for the 7

Table 17. Photometry of SN 1995al

JD-2.4e6	$U$	$B$	$V$	$R$	$I$
50024.990	—	13.45(0.02)	13.43(0.02)	13.32(0.06)	13.64(0.02)
50026.030	13.01(0.02)	13.40(0.02)	—	13.32(0.02)	13.61(0.02)
50030.010	13.23(0.04)	13.28(0.02)	13.25(0.04)	13.24(0.02)	13.66(0.02)
50032.000	13.35(0.02)	13.32(0.02)	13.28(0.02)	13.24(0.02)	13.70(0.02)
50035.020	13.48(0.04)	13.53(0.02)	13.33(0.02)	13.34(0.02)	13.82(0.02)
50037.020	—	13.69(0.02)	13.43(0.02)	13.32(0.10)	13.87(0.02)
50038.020	13.60(0.04)	13.70(0.02)	13.43(0.02)	13.48(0.02)	13.96(0.02)
50040.000	—	13.85(0.02)	13.55(0.02)	13.62(0.02)	13.99(0.02)
50042.000	14.16(0.06)	14.08(0.02)	13.71(0.02)	13.82(0.03)	14.20(0.07)
50047.980	—	14.55(0.02)	13.82(0.02)	13.81(0.02)	13.94(0.03)
50051.020	15.18(0.03)	15.00(0.02)	14.01(0.03)	13.88(0.03)	13.89(0.04)
50067.000	16.38(0.04)	16.06(0.02)	14.88(0.02)	14.50(0.02)	14.22(0.02)
50070.860	—	16.19(0.02)	15.07(0.02)	14.74(0.02)	14.47(0.02)
50078.950	—	16.38(0.06)	15.35(0.02)	14.99(0.06)	14.90(0.02)
50086.980	—	16.54(0.04)	15.55(0.03)	15.32(0.06)	15.25(0.05)
50088.900	—	16.51(0.06)	15.58(0.03)	15.33(0.05)	15.25(0.05)
50103.820	—	16.76(0.08)	16.02(0.04)	15.86(0.03)	15.91(0.05)
50136.900	—	17.31(0.12)	16.86(0.08)	16.90(0.12)	17.21(0.17)
50161.730	—	17.81(0.21)	17.53(0.16)	17.85(0.21)	17.83(0.45)

Table 18. Table 18: SN Observables<sup>a</sup>

SN	$U_{\max}$ (mag)	$B_{\max}$ (mag)	$V_{\max}$ (mag)	$R_{\max}$ (mag)	$I_{\max}$ (mag)	$\Delta m_{15}(B)$
SN 2002fk	—	13.32(0.02)	13.38(0.02)	13.39(0.03)	13.50(0.04)	1.08(0.03)
SN 1995al	13.01(0.05)	13.31(0.02)	13.27(0.02)	13.23(0.02)	13.62(0.03)	1.00(0.05)

<sup>a</sup>The uncertainty is given in parentheses.

hosts in Table 13. While one might invoke an unusual helium abundance as a possible explanation for the conflict with a single host (e.g., for NGC 4258 when Macri et al. 2006 showed the same discrepancy), this would be unlikely to explain why each of the 7 hosts in Table 13 are inconsistent with the Tammann et al. slope for  $P > 10$  d Cepheids.

We note that it is far more difficult to reliably measure the  $P - w$  (or  $P - L$ ) slope of Galactic Cepheids (from our vantage point within the Galaxy) than for extragalactic Cepheids. While Cepheids in an external host can be treated as coincident in distance, the estimate of the Galactic Cepheid slope suffers from the need for many individual, accurate distances. The cluster-based distances used for the longest period Galactic Cepheids are not very reliable as they frequently utilize tenuous stellar associations rather than cluster membership. In addition, past distance estimates to Galactic Cepheids using the Baade-Becker-Wesselink method did not consider a period dependence of the projection factor which may be significant (Gieren et al. 2005; Fouqué et al. 2007) and could lead to an inaccurate slope.

Geometric distance measurements via parallax are the "gold standard" for estimating distances. They are much more robust than the previous methods. The direct parallaxes of 10 Galactic Cepheids were measured by Benedict et al. (2007) using the Fine Guidance Sensor on *HST*. These 10 Cepheids alone or combined with Hipparcos parallaxes yield a  $P - w$  slope of  $-3.29 \pm 0.15$  (van Leeuwen et al. 2007), consistent with the SN hosts ( $-2.98 \pm 0.07$ ) and the LMC ( $-3.2$  to  $-3.3$ ).

The mean extinction of the Tammann et al Galactic Cepheids is high, with a mean of 1.8 visual magnitudes, and is even higher for the longest period Cepheids. A possible error in the assumed value of the reddening parameter (e.g.,  $\sigma_R \approx 0.5$ ) for these Cepheids would bias the pulsation relations by 0.3 mag if each had the same extinction. Thus, without more precise knowledge of this ratio of optical absorption to reddening, it does not seem possible to use the Galactic Cepheids with high extinction to determine  $H_0$  to better than  $\sim 15\%$ . Because younger and higher mass Cepheids have more than the average extinction, the *slope* of the inferred Galactic  $P - L$  can also be biased by an error in  $R$ . The mean of the Benedict et al Cepheids is a more modest 0.36 visual magnitudes which also adds to their reliability.

The Galactic measurement at the long-period end also suffers from limited statistics. The Tammann et al. (2003) sample has a mean period of 12 d with only 7 Cepheids at  $P > 30$  d and only 1 at  $P > 50$  d. In our SN hosts, over 200 Cepheids (more than half of the sample) have  $P > 30$  d. A Galactic sample of just 7 Cepheids at this range and with the aforementioned concerns would appear insufficient, even if their luminosities were accurate, to support a very precise measurement of the Hubble constant. However, the product of the 0.5 mag steeper slope from that of the Benedict et al sample or the SN host sample and difference in the mean period between the Galactic and SN host samples of  $\Delta \log P = 0.4 - 0.5$  causes a decrease in  $H_0$  of 10%-12% in Sandage et al.

Comparing results for the sum of the standardized peak magnitudes of nearby SNe Ia and the

Hubble diagram intercept,  $m_{v,i}^0 + 5a_v$ , a quantity which is invariant to the method of standardization, the difference of the weighted mean for the four (out of six) SNe Ia (SN 1981B, SN 1990N, SN 1994ae, and SN 1998aq) that are in common with Sandage et al. (2006) is  $0.02 \pm 0.04$  mag, showing excellent agreement. Sandage et al. (2006) also use SNe Ia data obtained from the photographic era (SN 1937C, 1960F, and 1974G) which R05 do not. There are clear reasons for not using the photographic data: they are not measured in the same way as for the Hubble-flow set, they have been shown to be unreliable, and they disagree with modern data (Riess et al. 2005). Even within the Sandage et al. analysis, the the absolute magnitude inferred from the photographic subset ( $-19.68 \pm 0.10$ ) differs from the modern set ( $-19.42 \pm 0.05$ ) by  $2.6\sigma$ , making the average brighter by 0.05 mag and decreasing  $H_0$  by 2.5%.

Little of the difference in  $H_0$  results from the determination of the absolute distance scale. Sandage et al. (2006) use an LMC distance modulus  $\mu_0 = 18.54$  mag as one route to their value. The implied LMC distance based on NGC 4258 and Galactic Cepheids (Macri et al. 2006; Benedict et al. 2007) is  $\mu_0 \sim 18.42$  mag, and Freedman et al. (2001) and Riess et al. (2005) adopted  $m_{u_0} \equiv 18.50$  mag.

## 6. Summary and Conclusions

(1) Using ACS we have observed a total of 237 Cepheids (216 with  $P > 20$  d) in three recent SN Ia hosts: NGC 1309 (SN 2002fk), NGC 3021 (SN 1995al), and NGC 3370 (SN 1994ae). We also present the multi-band light curves of SN 1995al and SN 2002fk.

(2) We reobserved the hosts of 6 reliable SNe Ia and the “maser galaxy” NGC 4258 in *HST* Cycle 15 (following the initial contiguous cycle of *HST* discovery observations) to identify longer period Cepheids. We found 57 with  $60 < P < 100$  d and 29 with  $75 < P < 100$  d which can aid in extending Cepheid measurements to greater distances.

(3) We have measured the metallicity parameter,  $12 + \log[\text{O}/\text{H}]$ , in H II regions to infer the metallicity of the Cepheid sample. We find the values for the Cepheids in the SN hosts and the inner region of NGC 4258 to be very homogeneous, all consistent with the solar value of 8.9.

(4) Based on 445 Cepheids across 7 hosts of solar metallicity we find the mean slope of the  $P - w$  relation using  $V$ -band and  $I$ -band measurements, the most commonly used for distance-scale work, to be  $-2.98 \pm 0.07$ . The 7 individual slopes are all consistent with the mean. The observed slope is fairly consistent with the slope of LMC Cepheids and consistent with the slope from Galactic Cepheid parallax distances. It is inconsistent with the slope of Galactic Cepheid distances from Tammann et al. (2003) using Baade-Becker-Wesselink and cluster distances. Using the slope derived here increases the value of  $H_0$  from that measured by Sandage et al. (2006) and Tammann et al. (2008) by  $\sim 15\%$  and constitutes the bulk of the difference in  $H_0$  with Freedman et al. (2001) and Riess et al. (2005). A companion paper (Riess et al. 2009) provides the addition of  $H$ -band measurements of the Cepheids in the 7 hosts and takes advantage of the

full reduction in systematic errors afforded by our refurbished distance ladder to provide a new determination of  $H_0$ .

We are grateful to Peter Stetson for making his DAOPHOT/ALLFRAME software available. Financial support for this work was provided by NASA through programs GO-9352, GO-9728, GO-10189, GO-10339, GO-10497 and GO-10802 from the Space Telescope Science Institute, which is operated by AURA, Inc., under NASA contract NAS 5-26555. A.V.F.'s supernova group at U.C. Berkeley is also supported by NSF grant AST-0607485 and by the TABASGO Foundation. KAIT was constructed and supported by donations from Sun Microsystems, Inc., the Hewlett-Packard Company, AutoScope Corporation, Lick Observatory, the US National Science Foundation (NSF), the University of California, the Sylvia & Jim Katzman Foundation, and the TABASGO Foundation. Some of the data presented herein were obtained with the W. M. Keck Observatory, which is operated as a scientific partnership among the California Institute of Technology, the University of California, and NASA; the observatory was made possible by the generous financial support of the W. M. Keck Foundation. We wish to extend special thanks to those of Hawaiian ancestry on whose sacred mountain we are privileged to be guests.

### Figure Captions

Figure 1: Image of a  $2' \times 2'$  region of the field of NGC 1309 from ACS WFC  $F555W$ . North is up and east to the left. The locations of the Cepheids identified are indicated by circles.

Figure 2: Same as Figure 1 but for NGC 3021.

Figure 3:  $F555W$  and  $F814W$  light curves of Cepheids in NGC 3021. For each of the Cepheid candidates listed by identification number in Table 8, the photometry is fit to the period-specific light-curve template.

Figure 4: Same as Figure 3 for NGC 1309 (see Table 7).

Figure 5:  $V$ -band,  $I$ -band, and Wesenheit dereddened  $[V - 2.45(V - I)]$   $P$ - $L$  relations for Cepheids identified in NGC 1309. The  $P$ - $L$  relation shown is from the LMC and is only fit to the filled symbols (see Figure 12 for a slope fit to the individual relations). An approximate instability-strip width of 0.35 mag is also given for comparison. Open symbols indicate short-period Cepheids in the period range which appears to suffer an incompleteness bias (preferentially bright or significantly blended with a blue source).

Figure 6: Same as Figure 5 but for NGC 3021.

Figure 7: Same as Figure 5 but for NGC 3370.

Figure 8: Dereddened distance modulus from the  $P - w$  relation as a function of the period cutoff. Although there is some evidence of an incompleteness bias at the short-period end of the  $V$ -band and  $I$ -band  $P$ - $L$  relations, there is no significant change in the dereddened distance modulus with period cutoff.

Figure 9: Composite  $V$ -band Cepheid light curves. For the Cepheids with  $P > 10$  d in each host, the fitted mean magnitude was subtracted from the observations which were then plotted as a function of their phase, as inferred from the fitted period. As seen and shown in Table 11, for each host the mean half-amplitude is consistent with 0.48 mag. This consistency indicates a lack of significant variation in blending from host to host and also provides a more direct probe of metallicity which can cause amplitude differences in the mean.

Figure 10: Composite  $V$ -band Cepheid light curves of the longer period Cepheids,  $P > 60$  d, whose discovery was enabled by reobservations of each host  $HST$  cycles subsequent to the discovery cycle. Although Cepheids at  $P > 60$  d have reduced amplitudes, they exhibit the characteristic sawtooth light curve of a classical Cepheid and serve to extend the use of the  $P$ - $L$  to greater distances.

Figure 11: Radial gradients of the oxygen-to-hydrogen ratios  $[O/H]$  of H II regions in the Cepheid hosts. Following the method of Zaritsky et al. (1994), emission-line intensity ratios of  $[O II] \lambda\lambda 3726, 3729$ ,  $[O III] \lambda\lambda 4959, 5007$ , and  $H\beta$  were used to derive values of  $12 + \log[O/H]$  for H II regions. The fitted linear gradient was used to determine the value of the metallicity correction



at the individual radii of the observed Cepheids. The variance in the data is dominated by spatial variations, not measurement errors.

Figure 12: The measured slopes of the dereddened (Wesenheit)  $P - w$  relations as a function of the mean metallicity parameter. The 7 hosts in Table 2 (including the inner region of NGC 4258) have solar-like metallicities and slopes which are mutually consistent with their mean of  $-2.98 \pm 0.07$ . This mean is consistent with the slope inferred from parallax distances to Galactic Cepheids (Leeuwen et al. 2007) indicated by the X, in good agreement with the LMC slope (square) and inconsistent with the Galactic slope (diamond) inferred from non-geometric distance measures (Tammann et al. 2003).

Figure 13: Ground-based comparison stars in the field of NGC 1309 (SN 2002fk; *left*) and NGC 3021 (SN 1995al; *right*) used to calibrate the light curves of the respective SNe Ia.

Figure 14: MLCS2k2 fits to the multi-band data for SN 1995al and SN 2002fk.

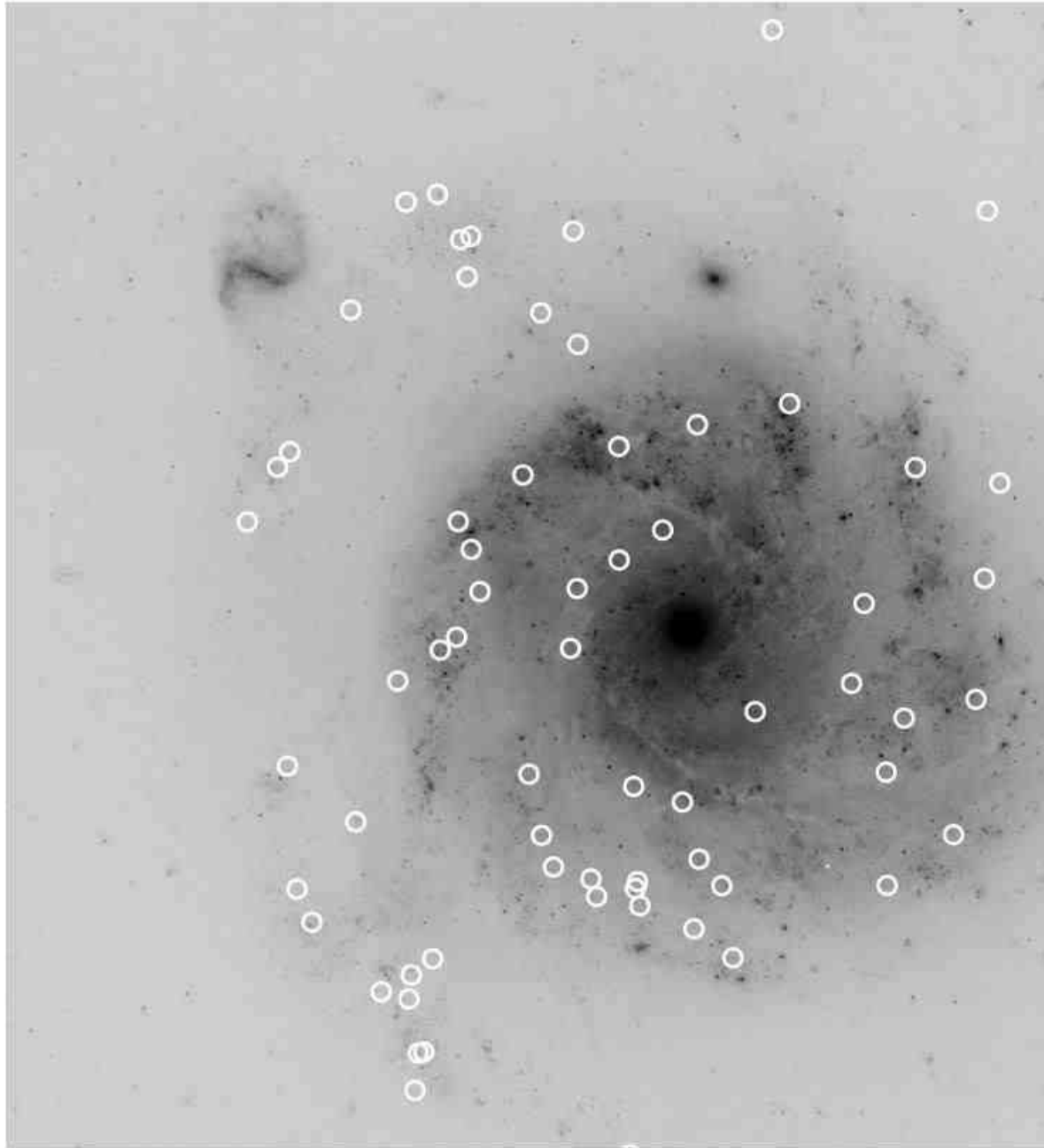


Fig. 1.—

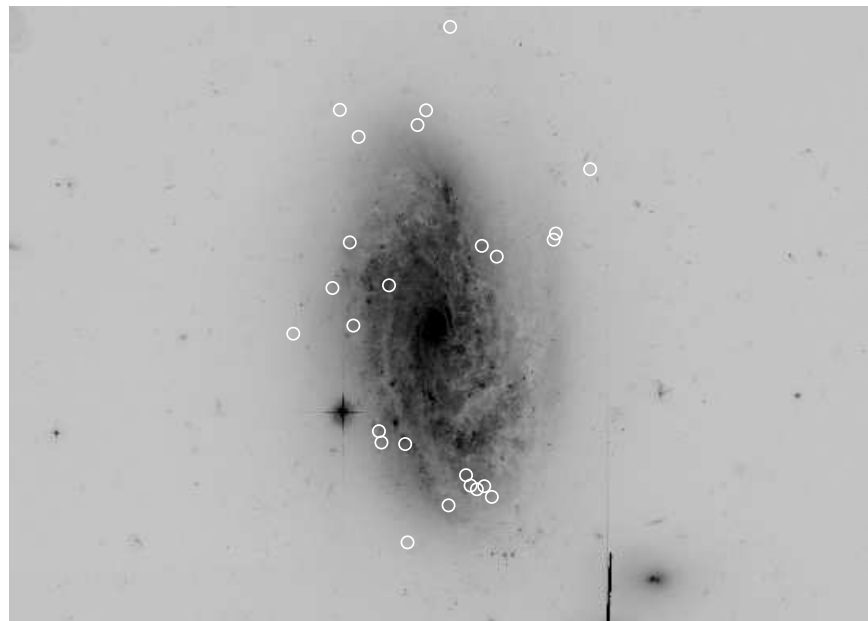


Fig. 2.—

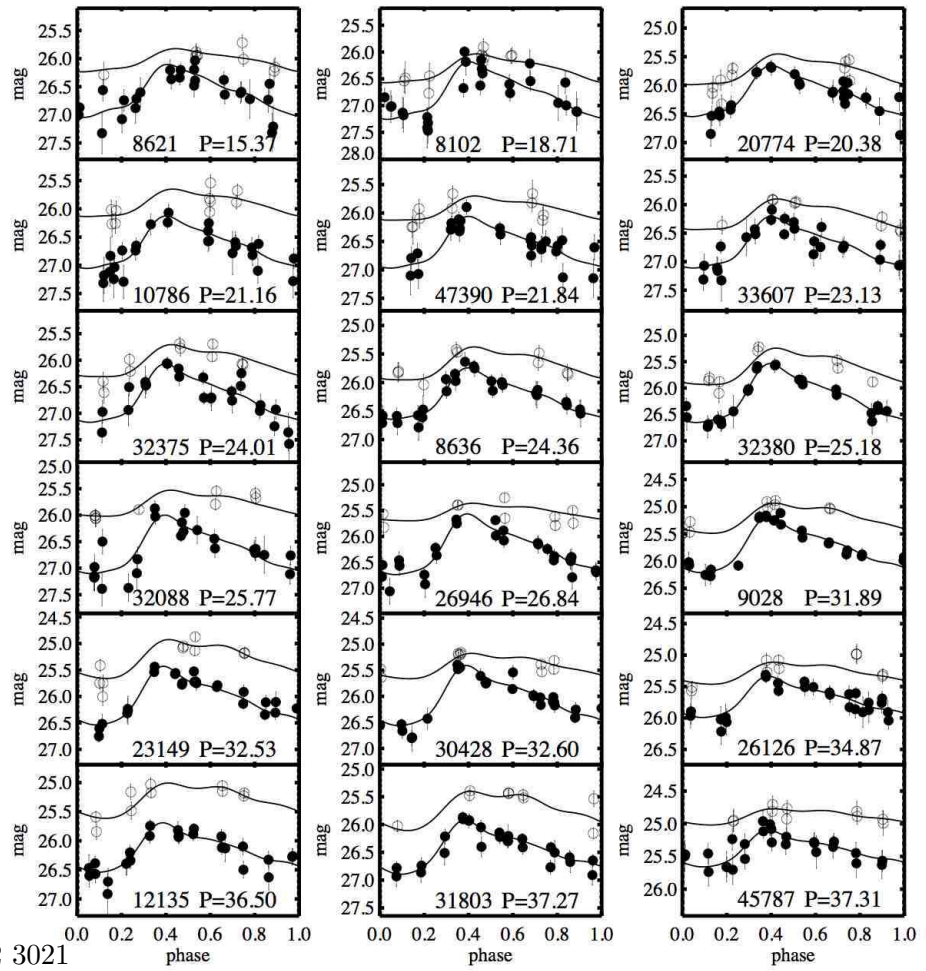


Fig. 3.— Page 1 of 2 3021

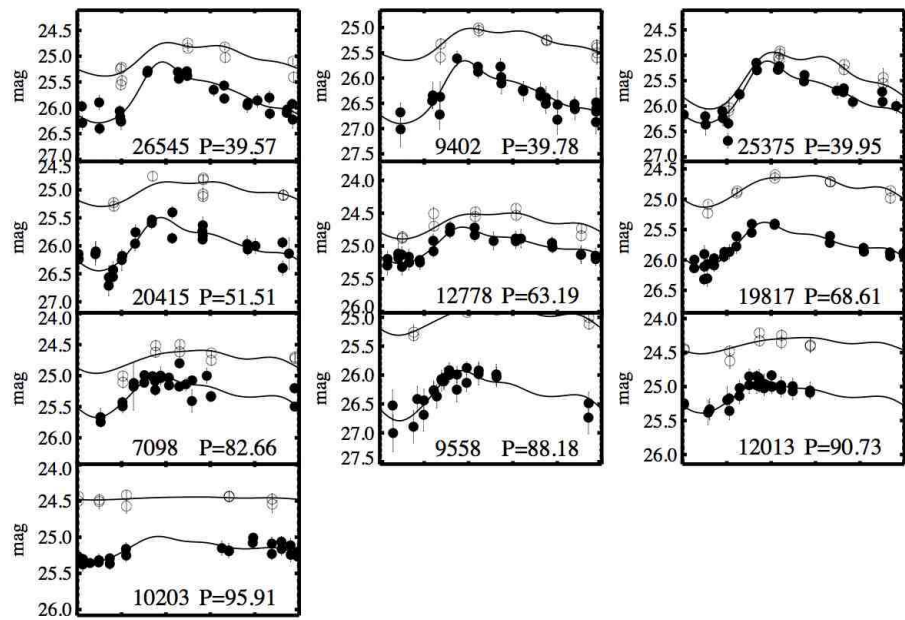


Fig. 3.— Page 2 of 2 3021

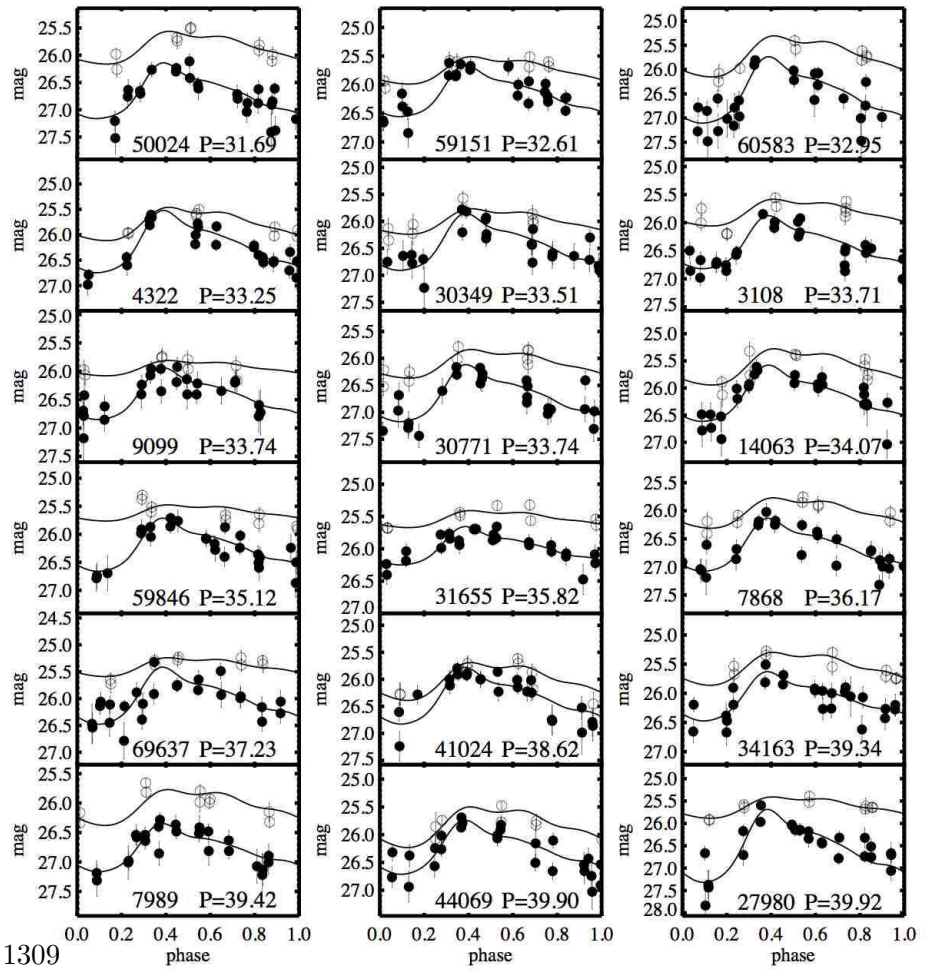


Fig. 4.— Page 1 of 5 1309

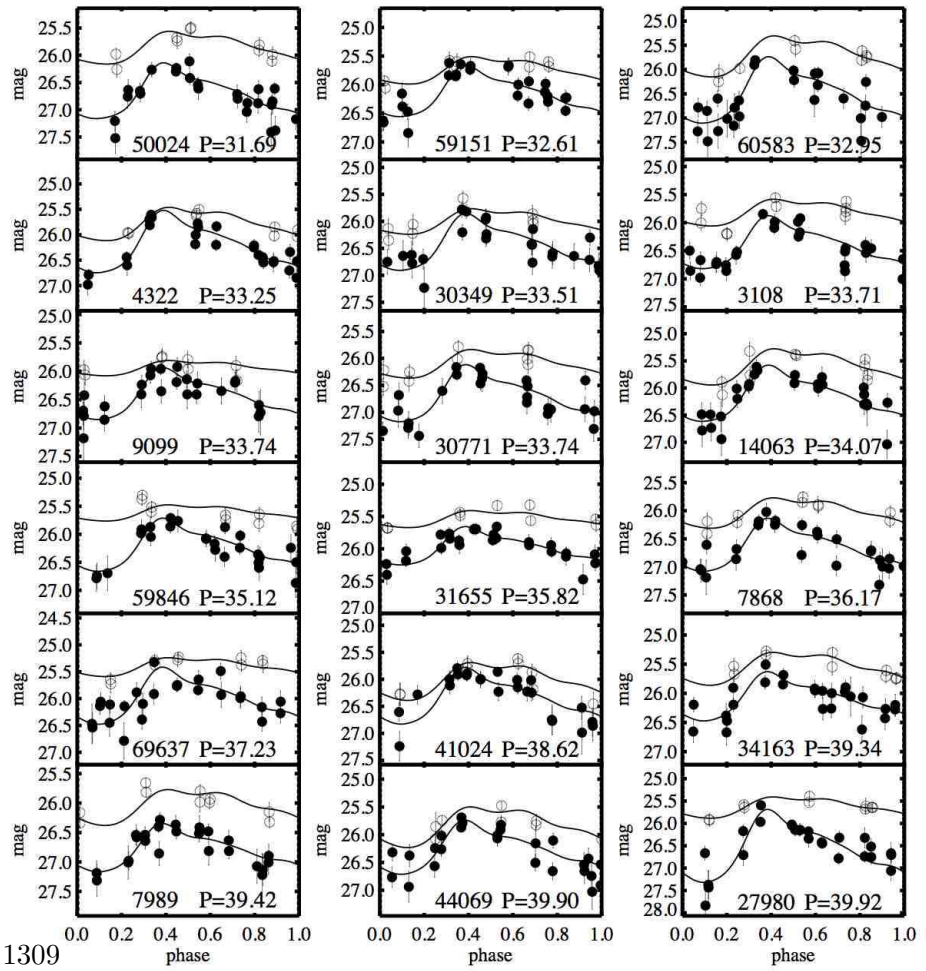


Fig. 4.— Page 2 of 5 1309

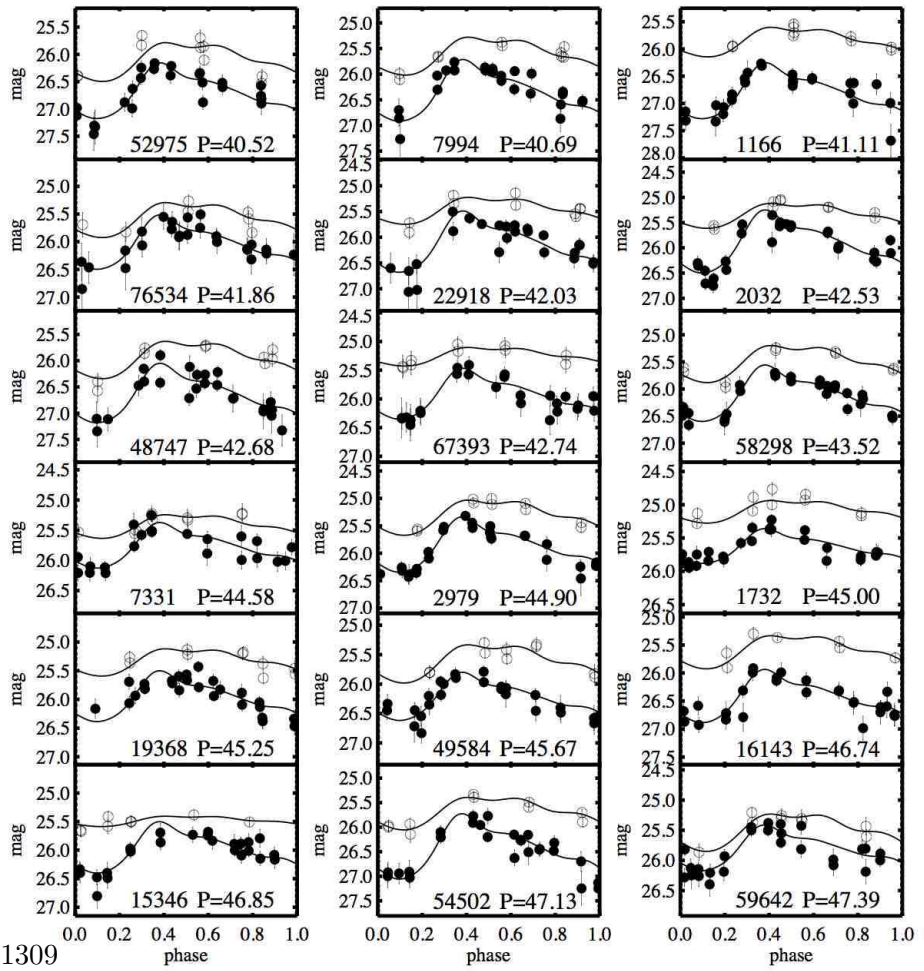


Fig. 4.— Page 3 of 5 1309



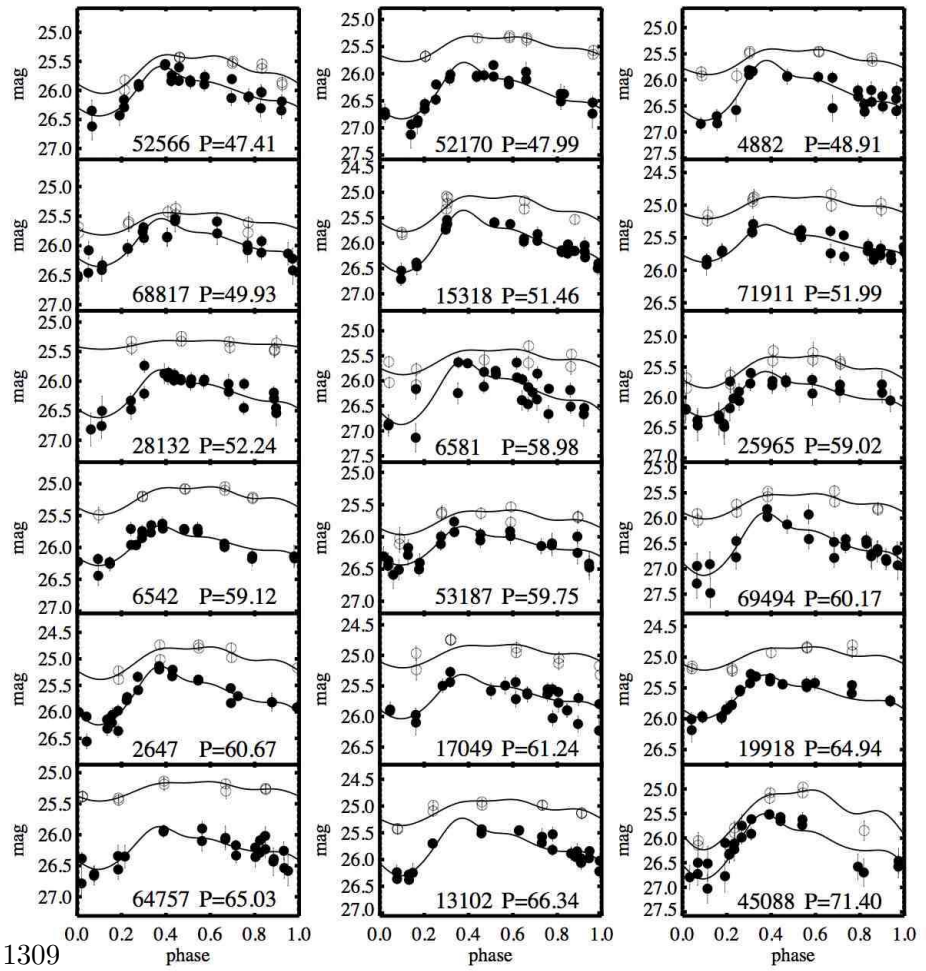


Fig. 4.— Page 4 of 5 1309

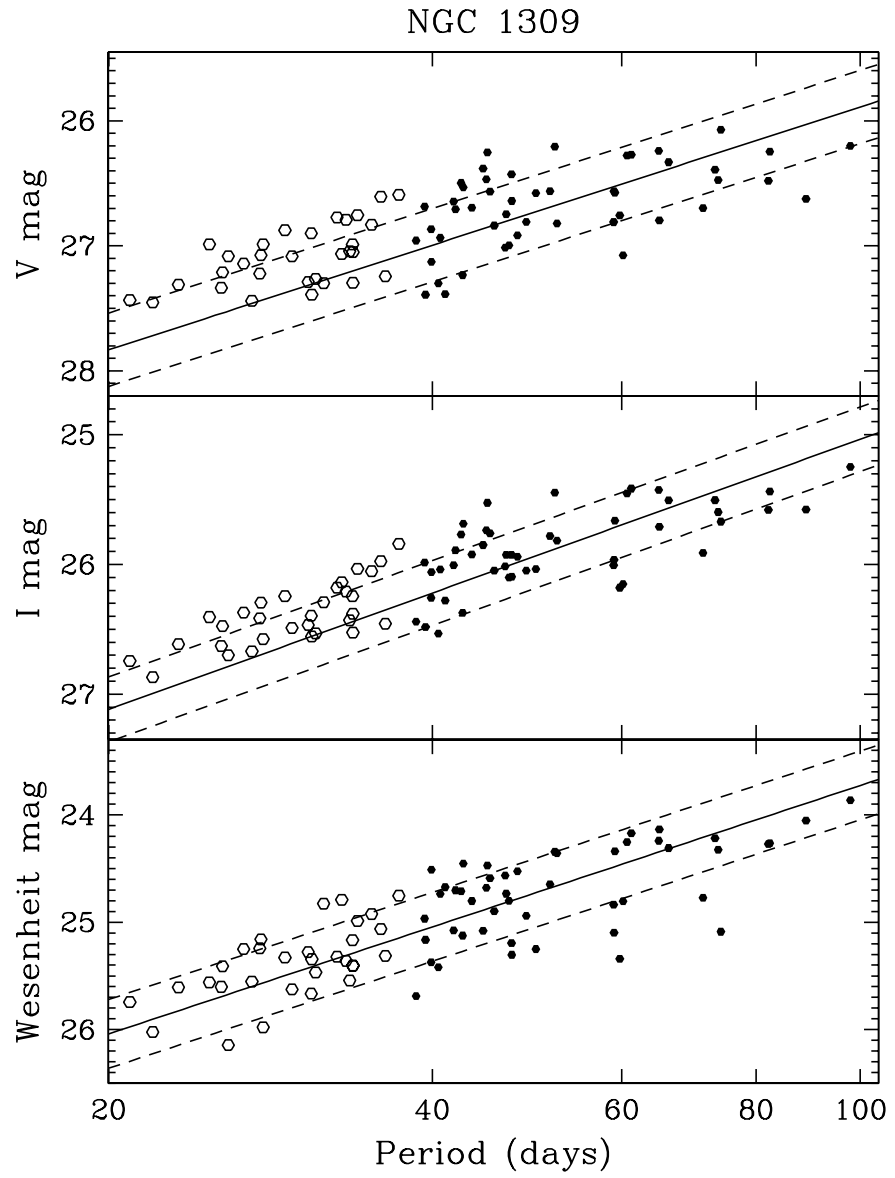


Fig. 5.—

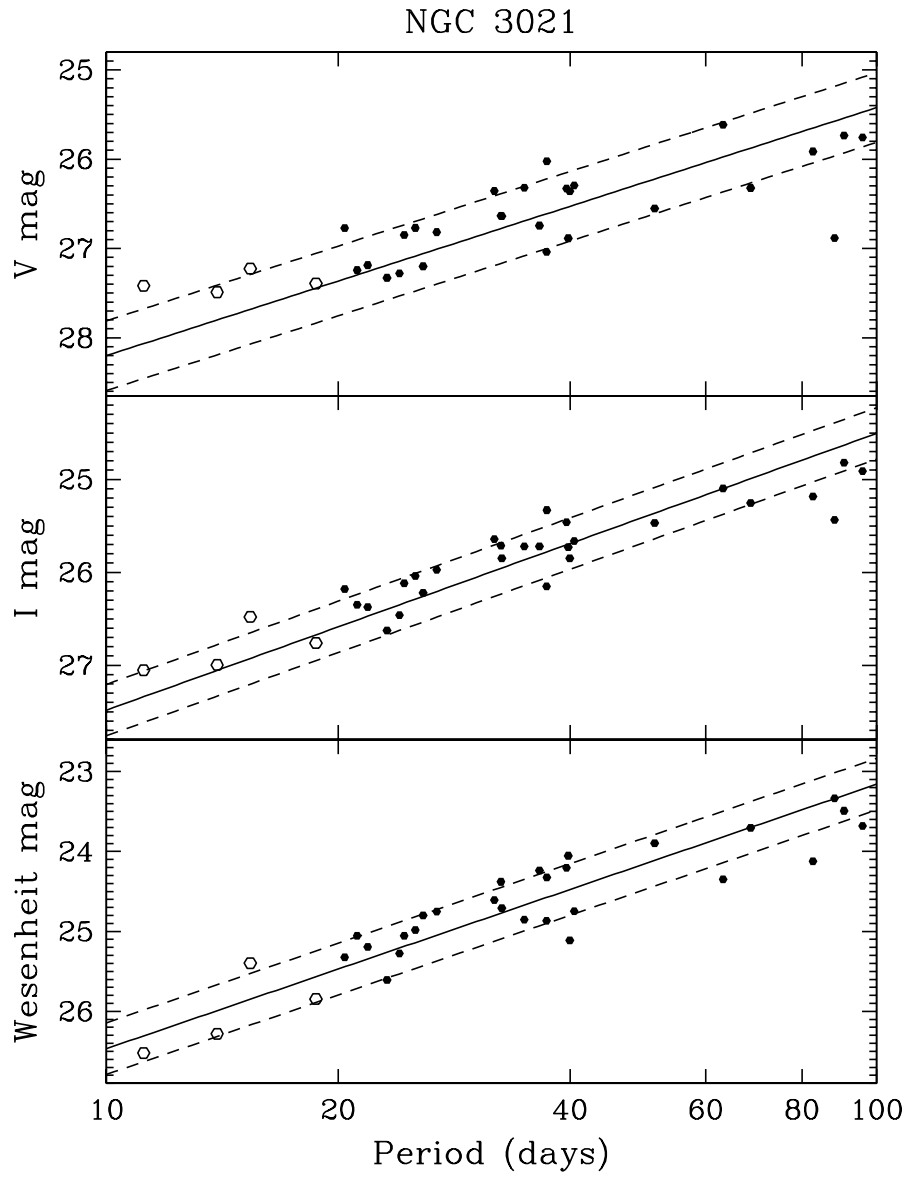


Fig. 6.—

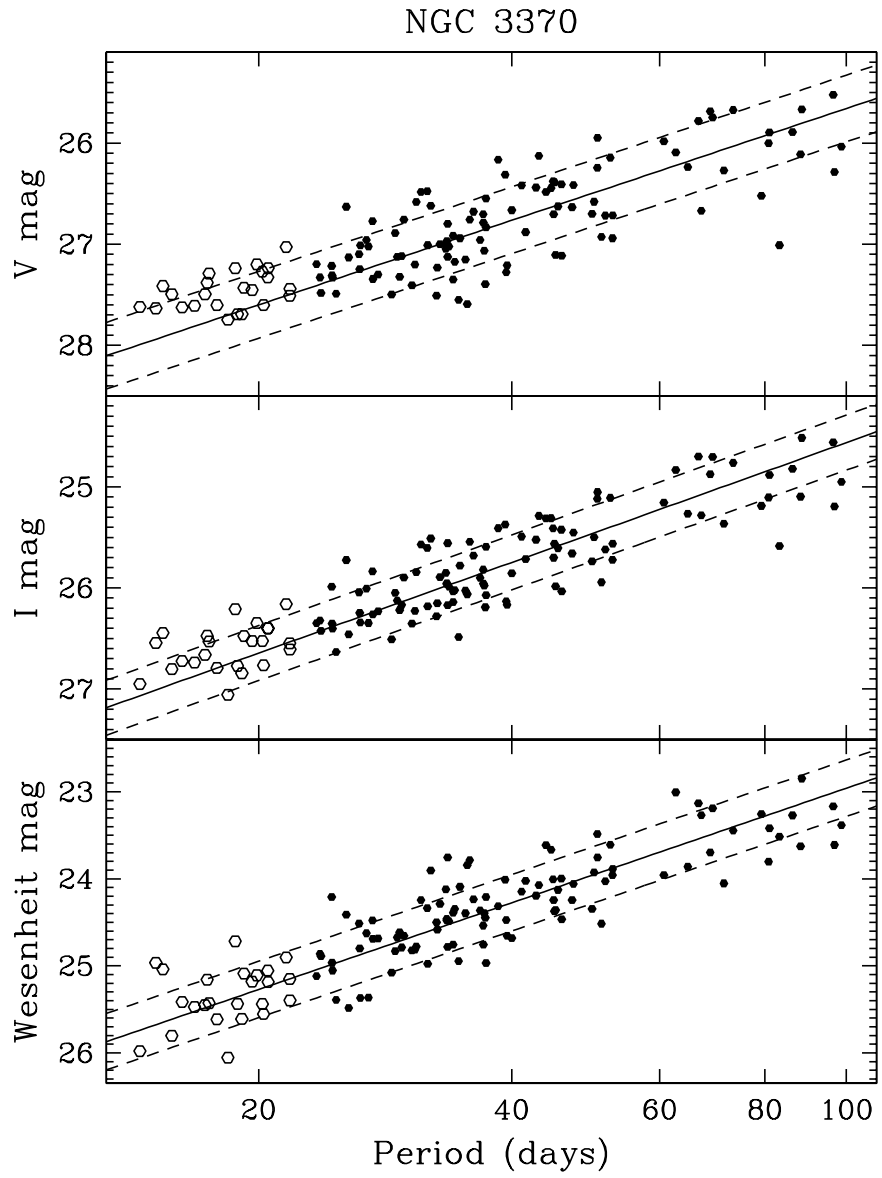


Fig. 7.—

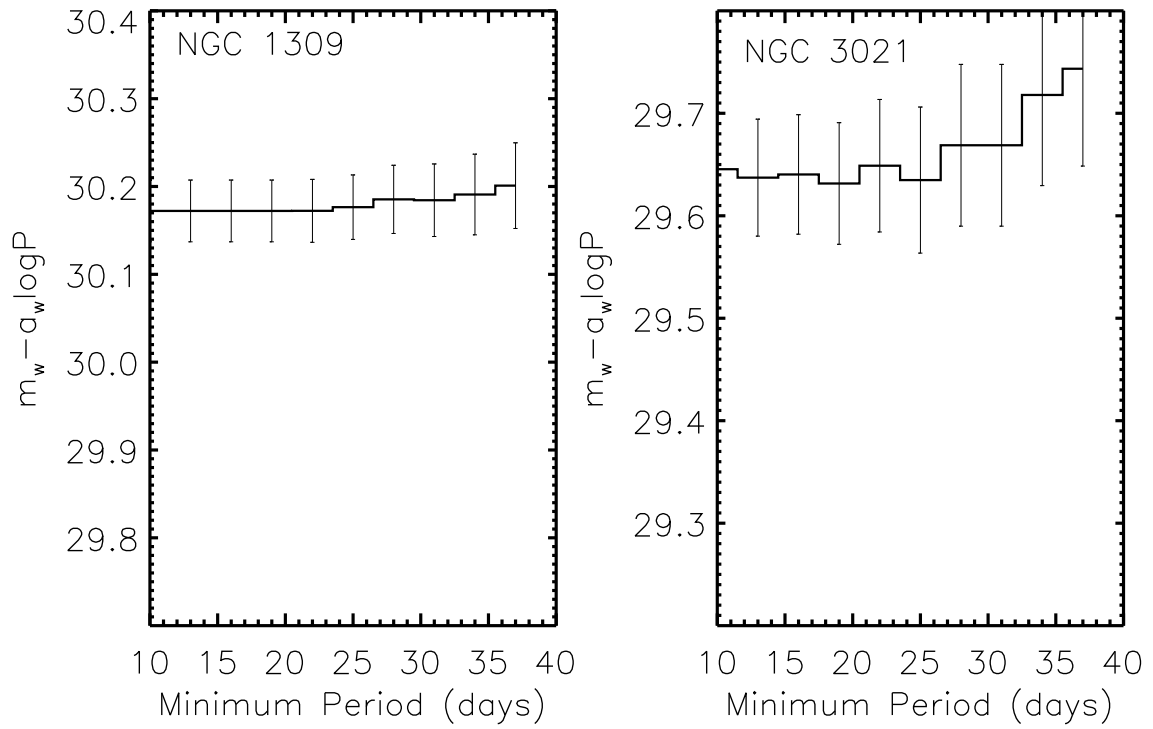
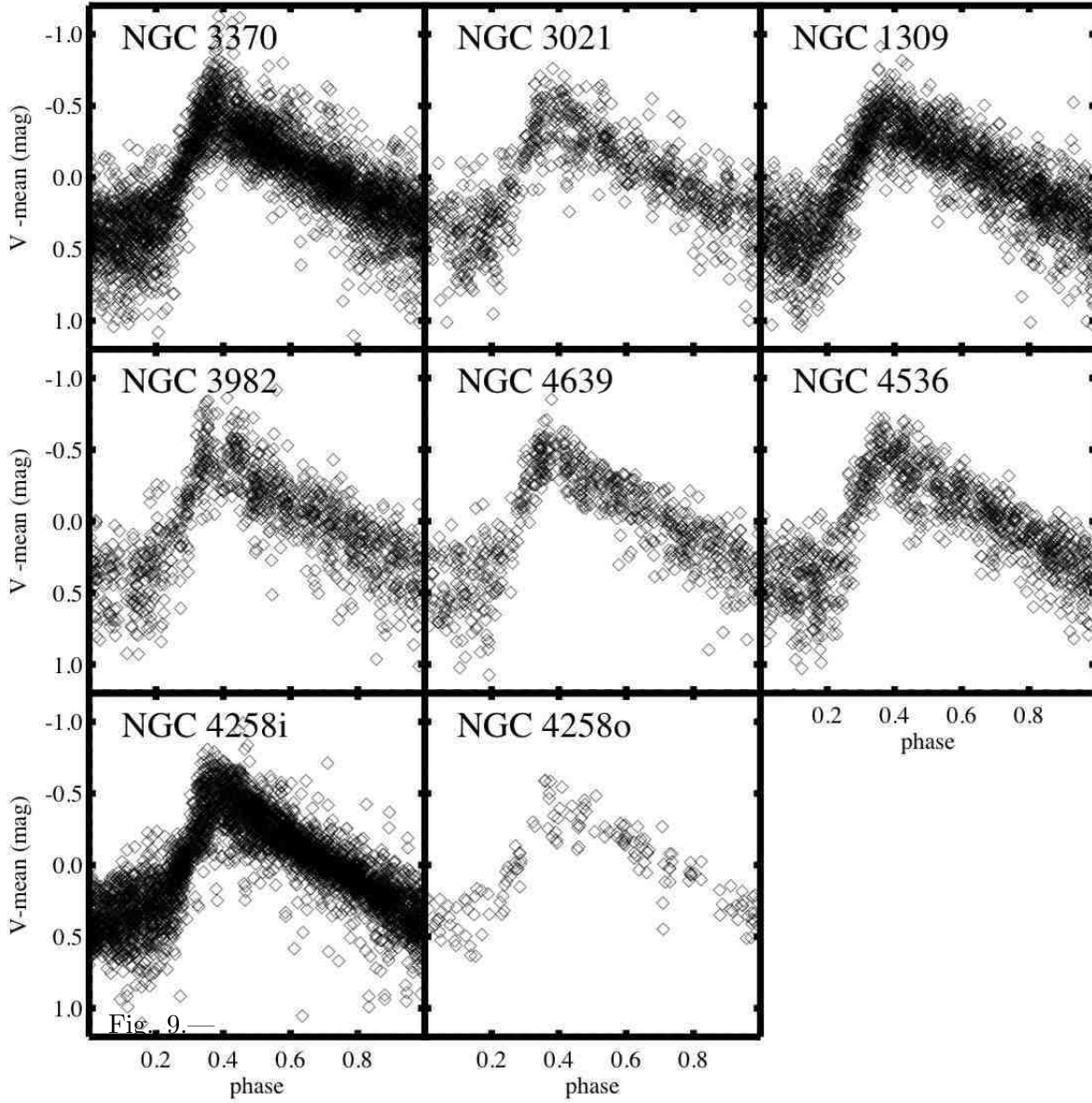


Fig. 8.—



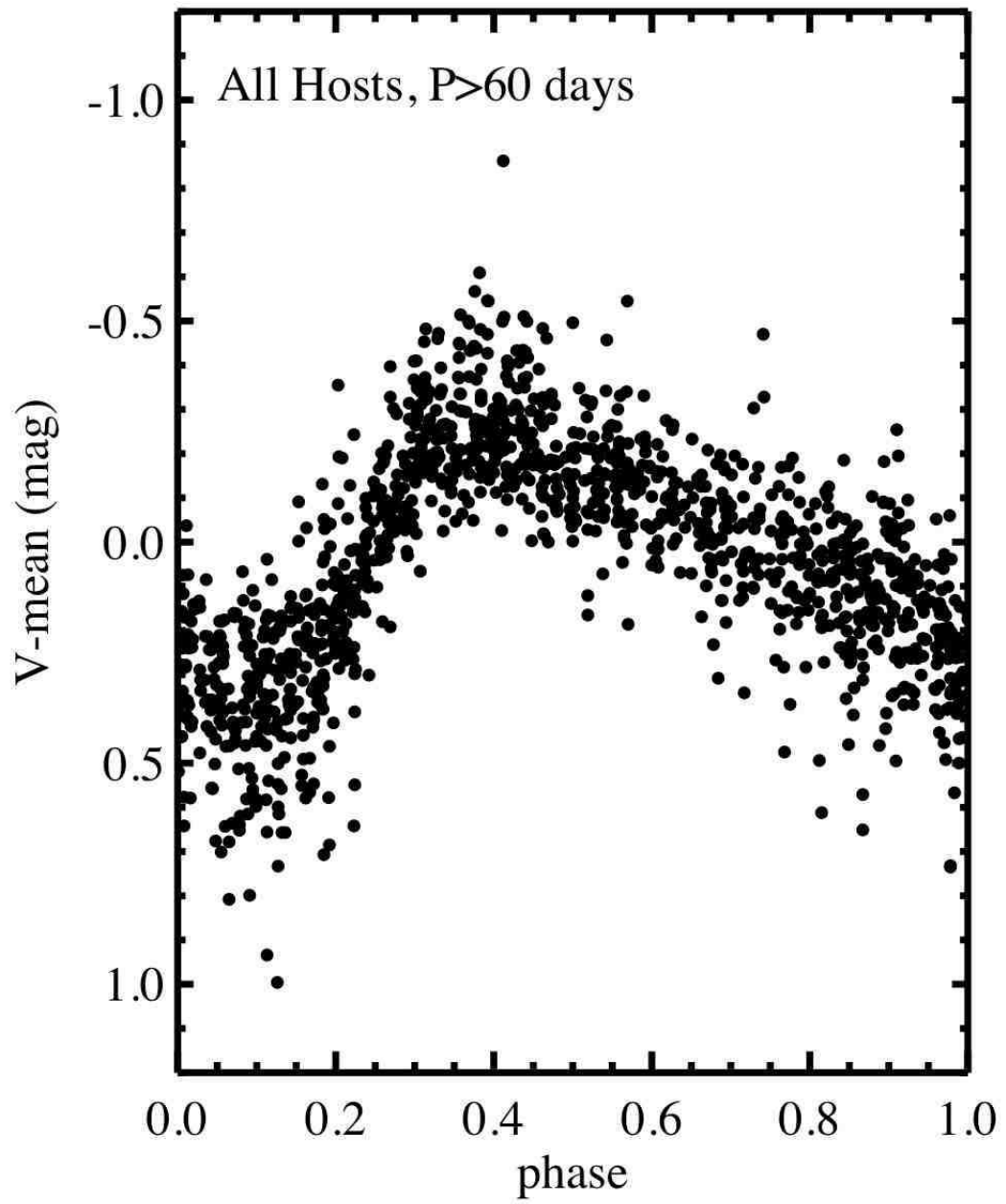


Fig. 10.—

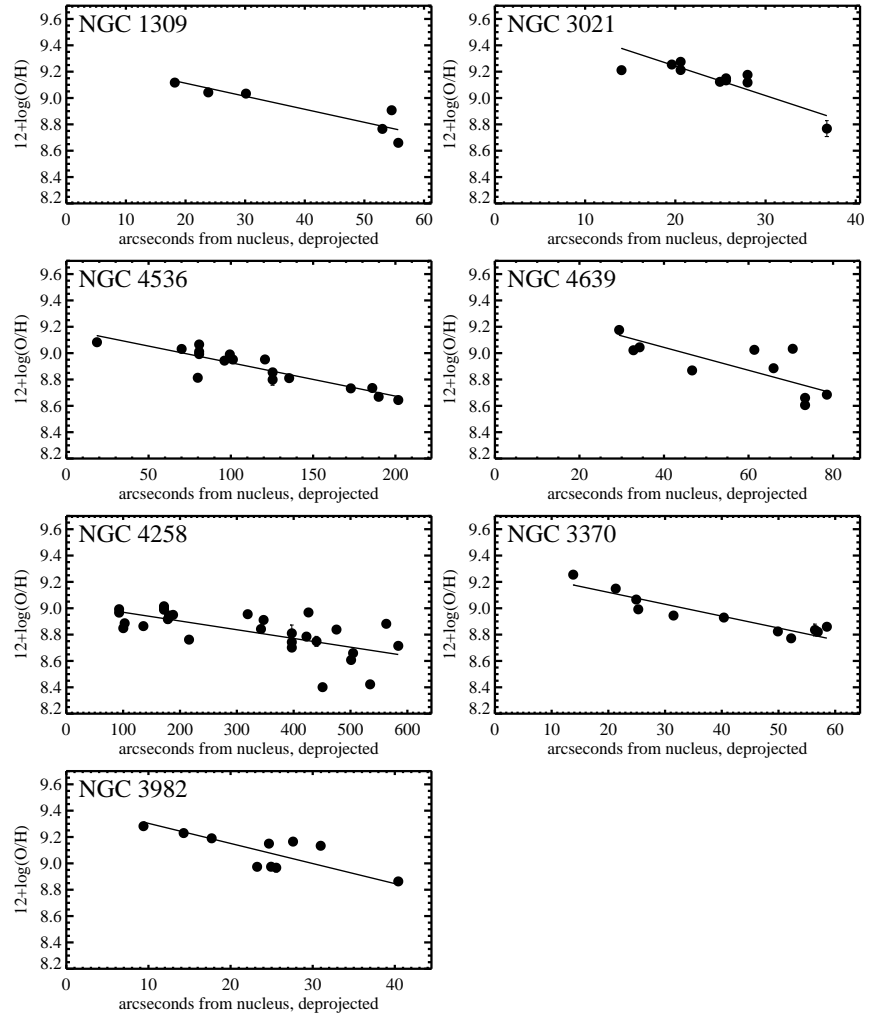


Fig. 11.—



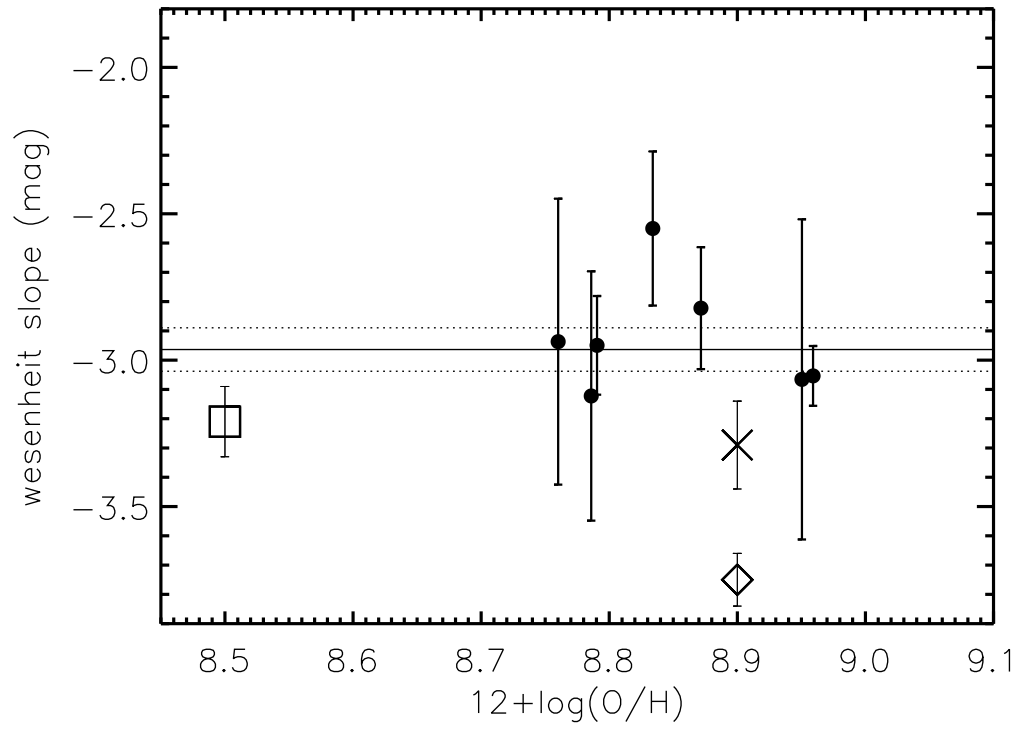


Fig. 12.—

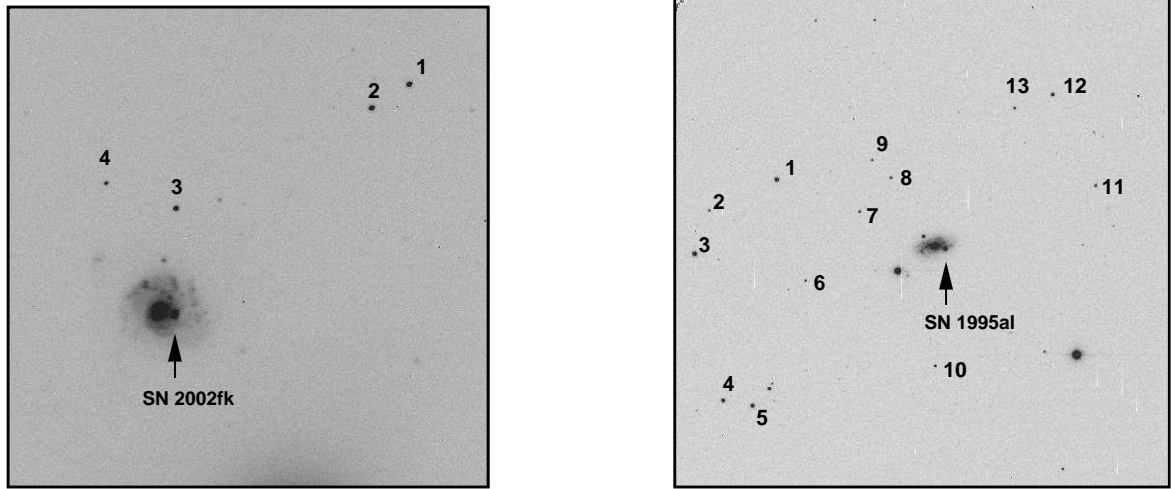


Fig. 13.— Comparison Star Finders for SNe

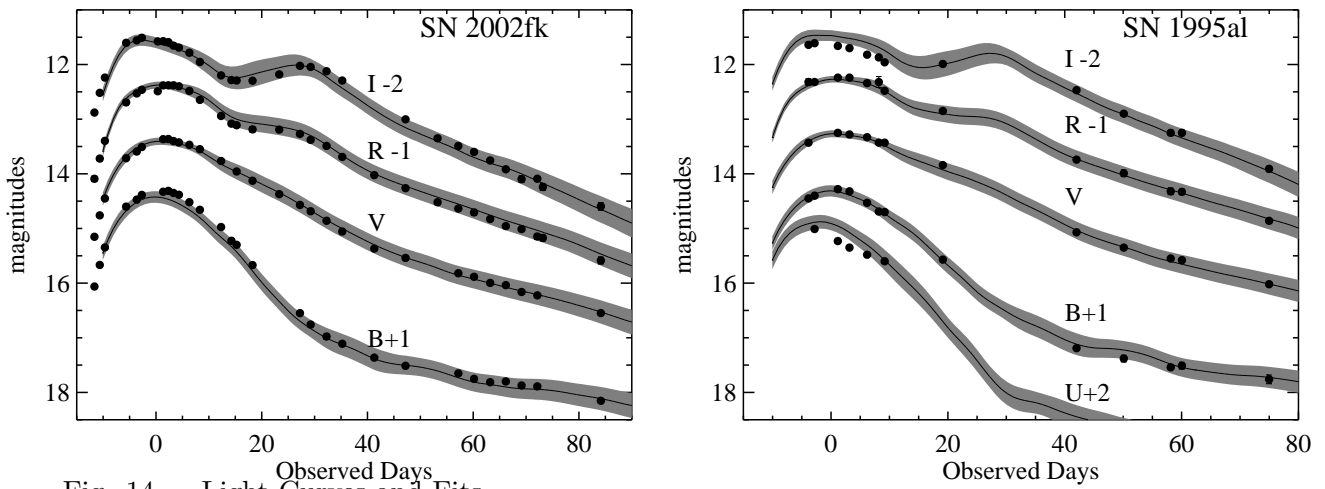


Fig. 14.— Light Curves and Fits

## REFERENCES

- Alibert, Y., Baraffe, I., Hauschildt, P., & Allard, F. 1999, *A&A*, 344, 551
- Andrievsky, S. M., Kovtyukh, V. V., Luck, R. E., Lépine, J. R. D., Maciel, W. J., & Beletsky, Y. V. 2002, *A&A*, 392, 491
- Andrievsky, S. M., Luck, R. E., Martin, P., & Lépine, J. R. D. 2004, *A&A*, 413, 159
- Ayani, K., & Yamaoka, H. 2002, *IAU Circ. No. 7976*
- Benedict, G. F., et al. 2007, *AJ*, 133, 1810
- Bird, J. C., Stanek, K. Z., & Prieto, J. L. 2009, *ApJ*, in press (arXiv:0807.4933)
- Bono, G., Caputo, F., Castellani, V., & Marconi, M. 1999, *ApJ*, 512, 711
- Buta, R. J., & Turner, A. 1983, *PASP*, 95, 72
- Chiaberge, M., et al. 2009, *HST ACS Instrument Science Report*
- Ferrarese, L., Silbermann, N. A., Mould, J. R., Stetson, P. B., Saha, A., Freedman, W. L., & Kennicutt, R. C., Jr. 2000, *PASP*, 112, 177
- Filippenko, A. V., Li, W. D., Treffers, R. R., & Modjaz, M. 2001, in *Small Telescope Astronomy on Global Scales*, ed. W. P. Chen, C. Lemme, & B. Paczyński (San Francisco: ASP), 121
- Ford, H. C., et al. 2003, *Proc. SPIE*, 4854, 81
- Fouqué, P., et al. 2007, *A&A*, 476, 73
- Freedman, W. L., Madore, B. F., Hawley, S. L., Horowitz, I. K., Mould, J., Navarrete, M., & Sallmen, S. 1992, *ApJ*, 396, 80
- Freedman, W. L., et al. 2001, *ApJ*, 553, 47
- Gibson, B. K., et al. 2000, *ApJ*, 529, 723
- Gieren, W., et al. 2005, *ApJ*, 627, 224
- Gieren, W., et al. 2008, *ApJ*, 683, 611
- Guy, J., Astier, P., Nobili, S., Regnault, N., & Pain, R. 2005, *A&A*, 443, 781
- Hamuy, M., Phillips, M. M., Maza, J., Suntzeff, N. B., Schommer, R. A., & Aviles, R. 1995, *AJ*, 109, 1
- Hamuy, M., Phillips, M. M., Suntzeff, N. B., Schommer, R. A., Maza, J., Smith, R. C., Lira, P., & Aviles, R. 1996, *AJ*, 112, 2438

- Holtzman, J. A., Burrows, C. J., Casertano, S., Hester, J. J., Trauger, J. T., Watson, A. M., & Worthey, G. 1995, *PASP*, 107, 1065
- Jha, S., Riess, A. G., & Kirshner, R. P. 2007, *ApJ*, 659, 122
- Jha, S., et al. 2006, *AJ*, 131, 527
- Kanbur, S. M., & Ngeow, C.-C. 2004, *MNRAS*, 350, 962
- Kanbur, S. M., & Ngeow, C.-C. 2006, *MNRAS*, 369, 705
- Kennicutt, R. C., et al. 1998, *ApJ*, 498, 181
- Kochanek, C. S. 1997, *ApJ*, 491, 13
- Landolt, A. U. 1992, *AJ*, 104, 340
- Leonard, D. C., et al. 2003, *ApJ*, 594, 247
- Li, W. D., et al. 2000, in *Cosmic Explosions*, ed. S. S. Holt & W. W. Zhang (New York: AIP), 103
- Macri, L. M., Stetson, P. B., Bothun, G. D., Freedman, W. L., Garnavich, P. M., Jha, S., Madore, B. F., & Richmond, M. W. 2001, *ApJ*, 559, 243
- Macri, L. M., Stanek, K. Z., Bersier, D., Greenhill, L. J., & Reid, M. J. 2006, *ApJ*, 652, 1133
- Macri, L. M., et al. 2009, submitted
- Madore, B. F. 1982, *ApJ*, 253, 575
- Madore, B. F. & Freedman, W. L., 2009, *ApJ* in press
- Marconi, M., Musella, I., & Fiorentino, G. 2005, *ApJ*, 632, 590
- Oke, J. B., et al. 1995, *PASP*, 107, 375
- Paczyński, B., & Pindor, B. 2000, *ApJ*, 533, L103
- Perlmutter, S., et al. 1997, *ApJ*, 483, 565
- Persson, S. E., Madore, B. F., Krzemiński, W., Freedman, W. L., Roth, M., & Murphy, D. C. 2004, *AJ*, 128, 2239
- Phillips, M. M., Lira, P., Suntzeff, N. B., Schommer, R. A., Hamuy, M., & Maza, J. 1999, *AJ*, 118, 1766
- Phillips, M. M. 1993, *ApJ*, 413, L105
- Riess, A. G., Press, W. H., & Kirshner, R. P. 1995, *ApJ*, 438, L17

- Riess, A. G., Press, W. H., & Kirshner, R. P. 1996, *ApJ*, 473, 88
- Riess, A. G., Press, W. H., & Kirshner, R. P. 1996, *ApJ*, 473, 588
- Riess, A. G., et al. 1998, *AJ*, 116, 1009
- Riess, A. G., et al. 1999, *AJ*, 117, 707
- Riess, A. G., et al. 2005, *ApJ*, 627, 579
- Riess, A. G., et al. 2009, submitted
- Saha, A., Sandage, A., Labhardt, L., Tammann, G. A., Macchetto, F. D., & Panagia, N. 1997, *ApJ*, 486, 1
- Saha, A., et al. 1996, *ApJ*, 466, 55
- Saha, A., et al. 2001, *ApJ*, 562, 314
- Saha, A., et al. 2006, *ApJS*, 165, 108
- Sakai, S., et al. 2004, *ApJ*, 608, 42
- Sandage, A., & Tammann, G. A. 2008, *ApJ*, 686, 779
- Sandage, A., et al. 2006, *ApJ*, 653, 843
- Sirianni, M., et al. 2003, *ApJS*, 148, 175
- Stetson, P. B. 1987, *PASP*, 99, 191
- Stetson, P. B. 1994, *PASP*, 106, 250
- Stetson, P. B. 1996, *PASP*, 108, 851
- Stetson, P. B. 2000, *PASP*, 112, 925
- Stetson, P. B., & Gibson, B. K. 2001, *MNRAS*, 328, L1
- Stetson, P. B., et al. 1998, *ApJ*, 508, 491
- Tammann, G. A., Sandage, A., & Reindl, B. 2008, *ApJ*, 679, 52
- Tammann, G. A., Sandage, A., & Reindl, B. 2003, *A&A*, 404, 423
- Udalski, A., et al. 1999, *Acta Astronomica*, 49, 223
- van Leeuwen, F., Feast, M. W., Whitelock, P. A., & Laney, C. D. 2007, *MNRAS*, 379, 723
- Valencic, Clayton, & Gordon, 2004, *ApJ*, 616, 912

Wang, X., et al. 2009, ApJ, submitted (arXiv:0811.1205)

Wei, J.-Y., et al. IAU Circ. No. 6256

Zaritsky, D., Kennicutt, R. C., & Huchra, J. P. 1994, ApJ, 420, 87

